UNIVERSITY OF CALIFORNIA

Los Angeles

Inhalability and Sampling of Large Particles

A dissertation submitted in partial satisfaction of the

requirements for the degree Doctor of Philosophy

in Environmental Health Sciences

by

Nola J. Kennedy

2000

INFORMATION TO USERS

This manuscript has been reproduced from the microfilm master. UMI films the text directly from the original or copy submitted. Thus, some thesis and dissertation copies are in typewriter face, while others may be from any type of computer printer.

The quality of this reproduction is dependent upon the quality of the copy submitted. Broken or indistinct print, colored or poor quality illustrations and photographs, print bleedthrough, substandard margins, and improper alignment can adversely affect reproduction.

In the unlikely event that the author did not send UMI a complete manuscript and there are missing pages, these will be noted. Also, if unauthorized copyright material had to be removed, a note will indicate the deletion.

Oversize materials (e.g., maps, drawings, charts) are reproduced by sectioning the original, beginning at the upper left-hand corner and continuing from left to right in equal sections with small overlaps.

Photographs included in the original manuscript have been reproduced xerographically in this copy. Higher quality 6" x 9" black and white photographic prints are available for any photographs or illustrations appearing in this copy for an additional charge. Contact UMI directly to order.

Bell & Howell Information and Learning
300 North Zeeb Road, Ann Arbor, MI 48106-1346 USA
800-521-0600

UMI®

UMI Number: 9981706

Bell & Howell Information and Learning Company
300 North Zeeb Road
P.O. Box 1346
Ann Arbor, MI 48106-1346

The dissertation of Nola J. Kennedy is approved.

Ann E. Carlson

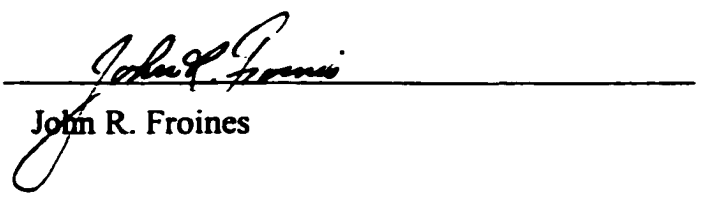

John R. Froines

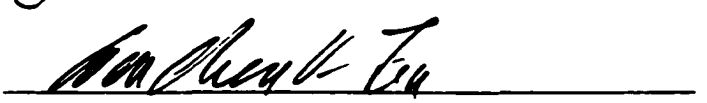

Wen Chen Victor Liu

William C. Hinds, Committee Chair

University of California, Los Angeles

2000

For Victor, Ellis and Amber

TABLE OF CONTENTS

LIST OF FIGURES AND TABLES

Figures

Tables

ACKNOWLEDGEMENTS

This research was supported by NIOSH research grant number 5-RO1/OH03196 and NIOSH Education and Research Center grant number T42/CCT910430. I wish to thank William Hinds for his guidance and mechanical expertise, Jinghui Zhang and Karina Tatyan for their assistance during the solid particle studies, and Yifang Zhu and Rose Siengsubcharti for their help during the liquid particle study.

VITA

September 17, 1962	Born, Concord, North Carolina
1984	B.A., Genetics University of California, Berkeley
1985-87	Industrial Hygiene Program Environmental Health Sciences Department University of California, Los Angeles
1986	Outstanding Graduate Student Award American Industrial Hygiene Association Southern California Section
1987-91	Manager, Industrial Hygiene Services Drucker Health & Safety Management, Inc. Manhattan Beach, CA and Atlanta, GA
1991-94	Staff Research Associate Environmental Health Sciences Department University of California, Los Angeles
1993-present	Certified Industrial Hygienist American Board of Industrial Hygiene, #5551
1993	M.S. – E.H.S. University of California, Los Angeles
1994-2000	Graduate Student Researcher Environmental Health Sciences Department University of California, Los Angeles
1994-2000	Teaching Assistant Environmental Health Sciences Department University of California, Los Angeles
2000	Teaching Assistant of the Year Award School of Public Health University of California, Los Angeles

PUBLICATIONS AND PRESENTATIONS

Perry, D.M.*, Froines, J.R., Sanchez, D., Kennedy, N.J., Sabty, R., Smalstig, T., Que Hee, S., and Hinds, W.C., Health and Safety Conditions in the Maquiladora Auto Parts Industry in Mexico. platform session at the American Public Health Association Annual Meeting, San Francisco, CA (1993).

Hinds, W.C.* and Kennedy, N.J., An Ion Generator for Neutralizing Concentrated Aerosol Streams. poster session at the American Association for Aerosol Research Conference, Orlando, FL (1996).

Kennedy, N.J.* and Hinds, W.C., Inhalability of Large Solid Particles. poster session at the American Association for Aerosol Research Conference, Denver, CO (1997).

Hinds, W.C., Kennedy, N.J., and Tatyan, K.: Inhalability of Large Particles for Mouth and Nose Breathing. *J. Aerosol Sci.* 29:S277-S278 (1998).

Hinds, W.C. and Kennedy, N.J.*, Performance of Personal Samplers for Inhalable Particles. poster session at the American Association for Aerosol Research Conference, Tacoma, WA (1999).

Hinds, W.C. and Kennedy, N.J.: An Ion Generator for Neutralizing Concentrated Aerosols. *Aerosol Sci. Tech.* 32:214-220 (2000).

Kennedy, N.J., Tatyan, K., and Hinds, W.C.: Comparison of a Simplified and Full-Size Mannequin for the Evaluation of Inhalable Sampler Performance. *Aerosol Sci. Tech.* (in press, accepted May 2000).

Hinds, W.C.*, Ashley, A.B., and Kennedy, N.J., Bulk Motion of Aerosols: Cloud Settling and Rayleigh-Taylor Instability. accepted for presentation at the International Association for Aerosol Research Conference, Dublin, Ireland (2000).

Hinds, W.C.*, Ashley, A.B., and Kennedy, N.J., Bulk Motion of Aerosols: Cloud Settling and Rayleigh-Taylor Instability. accepted for presentation at the American Association for Aerosol Research Conference, St. Loius, MO (2000).

ABSTRACT OF THE DISSERTATION

Inhalability and Sampling of Large Particles

by

Nola J. Kennedy

Doctor of Philosophy in Environmental Health Sciences

University of California, Los Angeles, 2000

Professor William C. Hinds, Chair

Inhaled large particles (10-150 μm) with systemic toxicity, such as, heavy metals, pesticides, radionuclides, or corrosive materials pose a health risk regardless of where they deposit in the respiratory tract. This research seeks to better define particle inhalability, the fraction of airborne particles that are inhaled as a function of particle size, for conditions found in occupational environments. This research also evaluated the performance of eight personal samplers for inhalable particles.

Measurements of inhalability and sampler performance were made for solid or liquid particles using an open-cycle, closed-jet, low-velocity wind tunnel. Wind tunnel air velocities were 0.4, 1.0, and 1.6 m/s. A modified full-size, full-torso mannequin was used to collect particles entering either the mouth or nose. Personal samplers were attached to the collar of the mannequin. Inhalation was simulated using a mechanical breathing machine at minute volumes of 14.2, 20.8, and 37.3 L. The mannequin either faced the oncoming wind or rotated slowly (0.06 rpm). Aerosol concentration in the test section was determined with three isokinetic samplers. At the test section, air velocity was uniform to within 10% and aerosol concentration was uniform to within 15%.

For particles larger than 50 μm, orientation-averaged mouth inhalability for both solid and liquid particles was significantly lower than the IPM criterion and the liquid particle results were 50% lower than the solid particle results. Facing-the-wind mouth inhalability was higher than the orientation-averaged results for both liquid and solid particles. For $d_a > 50$ μm, inhalability for solid particles was 4 times that of liquid particles. Wind velocity and breathing pattern had little effect on solid particle inhalabilty. Wind velocity did influence liquid particle inhalability. Nose inhalability is significantly different in trend and shape than mouth inhalabilty. Particle bounce seems to affect inhalabilty for solid particles larger than 50 μm. Two samplers showed good agreement with the IPM criterion: the IOM inhalable sampler and the 37-mm inline sampler with an 8-mm inlet positioned to face forward.

Chapter 1: Introduction to Inhalability and Sampling of Large Particles

1.0 Introduction

The studies presented in this dissertation investigate inhalability and sampling of large particles, those with an aerodynamic diameter (d_a) larger than 10 micrometers (μm). Inhalability is defined as the fraction of particles of a given size that can be inhaled either through the nose or mouth. Samplers designed to collect inhalable particles are evaluated by comparing their sampling efficiency for particles of a given size to inhalability data for the same size particles.

Inhaled particles are, by necessity, part of an aerosol. An aerosol is a two-phase system consisting of particles, either solid or liquid, suspended in a gas. Most commonly, the gas is air. Mechanical processes, combustion or resuspension of settled dust can form aerosols. The movement and behavior of aerosol particles is influenced by their size, their density and the forces that act on them, such as, gravity or an electric field. Aerosol particles cover a wide range of sizes, from "ultrafines" that have diameters in the nanometer (nm) range to the coarsest particles, which have an aerodynamic diameter (d_a) of 100 micrometers (μm) or more. The spectrum of aerosol particles is presented in Figure 1-1.

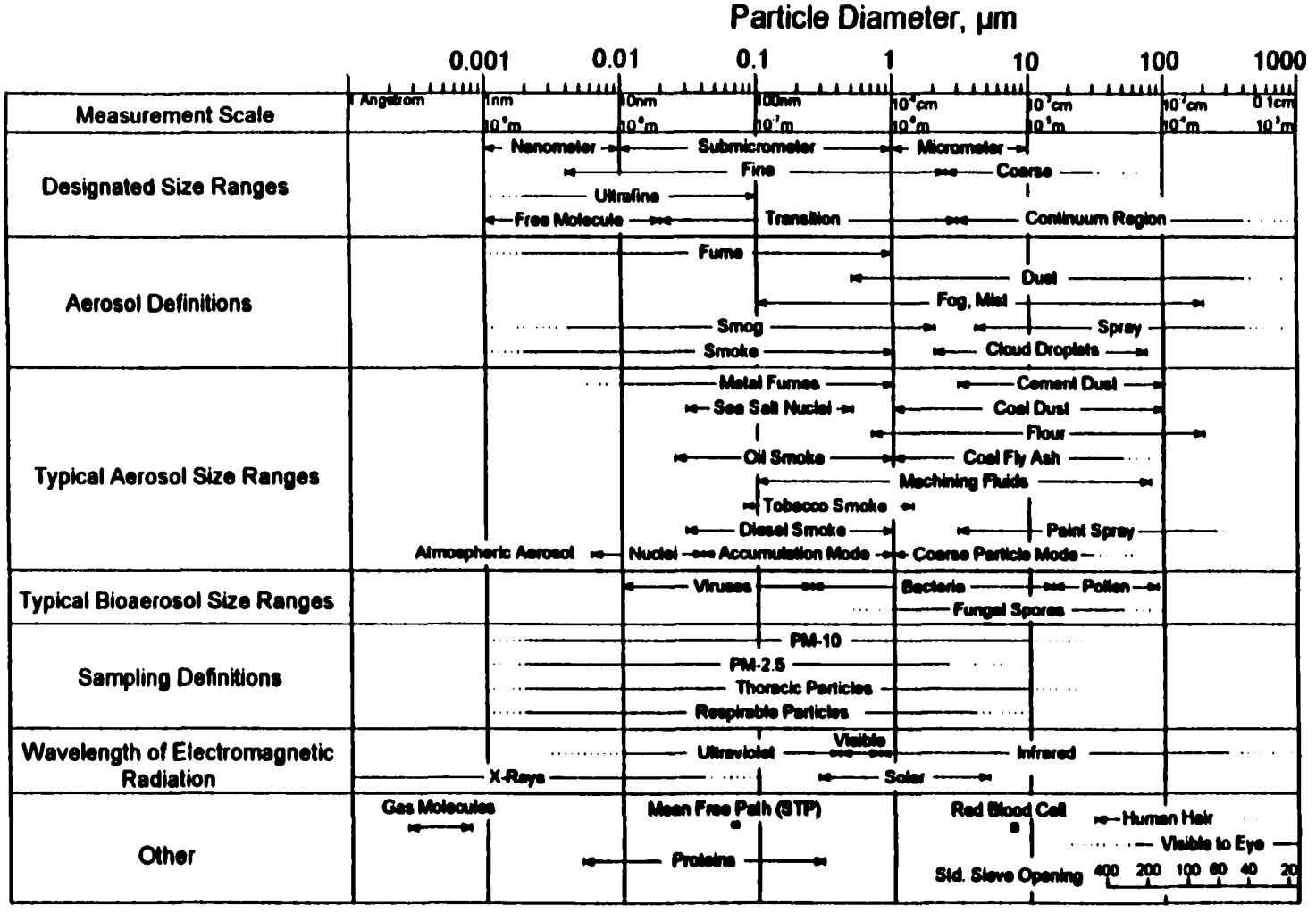

Figure 1-1: Size ranges and definitions of aerosol particles (Hinds, 1999).

Atmospheric aerosols are responsible for the color of a sunset, the dingy brown layer associated with smog, the haze of a summer day, and the salty, stickiness of a day at the beach. Therapeutic drugs and carcinogens are transported to the lung as aerosols, as is the case for asthmatics and smokers. Aerosolized particles are used in industrial processes, for example, the spray application of coating materials. Workplace aerosols also represent a common and well-recognized occupational exposure hazard. Throughout the world, governmental agencies have established occupational exposure limits (OELs) and community air pollution standards to protect workers and the public from health risks associated with exposure to airborne contaminants. For the most part, OELs are health-based and derive from epidemiological and toxicological data that relate exposure level, or dose, to an adverse health effect.

1.1 Background

Early concern about work-related health problems focused on occupational exposure to dusts, for example, coal dust and silica. Because of this, the first evaluations of occupational dust exposure were aimed at particles with aerodynamic diameters of 0.1 to 10 μm. Particles that are this small can penetrate to the gas exchange region (GER) of the lung, where they may cause disease, such as, pneumoconiosis or silicosis. During the last two decades, however, researchers and professionals interested in occupational health have begun to investigate the inhalation, deposition, and toxicity of large particles that can elicit a toxic effect regardless of where they deposit. Examples include heavy metals, pesticides, and radioactive materials.

For many years, the measurement of worker exposure to airborne particles relied on trapping particles, either in solution using an impinger or on a filter, then sizing and counting the particles. Particle count, along with the metered volume of air sampled, allows calculation of a number concentration. Exposures are reported as number of particles per unit volume. Typical number concentration units are million particles per cubic foot (mppcf) and particles/cm^3. The use of an optical microscope and the number of particles that need to be counted to optimize statistical accuracy make this a tedious and time-consuming process.

This created an impetus for developing methods that measure mass, instead of number. Mass is much simpler to evaluate. The only requirement is a suitable pre-weighed substrate and a scale or balance that offers sufficient precision. The mass of particles collected from a given volume of air allows calculation of mass concentration, usually expressed as mg/m^3 for occupational exposures. The disadvantage of this method is that the sample contains particles of all sizes, including sizes that may not be related to the health outcome of concern. Because particle mass is proportional to the cube of particle diameter, d_p^3, mass increases rapidly as size increases. A few large particles can obscure the mass contributed by many small particles. To explain by using a simplified example, consider the following:

An air sample is collected to determine worker exposure to nuisance dust in a workshop. A mass of 550 μg is collected from 100 L of air for a mass concentration of 5.5 mg/m^3. The same sample is evaluated for particle size and number. The dust is bimodally distributed; 90% of the particles have an aerodynamic diameter of 1 μm and the remaining 10% are 10 μm. The ratio of the mass contributed by the large particles (m_{lrg}) to that from the small particles (m_{sml}) is

$$\frac{m_{lrg}}{m_{sml}} = \frac{10\%\left(d_a^{\,3}\right)}{90\%\left(d_a^{\,3}\right)} = \frac{0.1\left(10^3\right)}{0.9\left(1^3\right)} = \frac{100}{9} = 111$$

and the mass contributed by the 1-μm particles is

$$550\ mg\left(\frac{1}{111}\right) = 4.95\ mg$$

So, the mass concentration of small particles is 0.05 mg/m^3, far below the total value of 5.5 mg/m^3. If only the 1-μm particles are responsible for an adverse health effect, then the "total" dust sample would drastically overestimate the exposure and the risk.

This illustrates the need for sampling only the fraction of particles that are physiologically significant. This is a simple concept, but it has only recently become a priority for agencies charged with the setting of occupational health standards. Research to define particle size-selective (PSS) criteria for large particles began only

a few decades ago. The PSS criteria are used as performance guidelines for aerosol samplers and to determine whether the hazardous particles in an aerosol are capable of reaching the portion of the lung where they can cause damage or disease.

1.1.1 Health-Related Aerosol Sampling

Inhalation is generally considered the most important route for occupational exposure to aerosols. Inhaled particles are deposited in the airways primarily as a result of gravitational and inertial forces for large particles ($d_a > 1$ μm) and diffusion for particles with an aerodynamic diameter less than 0.1 μm. The hazard associated with particles is a function of their chemical composition and the location of deposition. There are a number of mathematical models used to predict deposition location (Lippmann, 1995); all of them use particle size as a predictor.

1.1.2 Historical Framework

The British Medical Research Council introduced the first definition of the "respirable fraction" in 1952. It was defined as the portion of airborne dust able to penetrate to the alveolar region of the lung. The BMRC used a horizontal elutriator as a precollector and adopted a cut-off value based on available human respiratory tract deposition data. The definition of respirable fraction was applied specifically to aerosols associated with pneumoconiosis and was related to the terminal settling velocity of the particles by

$$E(d_a) = \frac{V_{TS}}{2(V_{TS,\,5\mu m})} \qquad (1.1)$$

where $E(d_a)$ is the collection efficiency of the precollector for particles with a given aerodynamic diameter, d_a, and settling velocity, V_{TS}. $V_{TS,\,5\mu m}$ is the settling velocity for a particle with an aerodynamic diameter of 5 μm. The criterion curve indicates that penetration is 100 percent for 1-μm particles and drops to zero when d_a = 7.1 μm, passing through 50 percent at d_a = 5 μm (BMRC, 1952).

Early in 1961, the Office of Health and Safety for the US Atomic Energy Commission (AEC) offered a definition of respirable particulate mass as the portion of inhaled dust that reaches the non-ciliated, gas-exchange regions of the lung. The associated size-selective sampling criterion was intended only for insoluble particles with a long retention time in the lungs, such as, silica and other minerals. Particles with high solubility or chemical toxicity, *e.g.*, metals were not the focus of the criterion. Respirable dust was defined by a curve with a 50% cut-off for d_a = 3.5 μm. The penetration efficiencies for other sizes were 100% at 2.0 μm, 75% at 2.5 μm, 25% at 5 μm, and 0% at 10 μm (Hatch and Gross, 1964).

In 1968, the ACGIH presented particle size-selective mass concentration TLVs® in their "Notice of Intended Changes". The "respirable" criterion selected by the ACGIH was based on alveolar deposition work conducted by the Task Group on

Lung Dynamics (1966). The criterion curve was similar to that described by the AEC, except the penetration efficiency for d_a = 2 μm was 90% instead of 100%. They used the respirable mass sampling criteria as part of their 1998 TLV® recommendations for silica, coal dust and nuisance dust. The recommended TLVs® for both silica and coal dust were based on health outcome. For silica, there was a convincing body of epidemiological evidence indicating a relationship between silica exposure, including count and mass concentrations, and the disease outcome, silicosis (Sutton and Reno, 1968). The health outcome considered for establishing the coal dust criteria was coal worker's pneumoconiosis (CWP). While there are other diseases related to coal dust exposure, such as, bronchitis, the TLV® was intended to prevent CWP. This marks the first time that health-based occupational exposure limits required the use of particle size-selective mass sampling to determine worker exposure.

The Federal Coal Mine Health and Safety Act of 1969 (Public Law, 1969) required the use of a Mining Research Establishment (MRE) horizontal elutriator as a precollector for the measurement of the respirable fraction of airborne dust. The MRE device was designed to meet the BMRC definition of respirable particulate mass. An elutriator uses competition between particle transport, related to aerosol flow rate, and gravitational settling, a function of particle size, to separate a given size fraction from the original aerosol. This was the first time that a governing

agency specified the use of a particular instrument for determining size-selective mass concentration.

The Federal Mine Safety and Health Act of 1977 (Public Law, 1977) released the requirement for use of the MRE. And, in 1980, the National Research Council (NRC) Committee on Measurement and Control of Respirable Dust in Mines (NRC, 1980) recommended the use of the ACGIH criterion for respirable dust instead of the definition provided by the BMRC. The ACGIH curve was shown to be a better match for human deposition data (Lioy *et al.*, 1985).

The early development of particle size-selective sampling criteria for the respirable fraction of airborne dust presented in the preceding paragraphs provides an historical perspective to the following discussion of particle size-selective criteria for large particles.

1.2 Particle Size-Selective Sampling Criteria for Large Particles

The late 1970's and early 1980's saw an increased effort to define the fractions of airborne aerosol capable of penetrating to different functional regions of the lung (Figure 1-2). Diseases, such as, nasal and bronchial cancers and chronic bronchitis were attributed to particles too large to penetrate to the gas exchange region (GER) of the lung. It had become apparent that size-selective criteria and occupational standards were needed for particles that enter the head airways region (HAR) and

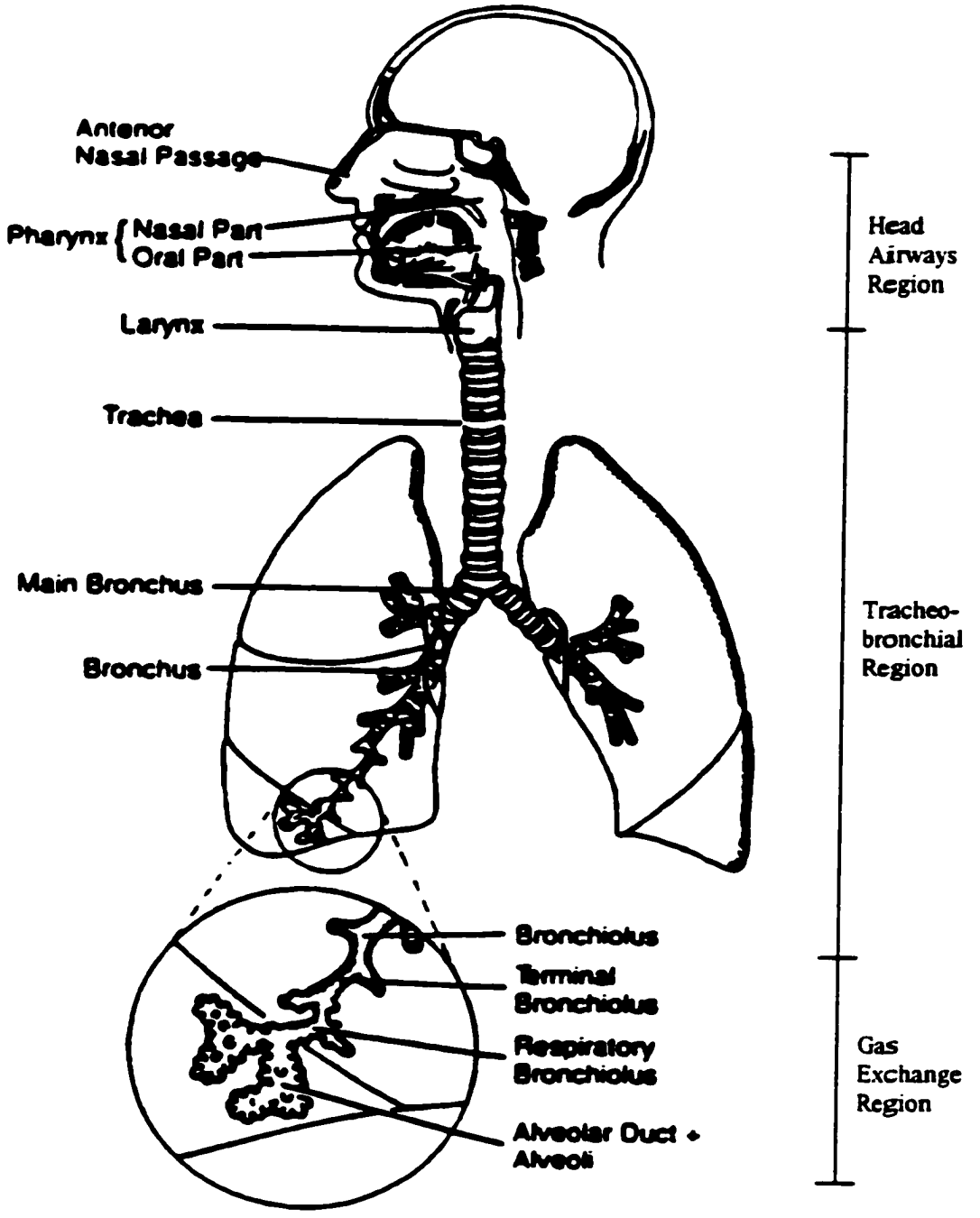

Figure 1-2: Functional regions of the respiratory tract.

reach the tracheobronchial region (TBR). It was during this time that the terms inhalable (originally, "inspirable") particulate mass (IPM), thoracic particulate mass (TPM), and respirable particulate mass (RPM) were adopted. The IPM fraction is defined as the portion of ambient aerosol particles, as a function of size, able to be inhaled through the nose or mouth. Particles in the TPM fraction are capable of penetrating past the larynx and RPM particles can reach the terminal bronchioles and the unciliated, gas-exchange region.

Both the International Standards Organization (ISO, 1981) and the American Conference of Governmental Industrial Hygienists (ACGIH, 1985) presented particle size-selective sampling criteria for large particles, those with an aerodynamic diameter above 10 μm, as well as for small respirable particles. Figure 1-3 shows the original IPM criterion curves developed by the ISO and ACGIH. Aspiration efficiency, the fraction of particles collected, is expressed as a percentage and plotted against aerodynamic particle diameter.

Much of the late 1980's and early 1990's was spent on discussion to resolve differences in the ISO and ACGIH definitions of the different particle size-selective sampling criteria. By 1995, the ACGIH criterion for inhalability found universal acceptance and was adopted by the ISO (1995) and the Comité Européen de Normalisation (CEN, 1993). During this "harmonization" process, agreement was also reached on the RPM and TPM criteria, resulting in a notable change in the long-

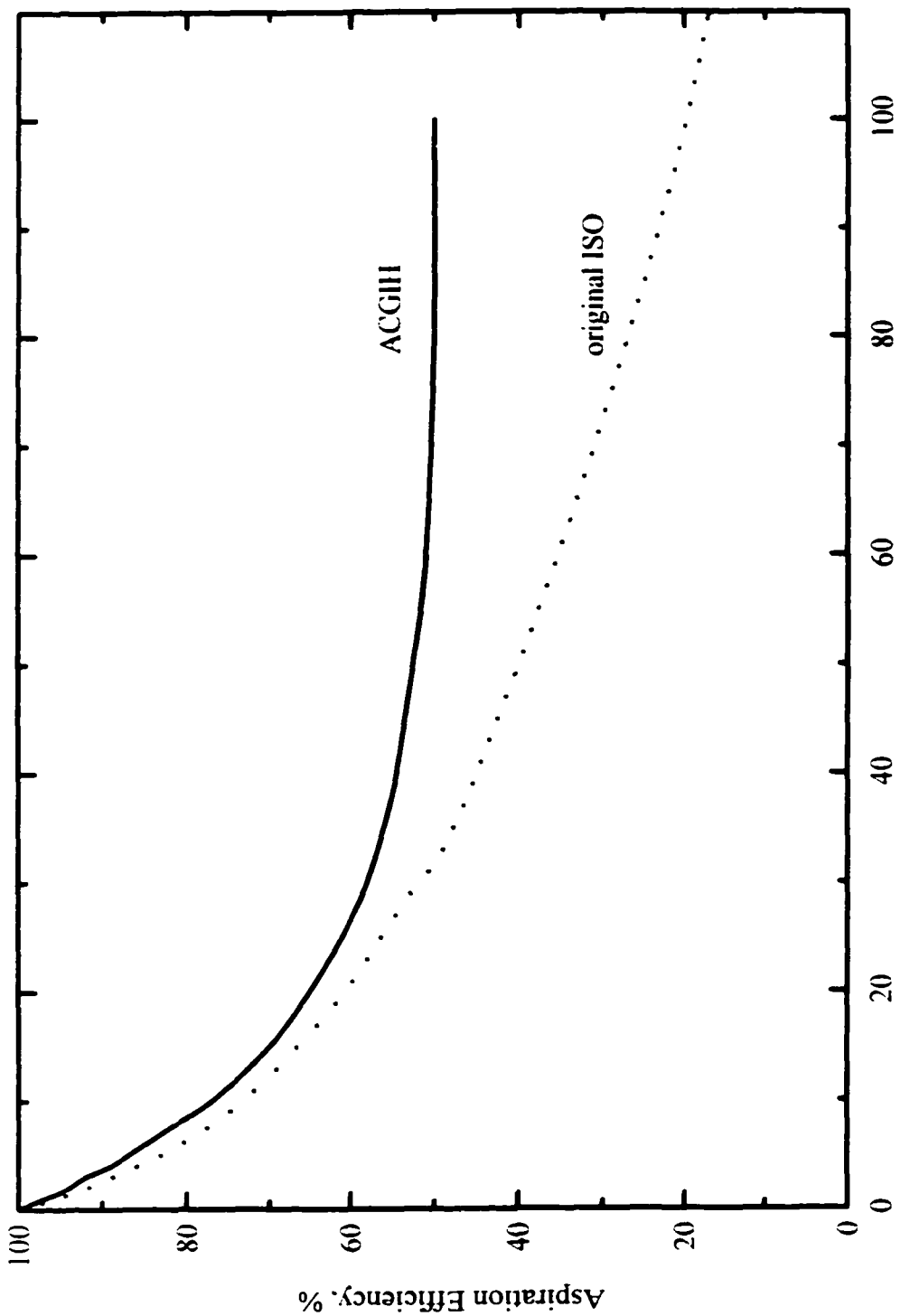

Figure 1-3: Original ISO and ACGIH IPM curves.

accepted definition of the RPM fraction. The cut-off diameter (d_{50}) for the respirable fraction was shifted from 3.5 μm to 4 μm.

The ACGIH/ISO/CEN (ACGIH, 1999) definition of the IPM criterion is

$$IF(d_a) = 0.5\left(1 + \exp(-0.06d_a)\right) \tag{1.2}$$

where $IF(d_a)$ is the inhalable fraction, or collection efficiency of an IPM sampler, for particles with aerodynamic diameter, d_a. The criterion, graphed in Figure 1-4, assumes that the sampler collects equally from all angles, 0° to 360°, with respect to wind direction. It also is limited to particles smaller than 100 μm and wind velocities below 4 m/s. In some situations, particularly for work conducted outside, wind velocity can exceed 4 m/s. Vincent *et al.* (1990) developed an expression for inhalability at higher wind velocities:

$$IF(d_a, U_0) = 0.5\left(1 + \exp(-0.06d_a)\right) + 10^{-5}U_0^{2.75}\exp(0.055d_a) \tag{1.3}$$

where U_0 is the wind velocity in m/s and the particle aerodynamic diameter, d_a, is in μm. This is also for orientation-averaged sampling and limited to particles smaller than 100 μm.

The TPM fraction (TF) is described by:

$$TF(d_a) = IF(1 - F(x)) \tag{1.4}$$

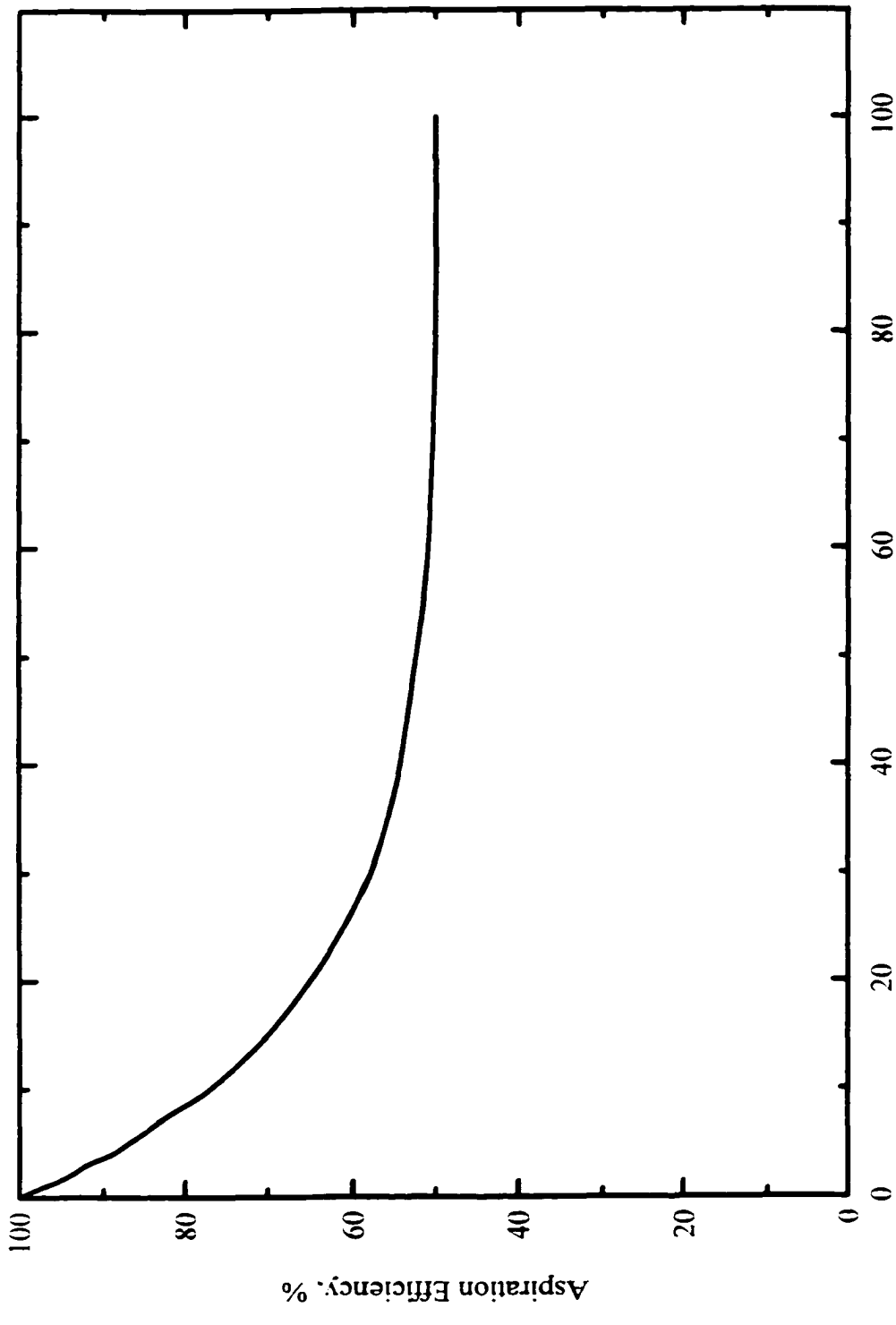

Figure 1-4: Criterion curve for the Inhalable Particulate Mass (IPM) fraction.

where *IF* is the inhalable fraction given in Equation 1.2. *F(x)* is the cumulative probability function of the standardized normal variable *x*,

$$x = \frac{\ln\left(\frac{d_a}{\Gamma}\right)}{\Sigma} \tag{1.5}$$

where the d_{50} cut off size, Γ, is 11.64 μm and the standard deviation, Σ, is 1.5. Figure 1-5 shows the TPM criterion curve.

The RPM fraction equation is similar in form to that for TPM,

$$RF(d_a) = IF(1 - F(x)) \tag{1.6}$$

except Γ is 4.25 μm and $\Sigma = 1.5$. The RPM criterion is shown in Figure 1-6.

1.3 National Ambient Air Quality Standards

Standards for workplace aerosols are not the only health-based environmental regulations. A brief mention of the status of particle size-selective sampling for ambient aerosols is warranted. The US EPA (1984) also chose to rethink its National Ambient Air Quality Standards (NAAQS) for particulate matter during the 1980's. In the 1970's, epidemiological studies began to investigate the link between ambient particulate concentration and human health effects. Comprehensive reviews of the literature are presented by Pope and Dockery (1999) and the US EPA (1996). Recent

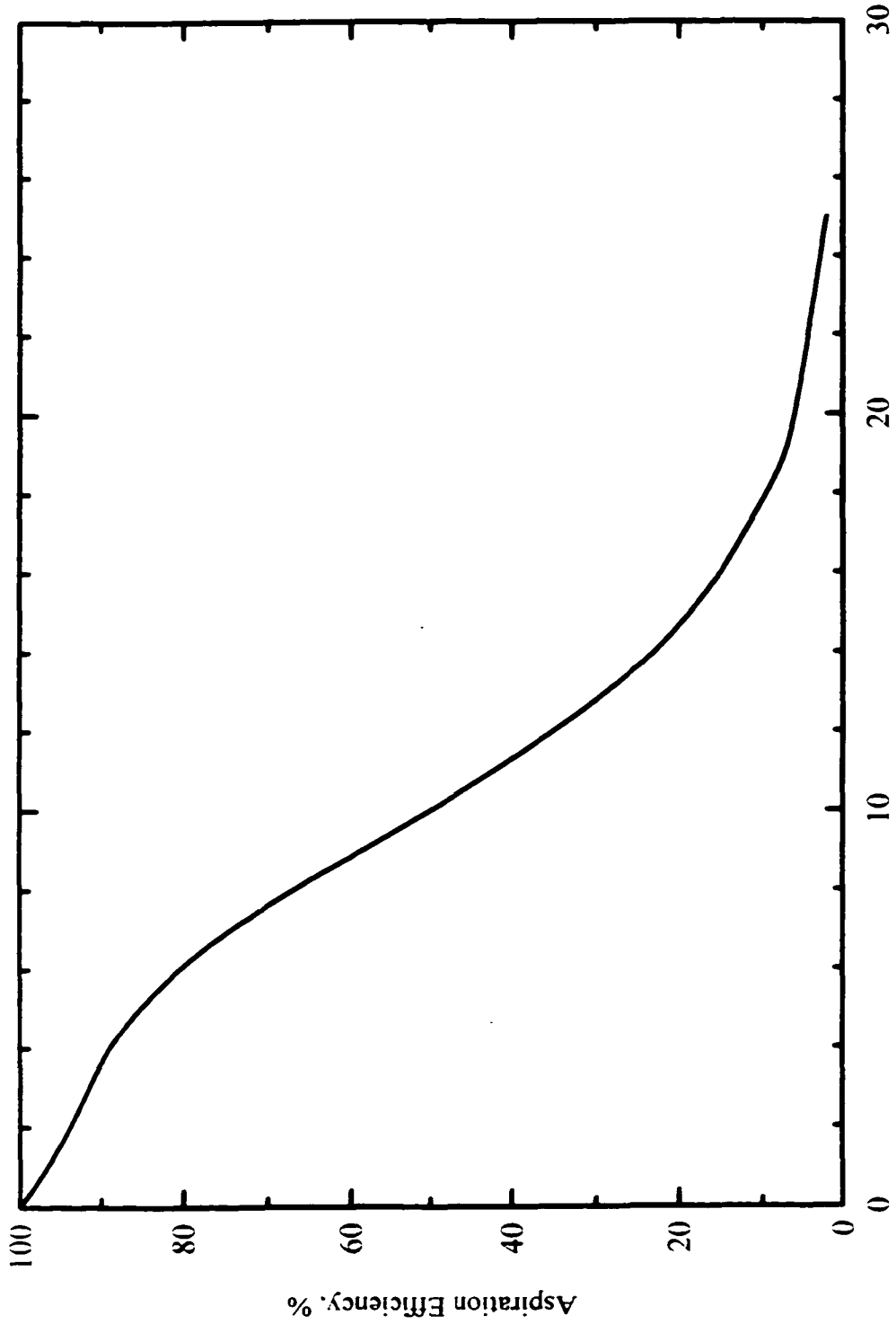

Figure 1-5: Criterion curve for the Thoracic Particulate Mass (TPM) fraction.

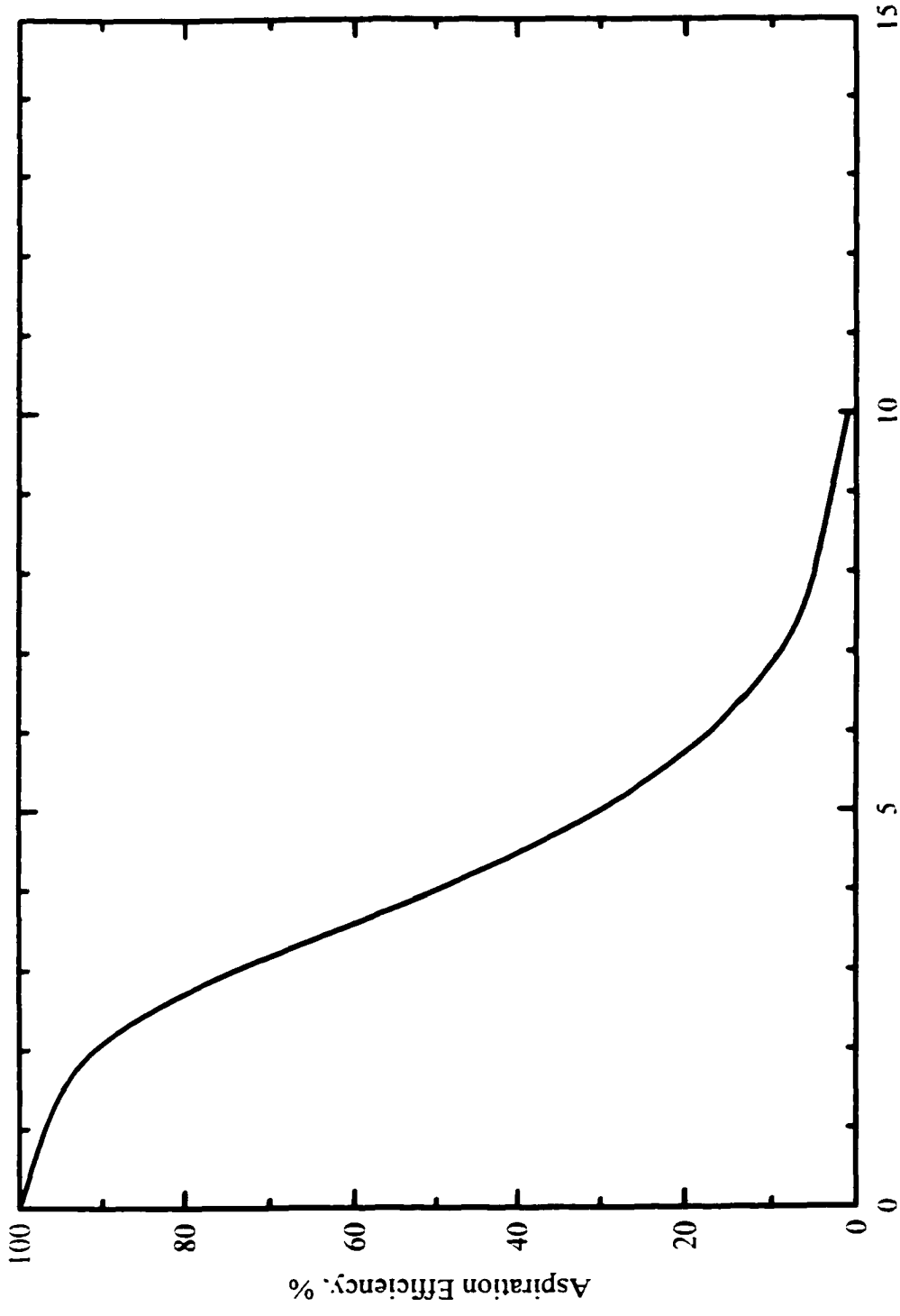

Figure 1-6: Criterion curve for the Respirable Particulate Mass (RPM) fraction.

studies indicate that relatively low increases in particulate pollution are linked with cardiopulmonary disease and early mortality (Dockery *et al.*, 1992, 1993; Pope *et al.*, 1992, 1995). A 1-8% increase in the number of deaths is associated with each increase of 50 $\mu g/m^3$ in ambient PM_{10} (see below) particulate concentration. This represents a major public health concern, because a one percent increase in mortality translates to 10,000 excess deaths in a population of one million.

Prior to 1984, the US EPA specified the measurement of total suspended particulate (TSP) as the index of particulate pollution in ambient air. An important activity of the EPA is the promulgation of ambient air quality standards to protect public health. Scientific recognition of the need for particle size-selective criteria led the EPA to re-examine their own air quality standard for particulate matter (PM). In response, they decided to focus only on those particles capable of penetrating to and beyond the tracheobronchial (TB) region, because these were responsible for diseases associated with particles in the environment. Initially, the EPA dictated a cut-off size of 15 μm, but subsequent review resulted in selection of sampling criteria with a cut size at 10 μm and a steep curve (CFR, 1987). This is referred to as the PM_{10} standard and it is similar to the ACGIH TPM fraction. In the 1990's, attention focused on fine particles, those with an aerodynamic diameter less than 2.5 μm, as an indicator of increased morbidity and mortality (Özkaynak and Thurston, 1987). The US EPA met the concern by adopting size-selective sampling criteria for $PM_{2.5}$ (CFR, 1997).

The $PM_{2.5}$ standard dictates an average annual level of 15 $\mu g/m^3$ and 65 $\mu g/m^3$ for a 24-hour period.

1.4 Public Health Implications

Based on Bureau of Labor Statistics reports (BLS, 1998) there are an estimated three million US workers employed in occupations where exposure to large particles may occur. These include machinists, wood workers, and farm workers. If only ten percent of these workers are exposed at levels that present a health hazard, there is still considerable public health concern. The majority of currently accepted OELs for workplace aerosols are based on "total" dust sampling. These may not be adequate to protect workers exposed to large particles. A number of studies have shown that traditional "total" dust sampling methods fail to collect most large particles greater than 20 μm and, as a result, underestimate their contribution to worker exposure.

It is the stated intention of the ACGIH and other occupational health policy organizations throughout the world to move from the use of OELs based on "total" dust sampling to those based on particle size-selective sampling criteria. The 1999 ACGIH TLVs® and BEIs® booklet contains seven IPM-TLVs® and ten more are listed in the "Notice of Intended Changes". EN 481 (CEN, 1993) and ISO 7708 (ISO, 1995) were adopted by the European community to provide guidelines for particle size-selective workplace aerosol sampling. In general, it has been difficult to

implement the IPM criterion. This is due to limitations of the criterion itself and to the sluggish development and evaluation of personal inhalable samplers (Kenny, 2000).

Figure 1-7 shows a simplified diagram of the ACGIH process involved in developing a TLV®. The information path is similar for both the traditional TLV® and the IPM-TLV®. The only difference being the use of particle size-selective sampling for the exposure assessment data as the basis of the standard. In an ideal situation, the ACGIH TLV® committee uses epidemiological studies that link exposure level with health outcome. The data allow creation of a dose-response relationship, which can be used to determine the exposure level at which nearly all workers may work safely without an adverse health effect. Although the two paths are identical in structure, the temporal distance between them is tremendous. Of the nearly 900 chemicals listed in 1999 ACGIH TLVs® and BEIs®, approximately 200 are aerosols. It has taken fifteen years to develop the seven IPM-TLVs® listed today.

The problem for development of IPM-TLVs® is that there are very few IPM exposure data. The IPM research community has been slow to develop inhalable samplers because it is experimentally difficult to test the devices and issues surrounding definition of the IPM criterion remain unresolved. For example, the importance of wind velocity and breathing pattern has not been fully addressed. Recent studies indicate that wind velocities in most work environments are lower than originally

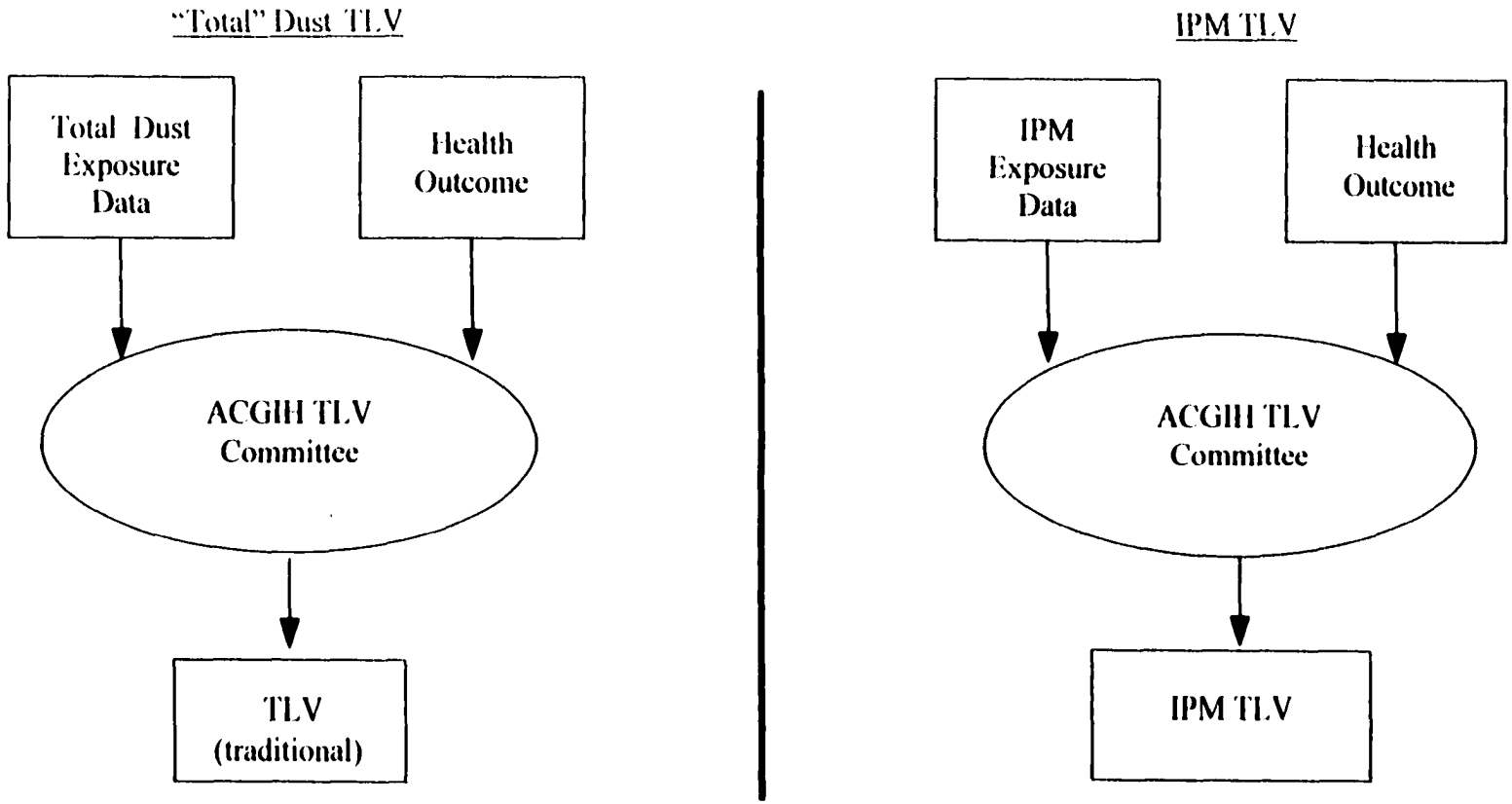

Figure 1-7: Diagram of simplified decision process for aerosol TLV® selection.

reported. Until there is agreement about the parameters that influence inhalability and those factors are sufficiently evaluated, there will be no meaningful development of sampling devices. Without IPM sampling devices, there are no IPM data for development of IPM standards.

Another reason IPM exposure data are limited is that practicing occupational health professionals continue to use traditional sampling methods because their primary goal is regulatory compliance. Well-documented, routine industrial hygiene monitoring can provide a great deal of information about exposures for a given operation, process or industry. Current US Occupational Safety and Health Administration (OSHA) standards dictate the use of "total" dust sampling. Until OSHA requires the use of IPM sampling methods, monitored occupational aerosol exposures will be reported as "total" dust concentrations. Without measurements of workplace IPM exposure levels, the ACGIH TLV® Committee must attempt to convert "total" dust data into IPM data for the purpose of determining a dose-response relationship. Figure 1-8 illustrates the information needed for such a conversion. Four pieces of information are required:

1) what was the size distribution of the sampled particles,
2) what is the inhalable fraction,
3) how does the sampling efficiency of the sampler used compare to that of an IPM sampler, and
4) what is the toxicity associated with deposition of the particles?

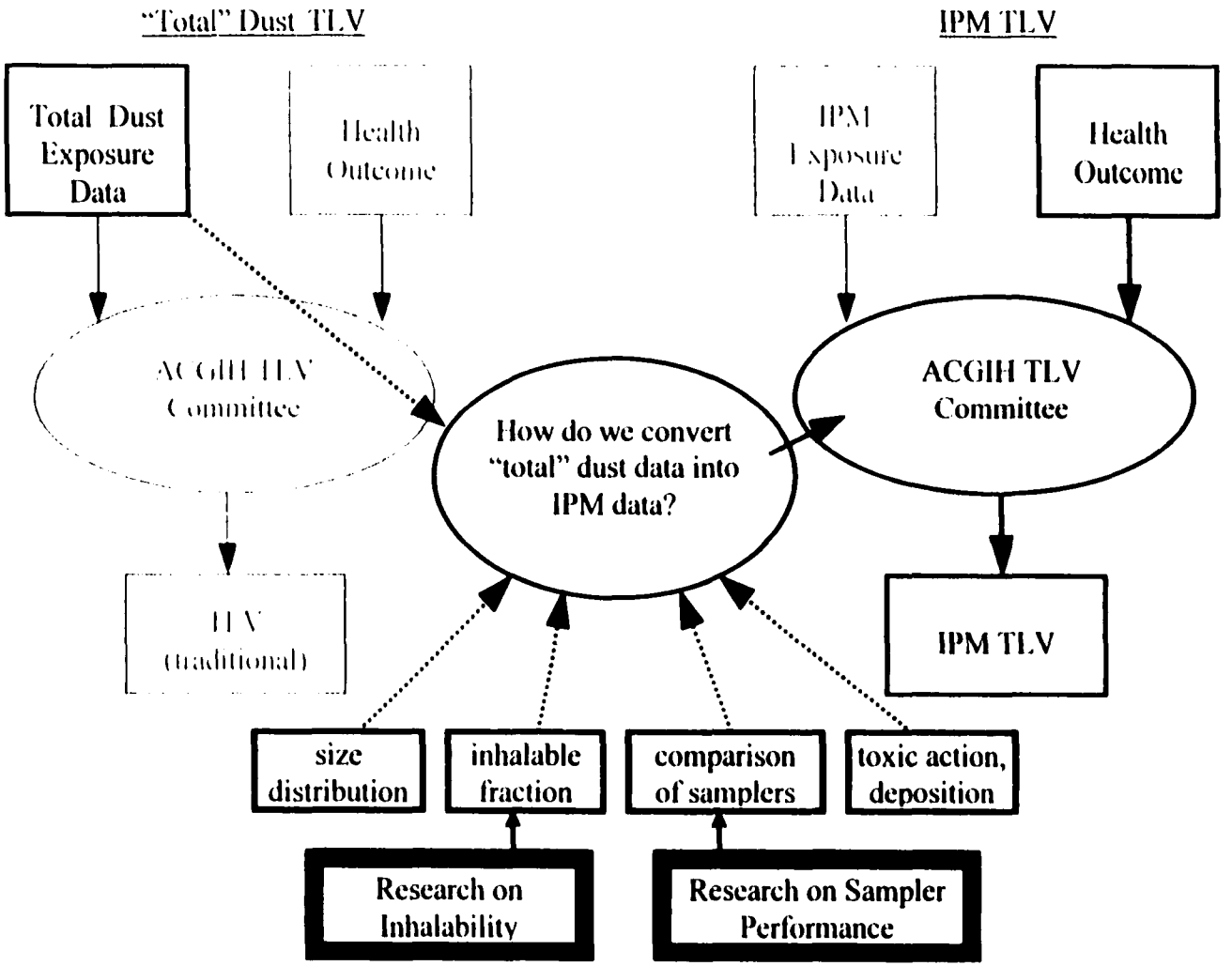

Figure 1-8: Diagram of simplified decision process for converting traditional TLVs® to IPM-TLVs®.

The research presented in this dissertation provides information that refines the definition of inhalable fraction and allows comparison of sampler performance. The inhalability data, coupled with knowledge of particle size distribution, can be used to determine the inhalable fraction. The study of inhalable sampler performance will help define the comparative efficiency, as a function of particle size, of devices for sampling the inhalable fraction. The primary usefulness of this research is in guiding future sampler design and providing conversion data for the establishment of particle size-selective sampling standards.

1.5 Wind Tunnel

Wind tunnels have been used to conduct a wide range of aerodynamics research. They are essential to the study of phenomena that either influence or are influenced by airflow or particle motion. The primary parameters that are considered during the design of a wind tunnel are cross-sectional size, wind velocity, and airflow characteristic. Cross-sectional size is important because blockage in the test section should be limited to minimize distortion of the flow pattern. Vincent (1989) recommends less than 10% blockage of the cross-sectional area, although blockage ratios up to 30% are considered acceptable for large wind tunnels. The range of wind velocities should be typical of those found in field situations. The airflow can be either laminar or turbulent and is defined by the Reynold's number, *Re*, a dimensionless number that characterizes the movement of air and is a ratio of inertial forces to frictional forces.

To study particle motion, it is necessary to maintain a consistent aerosol concentration within the test section of the wind tunnel. Spatial variation, an inability to maintain uniform concentration over the cross-sectional area, and temporal variation, changes in concentration along the length of the wind tunnel, can influence results and must be minimized. A test aerosol is usually delivered to the wind tunnel from a nozzle or mixing chamber that can be large or small compared to the cross-sectional area of the wind tunnel. Studies of inhalability and sampler performance require the use of a full-size mannequin because the flow of air near a sampler or the mouth is affected by the presence of a body (Vincent, 1989). This, in turn, dictates the need for a large wind tunnel cross-section to minimize the distortion of airflow around the mannequin. For a large wind tunnel, the point of aerosol delivery is small compared to the size of the wind tunnel, so a reliable mechanism is required to ensure that aerosol generation and delivery to the test section is consistent and uniform. The construction and maintenance of such a system is difficult and costly. Only a few such research facilities exist. Among these are the apparatus used by Kenny *et al.* (1995) which is 2.5 m × 2.5 m in cross-section, the National Institute for Occupational Safety and Health (NIOSH) wind tunnel that measures 1.22 m × 1.83 m, the 1.5 m × 2.5 m Institute of Occupational Medicine (IOM) wind tunnel (Mark and Vincent, 1986), and the UCLA low-velocity wind tunnel (Hinds and Kuo, 1995).

1.5.1 Alternatives to Large Wind Tunnels

Recent studies have focused on the possibility of using a smaller wind tunnel to conduct evaluations of sampler performance. Two approaches, the use of a simplified mannequin and the use of dimensional scaling, are proposed. Both remove the requirement to use a full-size mannequin, thus eliminating the need for a large wind tunnel. Witschger *et al.* (1998) and Aizenberg *et al.* (2000) have demonstrated that a simplified mannequin can be used to evaluate personal samplers by comparing their results to those obtained using a full-size mannequin. Aizenberg's group found reasonable agreement between the two systems for wind velocities of 0.5 m/s and 2.0 m/s and particle sizes with an aerodynamic diameter up to 70 μm.

Kennedy *et al.* (2000) used a simplified mannequin, like the one described by Witschger *et al.* (1998), to compare the performance of the IOM sampler (Mark and Vincent, 1986) to IOM sampler results for a full-size mannequin obtained during the sampler performance study presented in Chapter 4. They concluded that both mannequins give results that are reasonably close to the IPM sampling criteria for particles with $d_a < 80$ μm and wind velocities in the range of 0.4 m/s to 1.6 m/s. They also noted that for particles larger than 50 μm there were opposing trends in aspiration efficiency with increased wind velocity. Aspiration efficiency is the ratio of the sampled concentration to the true concentration; it is used as a measure of sampler performance. When the IOM sampler was mounted on the full-size

mannequin, the aspiration efficiency decreased with increasing wind velocity. On the simplified mannequin, the aspiration efficiency increased with increased wind velocity. It was proposed that the difference was due to "competition" between inertial projection of the particles and the airflow near the samplers. These are influenced by particle size and wind velocity and can account for the opposition of trends.

Dimensional scaling has also been proposed as a method to allow the use of smaller wind tunnels for personal sampler evaluation. Ramachandran *et al.* (1998) articulate that the use of large wind tunnels is not only difficult and costly, but also contributes to variability in the data related to differences in test systems. They argue that a smaller wind tunnel is easier to operate and reduces the likelihood of temporal and spatial variation in concentration, which, in turn, provides more reliable results. The difficulty with dimensional scaling is that there is no single scaling factor for air and particle motion. It is not a simple reduction. It requires the scaling of airflow and particle motion parameters, dimensional analysis, and the use of models for aspiration efficiency. Until an alternate method for testing personal samplers is fully developed, a large wind tunnel is needed for evaluations of inhalable sampler performance.

1.5.2 UCLA Low-Velocity Wind Tunnel

The UCLA low-velocity, open-ended wind tunnel (Hinds and Kuo, 1995; Kuo, 1993) was used as the test system. The wind tunnel is 4.8 m long and has a cross-section of 1.6 m × 1.6 m which is adequate to accommodate a full-size, full-torso mannequin. From front to back, the wind tunnel comprises a bell-mouth inlet, a screen and honeycomb to remove turbulence, the aerosol delivery manifold, a wooden lattice to introduce controlled turbulence, the test section housing the mannequin and samplers, a Faraday-cup sampler, the filter bank, and the fan. Figure 1-9 is a diagram of the wind tunnel.

The air that enters the wind tunnel is unfiltered room air. The bell-mouth inlet effectively smoothes the flow of air into the wind tunnel and minimizes the *vena contracta* that develops after the air enters the system (ACGIH, 1995). This reduces the static pressure loss associated with pulling air into the wind tunnel. This is the first of many design features that optimize airflow in the system.

At the inlet, there is a single layer of window screen with a 1.3 mm × 1.5-mm mesh followed by a paper honeycomb with 4-mm hexagonal cells and a 64 mm path length (depth). Together they reduce both the axial (direction of airflow) and lateral turbulence of the room air as it enters the wind tunnel.

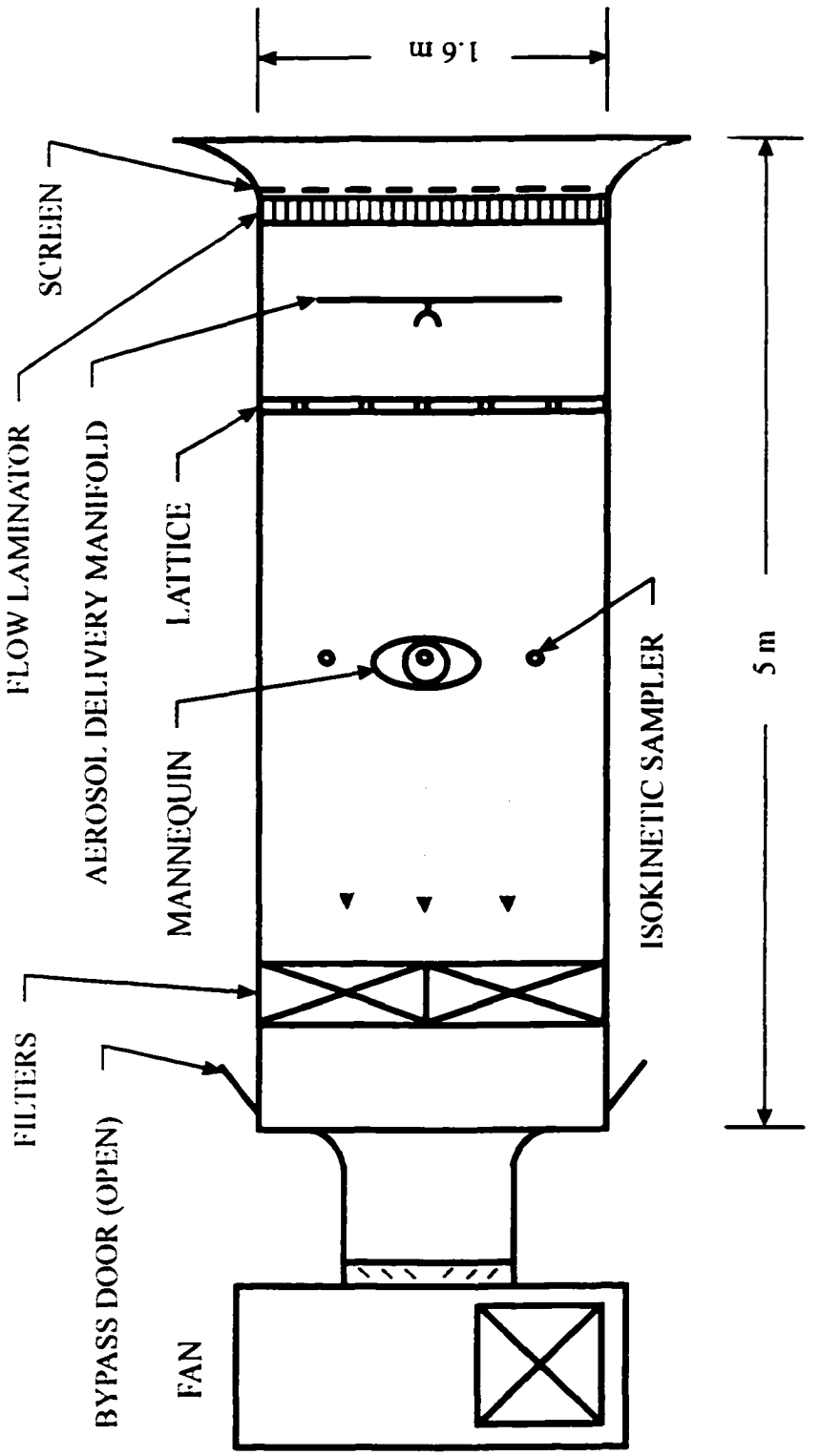

Figure 1-9: Diagram of the UCLA Low Velocity Wind Tunnel.

The aerosol delivery manifold underwent major redesign and retesting to provide a more reliable mechanism than the original unit. The original manifold used six aerosol outlets mounted horizontally and slowly moved up and down. Downstream measurements showed that there were gaps and overlaps in aerosol delivery, resulting in non-uniformity of particle concentration. Additionally, build up of dust inside the ungrounded copper nozzles was noted after a series of runs. Highly charged dust particles became a major concern of this project and are discussed in Chapter 2.

The redesigned manifold uses three nozzles mounted adjacent to each other on a sliding assembly that moves horizontally and vertically. The assembly moves back and forth across the wind tunnel every 6 seconds and travels up and down at 4-10 cm/s. This produces a uniform concentration within ± 15% over the central 1.3 m of the test section. The uniformity of dust concentration was measured using 11 sharp-edged isokinetic samplers placed in line, either vertically or horizontally, in the test section with the mannequin removed. The results are in Figures 1-10(a) and 1-10(b).

Several materials were tested for use as aerosol delivery nozzles, including conductive rubber, steel, stainless steel, aluminum, copper, polyvinyl chloride (PVC), and Tygon®. The interior diameter (ID) for the tubes ranged from 20.6 mm to 25.4 mm. The background current was 0.76 pico amperes (pA)[10^{-12} A]. The

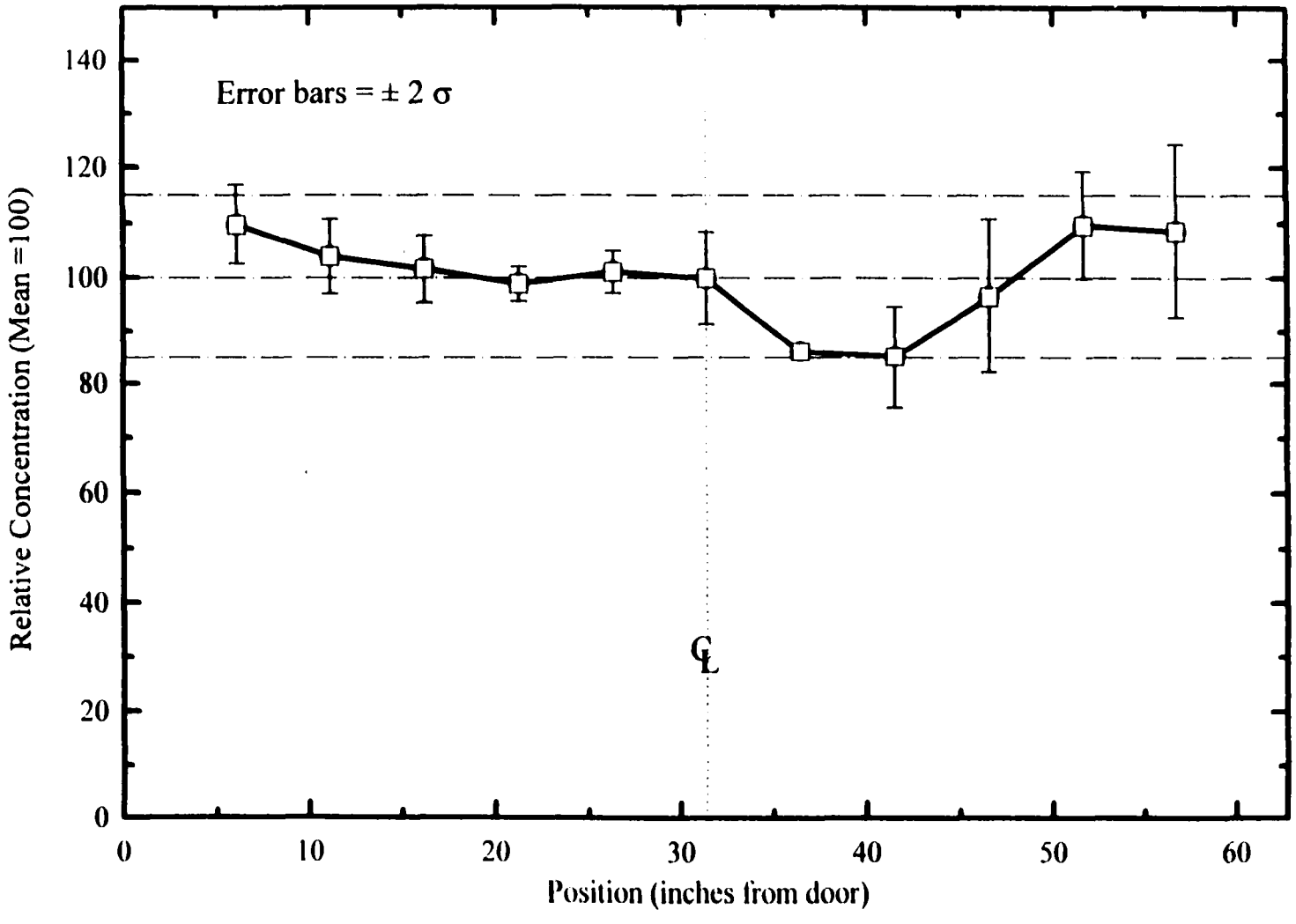

Figure 1-10(a): Horizontal concentration profile in wind tunnel test section.

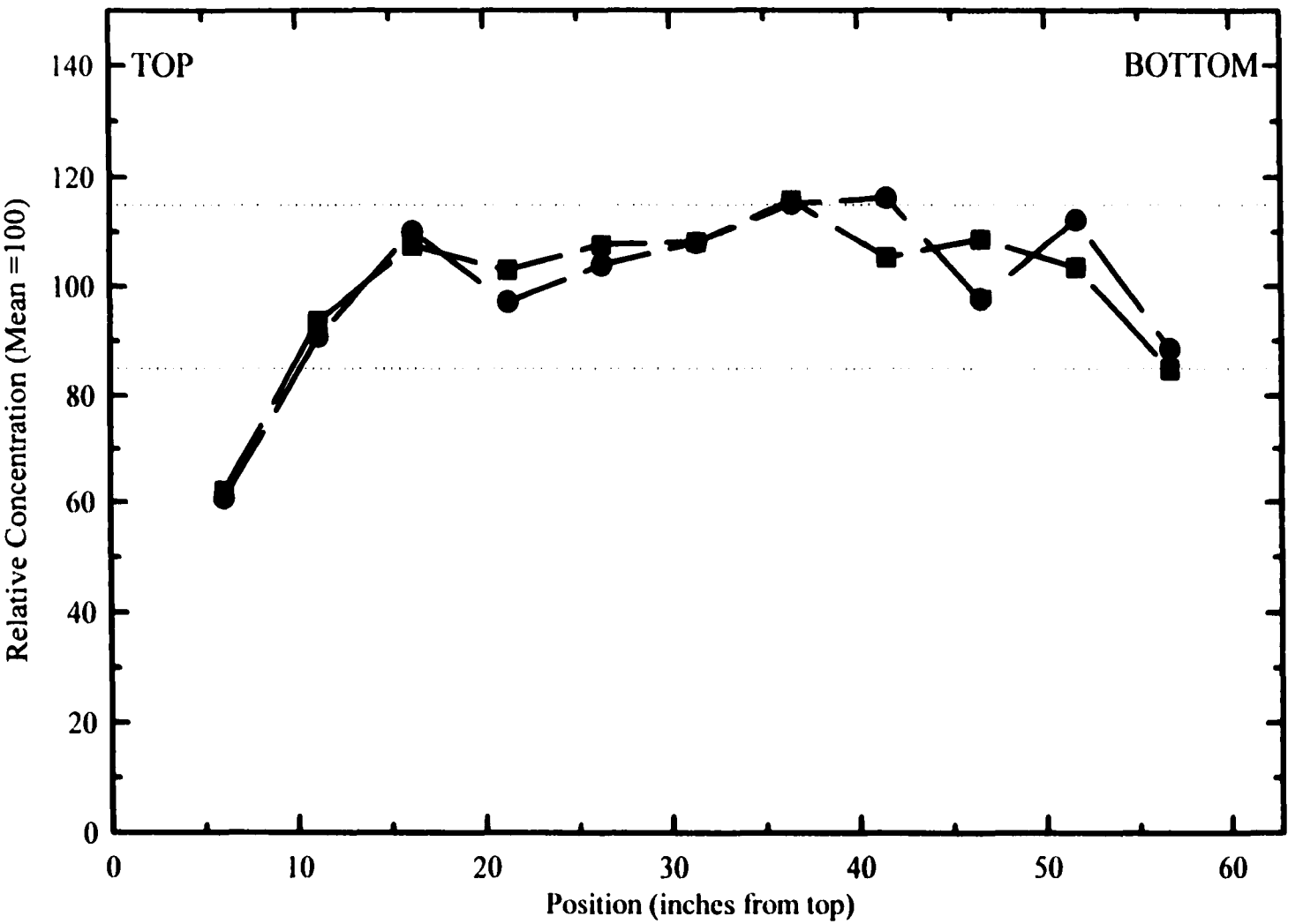

Figure 1-10(b): Vertical concentration profile of wind tunnel test section.

different nozzle materials were evaluated by monitoring the amount of charge carried by particles exiting the nozzle. Charge was measured as current and was adjusted for aerosol generation rate and tube size, because both factors can affect the build up of charge. The particle charge level was lowest for aerosol delivered through a copper nozzle. Table 1-1 shows the results.

Table 1-1: Materials Tested for Dust Delivery Tubes

Material	Tube ID, mm	Measured Current, pA
Conductive rubber	22.2	456.2
Steel	20.6	431.1
Stainless steel	22.2	403.9
Aluminum	20.6	279.1
Copper	**23.0**	**215.1**
PVC	20.6	435.6
Tygon®	25.4	380.0

The test dust, dispersed using three National Bureau of Standards (NBS) dust feeders (Dill, 1938) mounted on top of the wind tunnel, is carried to the three copper delivery nozzles through 18-mm ID conductive rubber tubes. The nozzles are grounded, as is the interior of the wind tunnel. All metal parts and fittings were grounded and all contact surfaces, including the floor and mannequin, were painted with conductive paint (EMI/RFI Shield Coating, distributed by McMaster-Carr, Santa Fe Springs, CA) to facilitate the removal of charge. Copper strips were adhered to the wind tunnel floor to provide a conductive path to ground.

The wood lattice located downstream of the aerosol delivery manifold serves to introduce controlled turbulence that aids the mixing of the aerosol to produce uniform concentration in the test section. The lattice is a square grid made of 1-inch square bars spaced 5 inches apart. The homogenous turbulence that is generated by the lattice is a turbulent field that decays as it moves away from the source of the turbulence (Baines and Peterson, 1951). The turbulence becomes homogenous within 10 bar sizes, or 0.25 m (10 inches), downstream of the lattice (Kuo, 1993).

When facing the wind, the mannequin has a projected area that is about 11% of the cross-sectional area (Hinds and Kuo, 1995). When positioned at 90° to the wind the mannequin blocks about 4% of the area. During the course of a sample run, as the mannequin rotates, the blockage varies from 4 - 11%. This is close to the 10% recommended for wind tunnel studies (Vincent, 1989).

Another necessary redesign was improvement of the mechanism for rotating the mannequin. The original set up used a fixed clevis mounted inside the center of the mannequin head. This was attached to a steel rod that extended through the top of the head and was connected to a drive shaft powered by a reversible gear motor located on top of the wind tunnel. It was necessary to manually reverse the direction of rotation, by stopping the motor and flipping a toggle switch, after each complete rotation to prevent kinks in the sampling hoses. In addition to operational awkwardness, the design presented a problem because there was play in the

connection between the drive shaft and the steel rod extended from the mannequin head. This caused the mannequin to rotate in a series of small jerks as the required torque built up and was lost.

The current design has the mannequin mounted on ball bearings and rotated by a Slo-Syn PT-230 stepping motor (Superior Electric Company, Bristol, CT) that is computer-controlled. The computer program, written by William Hinds, allows selection of sampling duration and automatically returns the mannequin to the start position at the end of each run, eliminating worry about kinks in the "breathing" hoses.

A Faraday-cup isokinetic sampler is located at the rear of the test section, just before the filter bank. It is used in conjunction with a Keithley Model 6512 electrometer, located outside the wind tunnel, to monitor the charge on the particles in the test aerosol. Particle charge was an issue during these investigations and its measurement, control and monitoring are discussed in Chapter 2.

The filter bank consists of four HEPA (high efficiency particulate air) filters stacked two high by two wide and a single layer of fiberglass prefilter. Each filter unit is 0.75 m on a side. HEPA filters remove 99.97% of particles with an aerodynamic diameter of 0.3 μm and are more efficient for particles of other sizes. They are often used in systems which require recirculation of air (Burgess *et al.*, 1989), as is the

case with the UCLA wind tunnel. Pressure drop across the filter bank is monitored using an inclined manometer mounted on the exterior of the wind tunnel. As the filter becomes loaded with dust, the efficiency increases, but the resistance also increases which results in a loss of ability to achieve the highest wind velocities. The fan that drives the wind tunnel is an 11,000 ft^3/min backward-curved air-foil fan (Chicago Blower Corp., Glendale Heights, IL, size 27) with a 7.5 horsepower electric motor. A radial seven-vane control damper allows adjustment of airflow down to 5% of maximum. The wind tunnel is capable of wind velocities in the range of 0.2 - 2.0 m/s. Lower wind velocities can be achieved by opening the bypass doors located downstream of the filter bank. The exhausted air is recirculated back into the room through a muffler designed to reduce both noise and room air turbulence.

The UCLA Low-Velocity Wind Tunnel was designed for studies of particle inhalability and sampler performance. It meets the requirements outlined by the CEN (1993) for such test systems.

Chapter 2: An Ion Generator for Neutralizing Concentrated Aerosols

The information in this chapter was published in the peer-reviewed journal *Aerosol Science and Technology* (Hinds and Kennedy, 2000).

2.0 Introduction

As mentioned in the description of the wind tunnel, preliminary work indicated that the test dust contained charged particles. Highly charged particles present a problem for aerosol sampling because electrostatic attraction can influence the motion of the particles and affect the results. It was necessary to effectively neutralize the charge. To do this, several things had to be accomplished, including:

1. minimize potential for build up of charge,
2. develop method for measuring charge on the particles,
3. determine amount of charge carried by particles,
4. provide enough ions for neutralization, and
5. evaluate effectiveness of neutralization.

2.1 Background

Previous studies conducted using the UCLA low-velocity wind tunnel (Kuo, 1993) approached the problem of particle charge by humidifying both the room air (to a

minimum of 50% RH) and the dispersion air used to carry the particles into the wind tunnel (to 65% RH). High humidity provides a surface layer of water molecules that allow charge to bleed away. This was thought adequate to prevent the build up of static charge. In addition, it is a reasonable assumption that large particles, because of their mass, are less likely to be influenced by a small amount of charge than by their inertia or gravitational force.

In general, solid particles acquire charge by static electrification or by collision with bipolar ions (Hinds, 1999). As the test dust bumps and scrapes along the various metal, plastic and rubber pieces used to suspend and transport the aerosol into the wind tunnel, there is plenty of opportunity for acquisition of charge. There are two basic approaches to minimizing the charge on particles. The first is to prevent build up of charge by the careful selection of materials, reduction of contact with surfaces, and humidification of the air. The second is to neutralize charged particles by providing contact with a surface or ions of the opposite sign. A common neutralization method is to mix the charged particles with high concentrations of bipolar ions, usually generated by a radioactive source, such as, polonium^{210} or krypton^{85} or by corona discharge (Liu and Pui, 1974; Yeh, 1993; Hinds, 1999; Cooper and Reist, 1973; Zamorini and Ottobori, 1978; Adachi *et al.*, 1993; Romay *et al.*, 1994).

The smallest amount of charge possible on an aerosol particle is zero, however, this is rarely the case because of random charging from ions that exist in ambient air. The concentration of bipolar ions in air is approximately 10^9 ions/m^3 (Hinds, 1999). In the free atmosphere, an uncharged particle will gain charge by random collision with ions in the air (Yeh, 1993). A particle with excess charge will lose charge by the same mechanism. The desired endpoint for neutralization of particles is to bring the level of charge to the Boltzmann equilibrium charge distribution. This is a steady-state condition resulting from competition between neutralization and the acquisition of charge from the ions in the air. The fraction of particles of a given size carrying n charges, f_n, is expressed as (Hinds, 1999):

$$f_n = \left(\frac{K_E e^2}{\pi d_p kT}\right)^{\frac{1}{2}} \exp\left(\frac{-K_E n^2 e^2}{d_p kT}\right) \qquad (2.1)$$

where K_E is a constant of proportionality, 9×10^9 N·m^2/C^2,

e is the charge on an electron, 1.60×10^{-19} C,

d_p is particle diameter,

k is boltzmann's constant, 1.38×10^{-23} N·m/K, and

T is absolute temperature.

Equation 2.1 is valid for d_p larger than 0.05 μm. At Boltzmann's equilibrium, the amount of charge on the particle is minimal and not likely to result in sampling

artifacts. For a 30-μm particle, the average number of charges, n_{avg}, at Boltzmann's equilibrium is 12.9 when calculated using

$$n_{avg} \approx 2.37\sqrt{d_p} \tag{2.2}$$

where d_p is in μm (Hinds, 1999).

When particles are highly charged or time available for neutralization (residence time) is short, a high concentration of bipolar ions is required. The maintenance of a high concentration of bipolar ions is not easy because ions of opposite sign can recombine at a rate nearly equal to their rate of generation. The rate of neutralization is dependent on the product of ion concentration, N_i, and residence time, t. In general, a value for $N_i t$ greater than 6×10^{12} ion·s/m^3 is needed for full neutralization of highly charged particles (Hinds, 1999). N_i depends on the strength of the ion source and t depends on flow rate.

2.2 Experimental

Because particle charge could influence the results of the inhalability and sampler performance studies, every effort was made to ensure that the wind tunnel and its components were conductive. The aerosol dispersion air was humidified, all metal fittings were grounded, all contact surfaces were painted with conductive paint and copper strips were adhered to the floor of the wind tunnel and grounded. The aerosol streams from the NBS (National Bureau of Standards) dust feeders (Dill, 1938) were

conveyed through conductive 18-mm ID (25-mm OD), carbon-filled EPDM (ethylene propylene dimonomer) rubber tubing (Technical Specialties Company, Inc., Odessa, FL) to the 23-mm ID copper delivery nozzles. Using an extrapolation of data for coal, mica, and silica (Johnston *et al.*, 1986) the process of aerosolization, using NBS dust feeders, is not expected to contribute an excessive amount of charge to the particles. The anticipated charge on a 30-μm particle, after aerosolization, is approximately 10,000 charges. At this charge level, the motion of the particles is affected much more by gravitational force than by electrostatic force. The settling velocity of the particle is 10^6 greater than the velocity due to electrical mobility, assuming a field strength of 1 V/m.

Aluminum oxide (Al_2O_3) optical abrasive powder (General Abrasives/Treibacher, Inc., Niagara Falls, NY) with a mass median physical diameter of 30 μm (MMAD = 52 μm) was selected for evaluating particle charge. The density of the bulk material is 3960 kg/m^3, which means that a 30-μm particle has a mass of 5.6×10^{-11} kg. Al_2O_3 presents a particular problem, when concerned with particle charge, because the material has an extremely high electrical resistivity, 10^{14} Ω· m (CRC, 1983). This is so high that a charged 30-μm particle would require hours of contact with a grounded surface for the charge to bleed through the particle.

The charge on the particles was measured using a Faraday-cup isokinetic sampler (Figure 2-1) connected to an electrometer. A 47-mm stainless steel filter holder

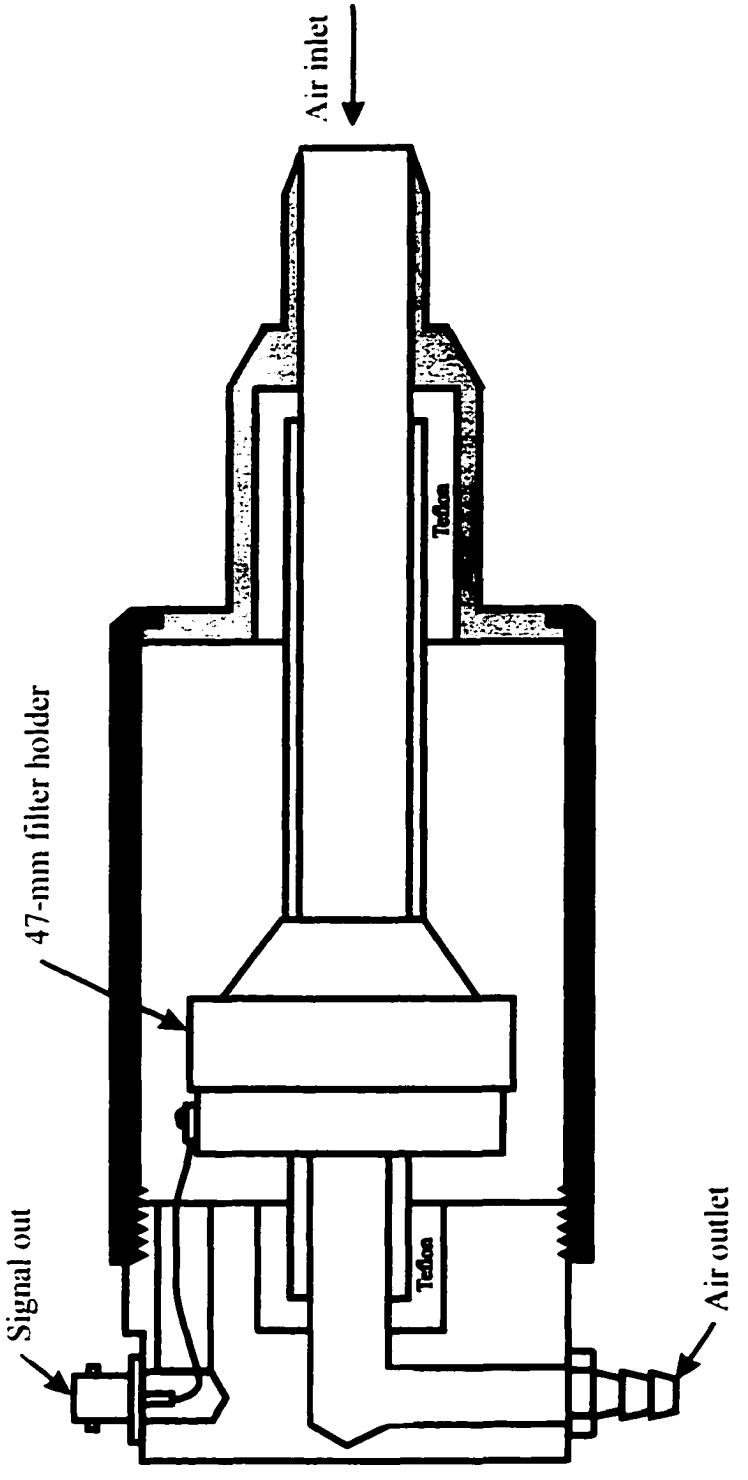

Figure 2-1: Diagram of the Faraday-cup isokinetic sampler.

served as the Faraday-cup, an insulated receptacle for the capture of charge. The cup is insulated with a Teflon® ring and housed in a 90-mm stainless steel cylinder with a 21-mm sharp-edged inlet. The design is similar to that given by John (1980). A sampling flow rate of 20.8 L/min is required to meet isokinetic conditions when the wind velocity is 1.0 m/s. Particles were collected on 47-mm glass-fiber filters cut from Whatman EPM 2000 filter paper sheets (Whatman International Ltd., Maidstone, England). The Faraday-cup isokinetic sampler was placed 2 m directly downstream of the aerosol stream during sampling. This was done to optimize sample collection and determine the maximum ion concentration for the aerosol.

The Faraday-cup isokinetic sampler is connected, using a shielded cable, to a Keithley Model 6512 electrometer (Keithley Instruments, Cleveland, OH) capable of resolution to 0.1 femto amperes (fA)[10^{-15} A]. The instrument is autoranging and can store up to 100 data points. Figure 2-2 shows the Faraday-cup isokinetic sampler and the electrometer. The charge collected on the filter is measured as current. A measurement was taken every 10 seconds and the accumulated charge was calculated. By differencing subsequent measurements, the amount of charge arriving in the Faraday-cup for each interval was determined. The system was stable and reliable. The charge carried by the 30-μm particles was found to be 240,000 positive charges per particle.

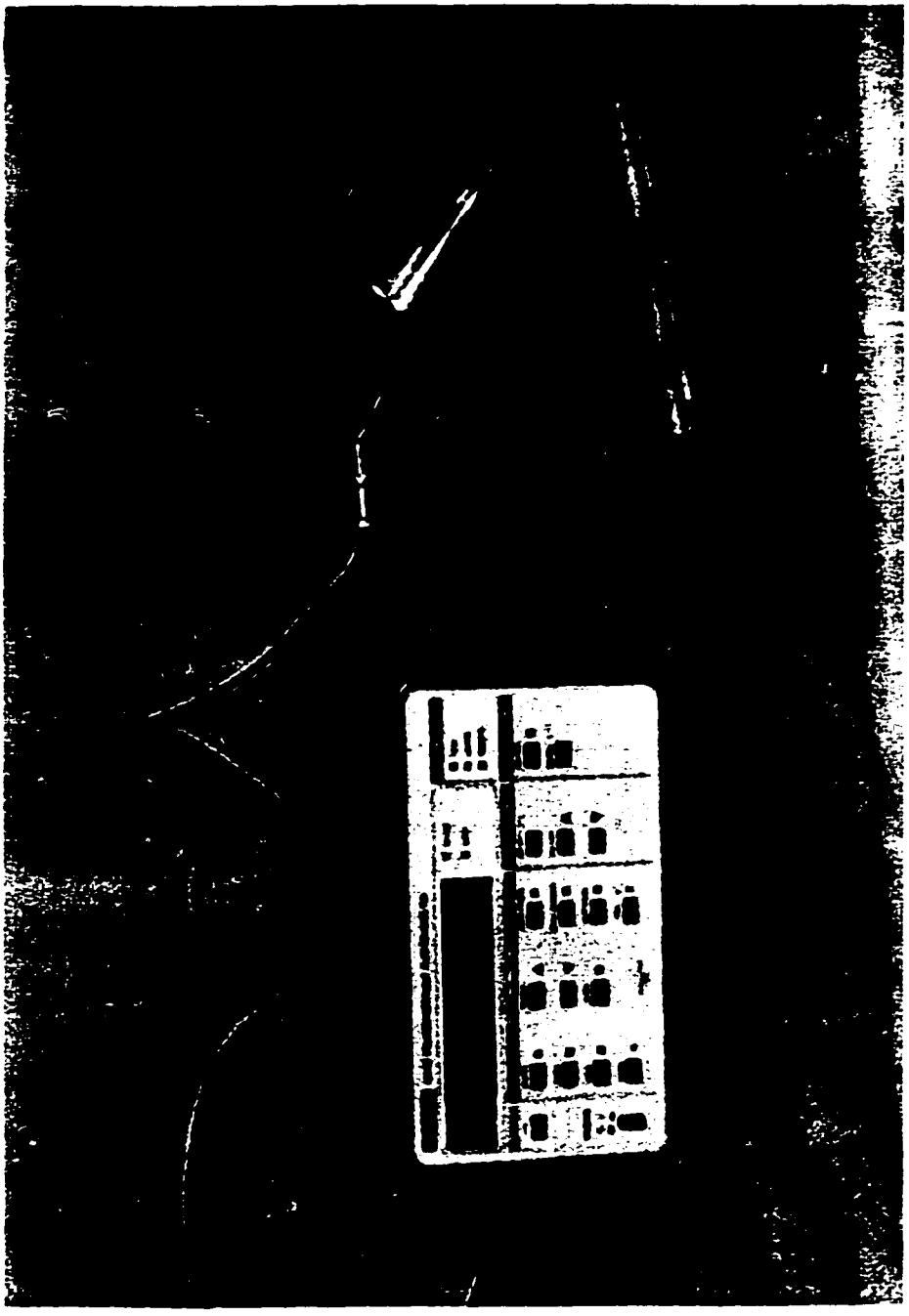

Figure 2-2: Photograph of (a) the electrometer and (b) the Faraday-cup isokinetic sampler.

At an output concentration of $1.05 \times 10^9/m^3$ and delivery flow rate of 160 L/min, 6.6×10^{11} negatives charges per second (0.11 μA) are required to neutralize the aerosol in each of three streams. This corresponds to a negative ion concentration of $2.5 \times 10^{14}/m^3$. To discharge the aerosol using bipolar ions requires an excess of bipolar ions; at least ten times the required negative ion concentration, or $2.5 \times 10^{15}/m^3$.

Po^{210} and Kr^{85} generate bipolar ions by radioactive decay. A commonly used aerosol neutralizer, the TSI Model 3054, contains a 10-mCi Kr^{85} source sealed in a stainless steel cylinder that is 0.5 m long. At a flow rate of 150 L/min, the residence time inside the device is nearly 2 seconds and the ion concentration is approximately $8.8 \times 10^{12}/m^3$ (Teague *et al.*, 1978). Not only is this insufficient to meet the ion concentration requirement, but the geometry of the device prohibits its for large particles.

It was necessary to develop an ion generator capable of providing enough negative ions to neutralize the charged aerosol. This led to the design of a five-electrode, flow-through ion generator (Figure 2-3). The body of the ion generator is constructed from standard sizes (21-mm and 32-mm) of PVC (polyvinyl chloride) pipe available at hardware stores. The peripheral electrodes are made of tungsten wire with a diameter of 0.5 mm. The diameter of the central electrode, which is positioned axially, is 2 mm. For each of the three aerosol streams, one of these devices is placed just downstream of the NBS dust feeder. The electrodes were

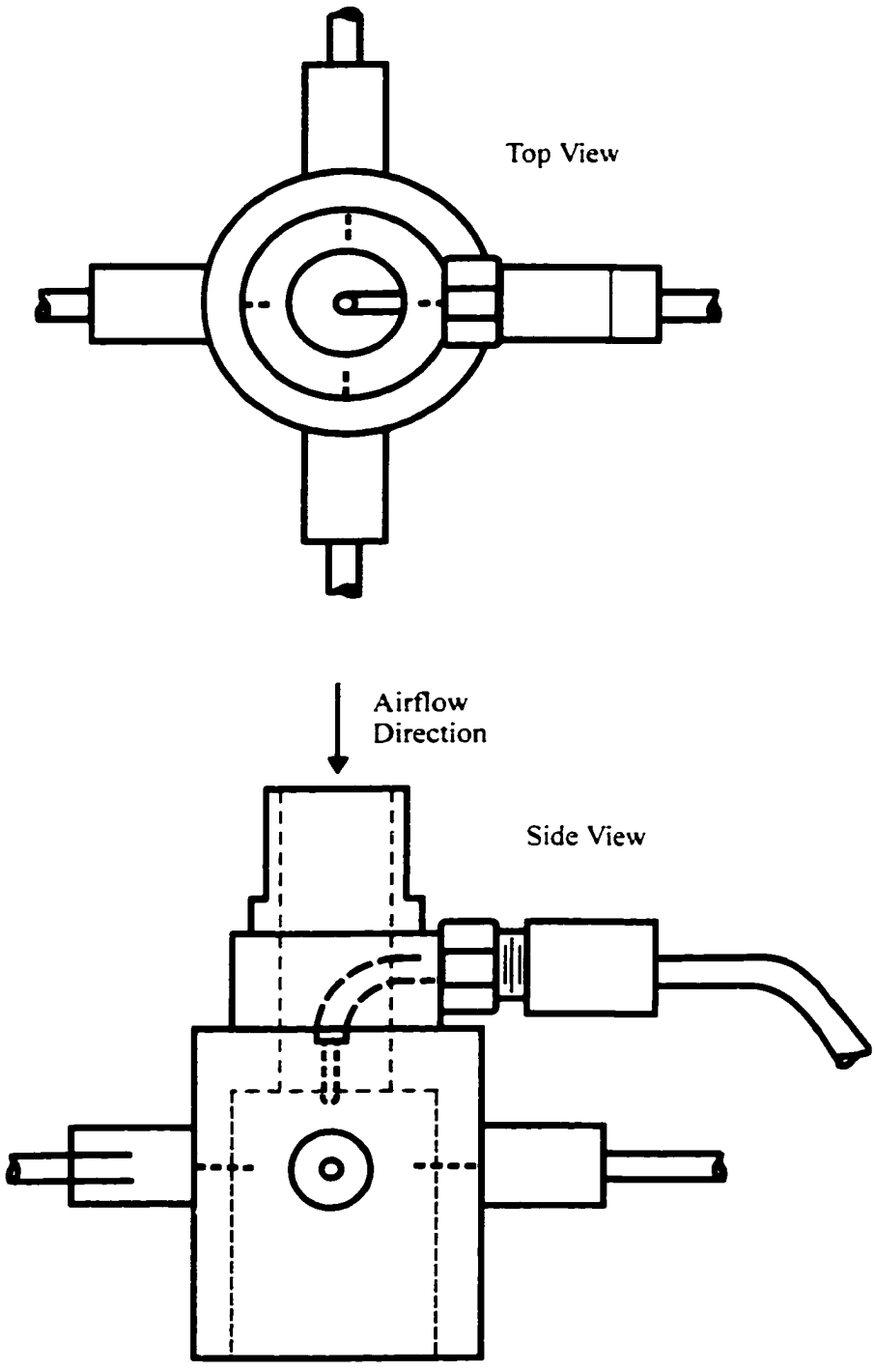

Figure 2-3: Diagram of the Ion Generator.

connected to the power supply with high voltage wire and high voltage connectors. The power supply is used to establish an electric field between the center electrode (positive) and those on the periphery. The polarity of the electrodes can be reversed, if necessary, to accommodate changes in net charge on the particles. The electric field produces a negative corona at the four peripheral electrodes, which generates many more negative ions than positive ions. The ions are located at the edge of the aerosol stream, as it flows axially through the device, where they quickly contact the charged particles.

Adjusting the voltage of the power supply controls the number of ions produced. The instrument must be adequate to power all three ion generators. The power supply chosen was a Richmond Model AB-250 (Richmond Static Control Services, Palm Springs, CA). It allows precise voltage control up to ± 8.5 kV with a maximum current of 150 μA.

2.3 Results and Discussion

At the start of each run, background levels of particle charge were measured. Then, the output voltage from the power supply was adjusted to minimize the current measured by the Faraday-cup isokinetic sampler. The ion generator is capable of reducing the charge to about one percent of the original charge. Figure 2-4 shows the average results for a series of runs. The resulting charge on a 30-μm particle is approximately 2,400 charges/particle. This is much higher than the Boltzmann's

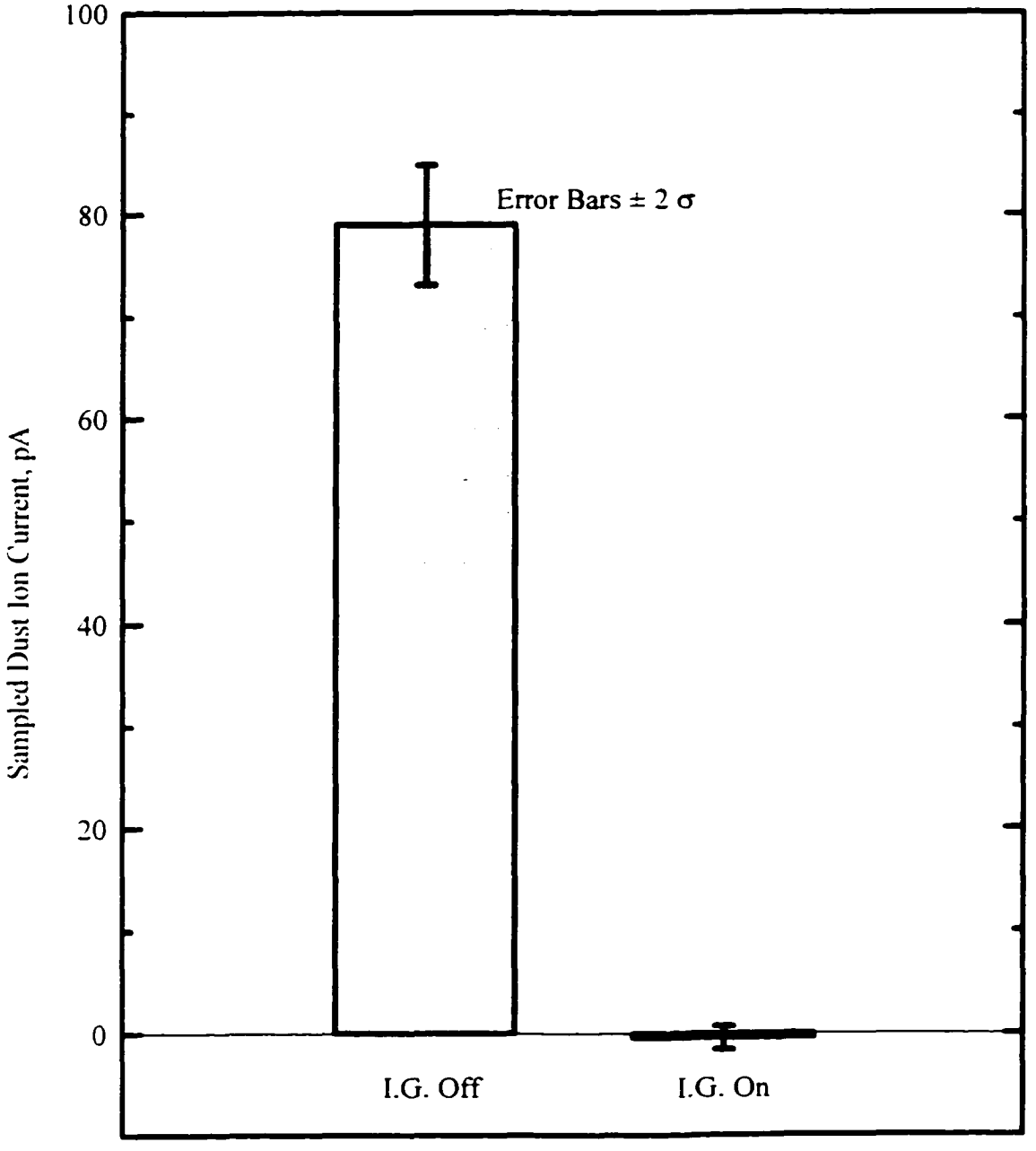

Figure 2-4: Charge reduction for 30-μm aluminum oxide particles.

equilibrium charge of 13 charges/particle, but still low enough to prevent errors in the evaluation of inhalability or sampler performance associated with electrostatic charge (Johnston *et al.*, 1986).

The ion generator was tested for stability by adjusting it to minimize ion current and then allowing continuous operation, without further adjustment, for one hour. The results are shown in Figures 2-5(a) and 2-5(b). With the ion generator on, 95% of the measurements of ion current are within 1.6 pA of zero, which is ± 2% of the ion current measured when the ion generator is off. Occasionally, there is an arc between the axial electrode and one of the peripheral electrodes. When this occurs, there is a momentary shift in the charge condition of the aerosol that returns to normal in a few seconds. The ion generator was found to be stable for long periods of time, however, dust builds up on the electrodes and must be removed occasionally. This was accomplished by increasing the airflow through the ion generator and simultaneously tapping the exterior body of the ion generator. The power supply is shut off during this procedure.

2.4 Conclusion

Unneutralized 30-μm aluminum oxide particles were found to carry ± 240,000 charges. In order to minimize the effect of charge on inhalability measurements, it was necessary to neutralize the particles. The ion generator described in this study provides adequate and stable reduction of charge carried by aluminum oxide particles

to approximately 1% of their initial charge amount. At the reduced charge level, the sampling effects due to electrostatic charge are negligible. The Faraday-cup isokinetic sampler and electrometer provide an accurate and simple method for monitoring the charge on the particles.

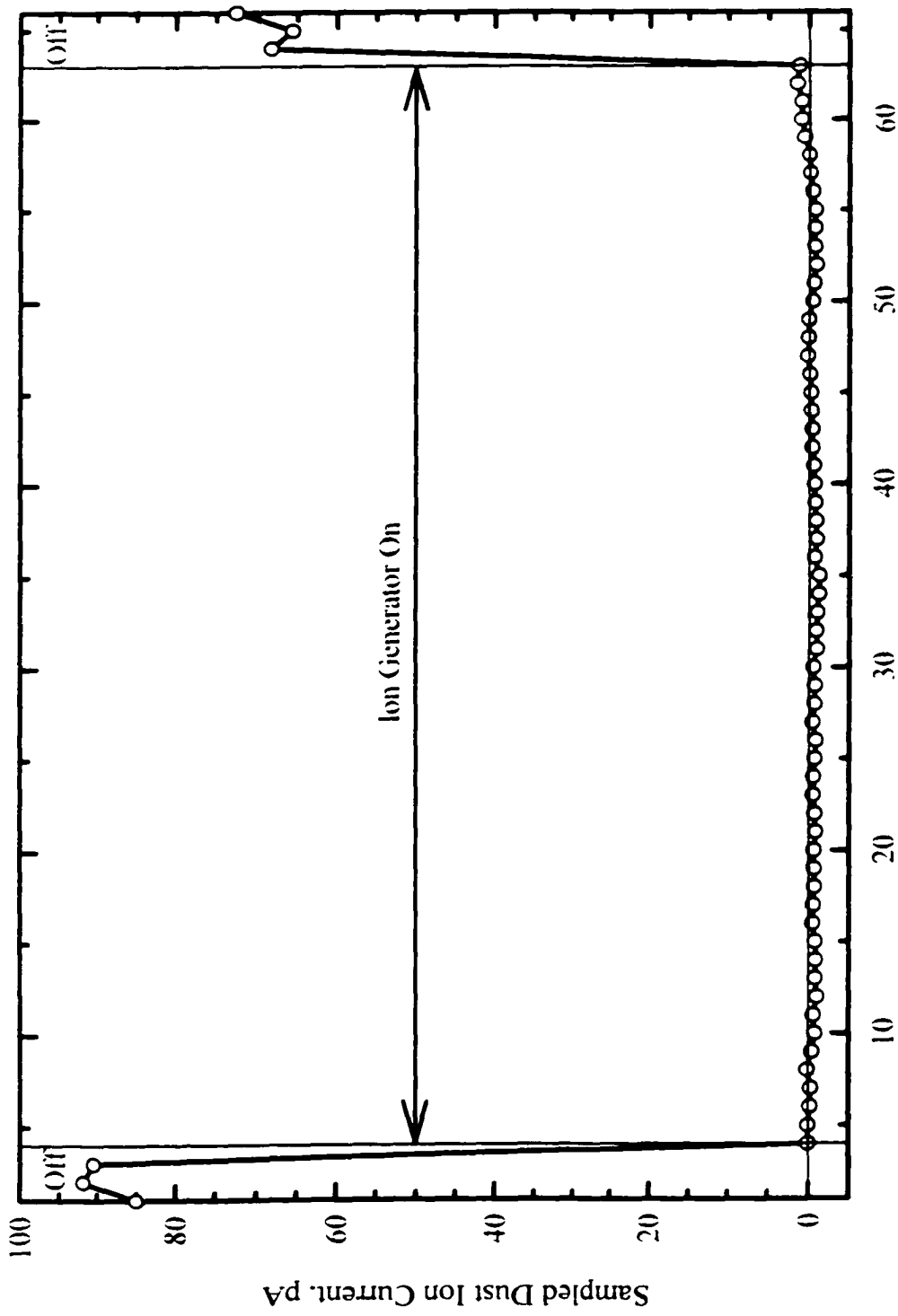

Figure 2-5(a): Charge reduction over a one-hour period.

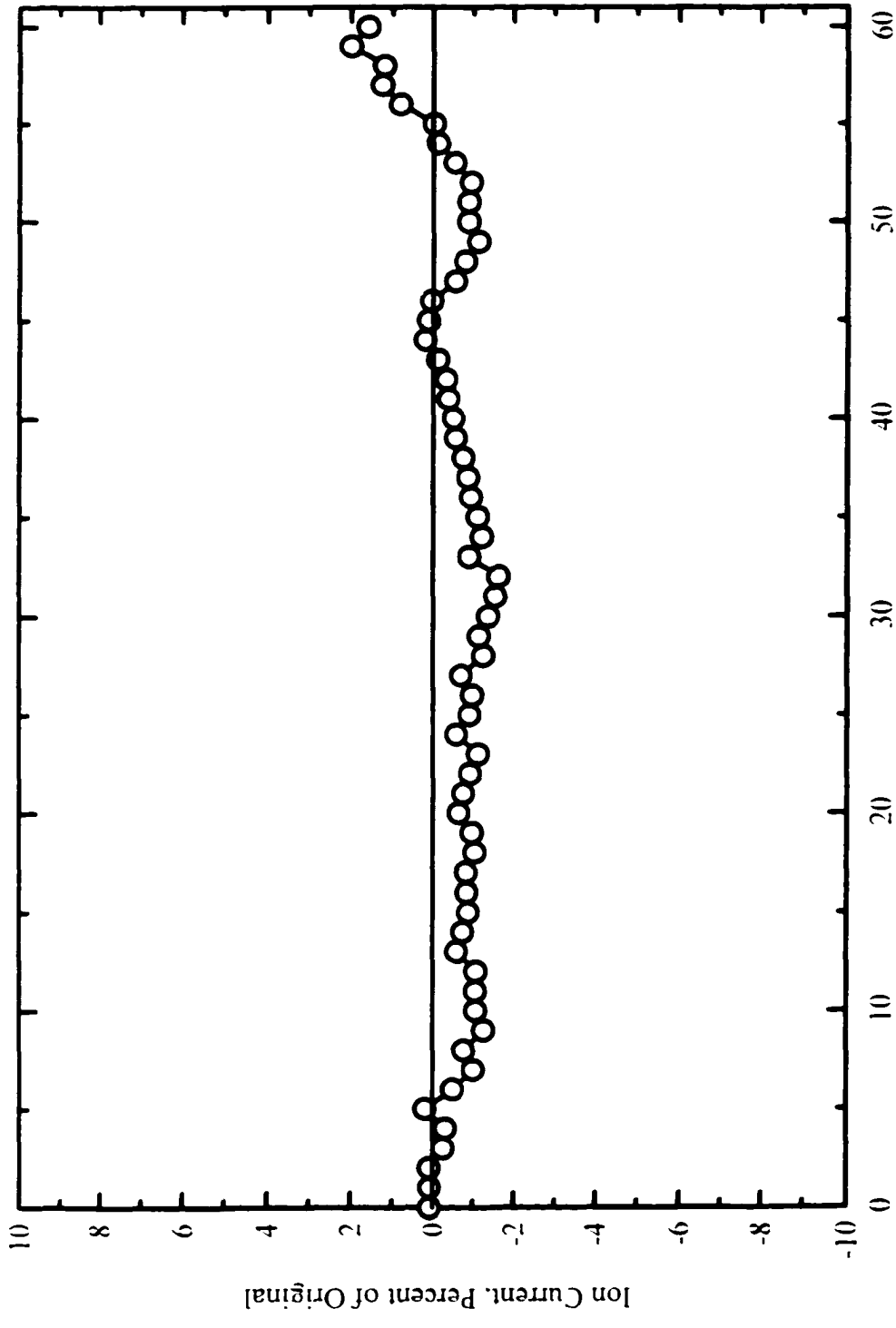

Figure 2-5(b): Stability of charge reduction over a one-hour period.

Chapter 3: Inhalability of Large Solid Particles

3.0 Introduction

The traditional approach to evaluation of worker exposure to hazardous particulate air contaminants has been the measurement of either the "total" dust exposure or the exposure to small particles (d_a < 10 μm) which can reach the alveolar region of the lungs. Recognition that health-based OELs should require sampling methods that collect the relevant or toxicologically important particles has lead to the development of particle size-selective sampling criteria for aerosols. The ACGIH (1985), CEN (1993) and ISO (1995) have defined three progressively finer size fractions for airborne particles, based on where the particles deposit in the lungs.

The inhalable particulate mass (IPM) fraction contains particles that can be inhaled, either through the nose or mouth. This fraction includes the largest aerosol particles, which have an aerodynamic diameter larger than 10 μm and generally deposit in the head airways. The thoracic particulate mass (TPM) fraction defines particles capable of penetrating past the larynx. TPM particles deposit in the ciliated lung airways where they can be cleared by mucociliary transport. The smallest mass fraction is the respirable particulate mass (RPM) fraction that contains particles capable of reaching the gas exchange region of the lungs. Clearance of RPM particles is largely

a function of their chemical and physical characteristics. Figure 3-1 presents the criteria for the three particle size-selective criteria.

When looking at the three curves in Figure 3-1, one feature immediately distinguishes the IPM curve from the TPM and RPM curves. The TPM and RPM curves drop to zero percent penetration at some point, while the tail of the IPM curve abruptly ends at about 50% penetration for 100-μm particles. The inclusion of an inhaled particle in either the TPM or RPM is related to its ability to penetrate past the head airways to either the tracheobronchial region (TBR) or the gas exchange region (GER) of the lung, respectively. Particles included in the TPM and RPM are influenced by deposition mechanisms in the previous airway sections, while particles in the IPM are governed by sampling mechanisms. This means that the inhalability of a particle is not only related to its size, but to external environmental factors that influence particle motion.

The IPM criterion curve is defined by the equation

$$IF(d_a) = 0.5\left(1 + \exp(-0.06d_a)\right) \qquad (3.1)$$

where $IF(d_a)$ is the inhalable fraction and d_a is the aerodynamic diameter in μm. The IPM criterion is limited to wind velocities below 4 m/s and particles smaller than 100 μm. Certainly, particles larger than 100 μm can be inhaled, but the maximum size

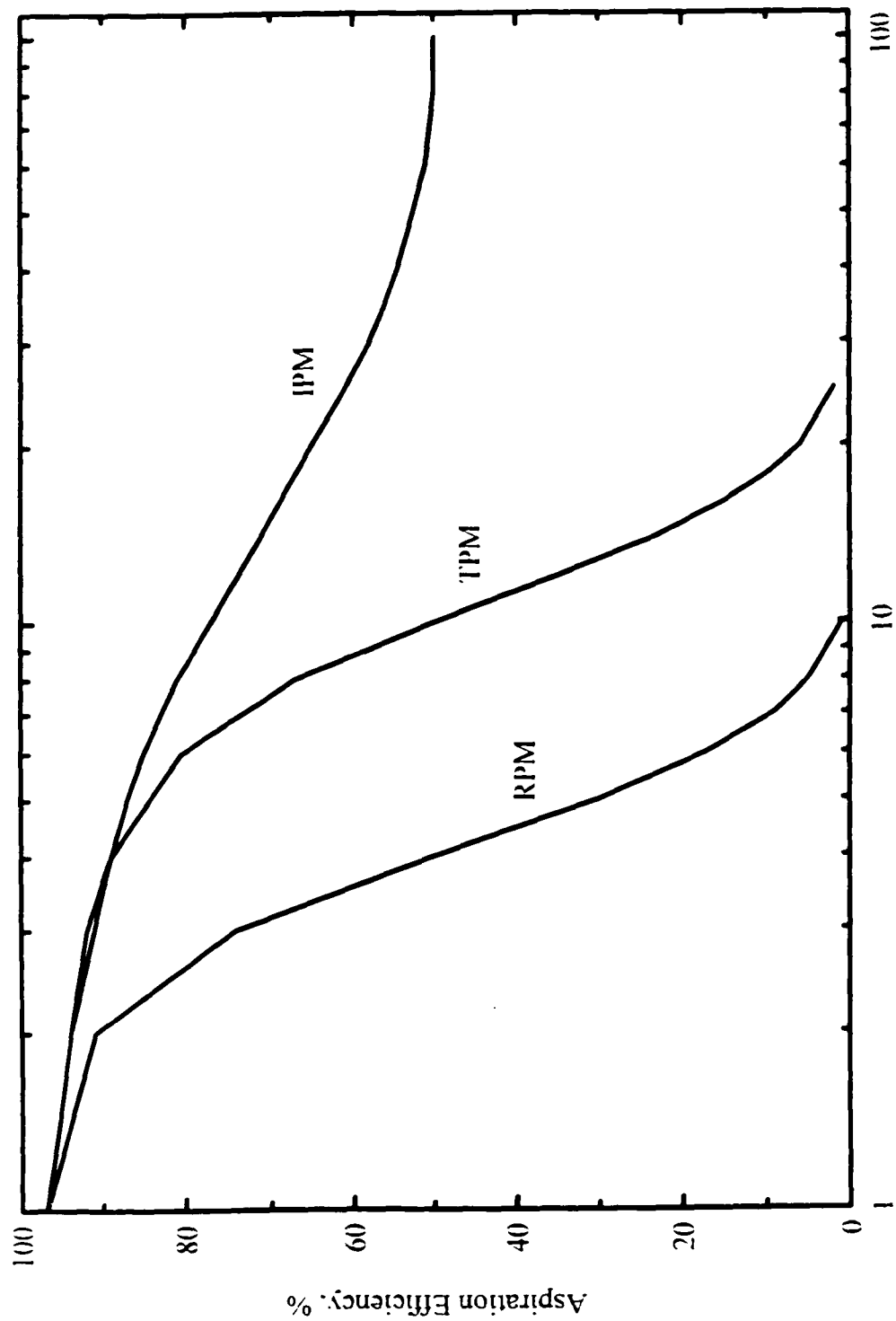

Figure 3-1: IPM, TPM and RPM criteria curves.

for inhalable particles has not been determined. Data to permit an extension of the IPM criterion curve beyond 100 μm is needed.

The accepted IPM criterion is further limited because it does not account the effect of wind velocity or breathing rate. It is representative only of mouth breathing that is orientation-averaged with respect to wind direction. Until the present study, nose inhalability has been neither investigated nor used for development of inhalability criteria. Whether a worker uses nose or mouth breathing is largely dependent on work rate and, thus, related to breathing pattern. Because all of these factors influence the sampling of particles, they should be investigated for any determination of inhalability.

Particles in the IPM fraction deposit in head airways where they are either absorbed at the site of deposition, swallowed or expelled from the body by bulk cleaning methods, such as, sneezing, spitting or nose blowing. Large particles in the inhalable fraction can present a health hazard if the contaminant has one of the following toxicological properties: 1) the material is highly soluble and quickly absorbed into the blood, for example, soluble salts and nicotine; 2) the material can be absorbed from the gastrointestinal tract, *e.g.*, lead, cadmium and pesticides; and 3) the material exerts its toxicity at the site of deposition, such as, radionuclides, acids, and nasal carcinogens, such as, wood dusts (Soderholm, 1985).

For the purpose of creating health-based OELs to assess the hazard associated with large airborne particles, five questions must be answered:

1) where are the sites of toxic action for the material,

2) how is toxicity influenced by particle size and deposition site,

3) what is the size distribution of the particles,

4) which particle sizes can be inhaled under the work conditions, and

5) what type of sampler will accurately reflect the hazard of the inhaled particles?

The questions of toxicity are fodder for other studies, as is the measurement of particle size distributions. This study seeks to answer the fourth question by providing information about inhalability under a variety of conditions that are typical of most workplaces. The overall objective is to evaluate the inhalability of large particles as a function of wind velocity and wind direction (environmental factors) breathing pattern (worker/sampler factors). The results provide data for refinement of the IPM criterion. A study of sampler performance, which addresses question (5) above, is presented in Chapter 4.

3.1 Background

Aerosol measurements are not only used to determine exposure, but also to define risk. Occupational epidemiology and toxicology studies seek to evaluate risk by comparing exposure measurements to health outcomes. Aerosol measurements are

key to hazard assessment and they should accurately reflect exposure. In the ideal case, isokinetic sampling is used to collect a sample that accurately represents the aerosol in a moving stream of gas. As the name "isokinetic" implies, the aerosol is sampled under conditions that maintain the motion of the particles in the freestream. An isokinetic sampler uses a thin-walled tube as a probe that is aligned with the oncoming wind. This minimizes obstruction or blockage of the air movement. Badzioch (1959) investigated the impaction of aerosol particles at the inlet of thin-walled samplers and Belyaev and Levin (1972) and Rouillard and Hicks (1978) have studied the effect of wall thickness on the performance of isokinetic samplers. For isokinetic sampling, the sampling flow rate must be adjusted so that the velocity of the air entering the probe is the same as the velocity of the air outside the probe. This prevents distortion of the air stream and consequent loss or gain of particles in the sampled air volume. Vincent (1989) presents an overview of isokinetic sampling and its practical uses.

Most samplers are not thin-walled and there is a large body of work that investigates and models the movement of air around blunt samplers. Among these are studies by Liu and Pui (1981), Vincent and Mark (1982), Vincent *et al.* (1982), Vincent (1984), Vincent (1987), Dunnett and Ingram (1988), Chung and Dunn-Rankin (1992), and Erdal and Esmen (1995). In effect, the human head is a blunt sampler. Its cyclic breathing and location on top of a broad body result in complex airflow patterns in the vicinity of the samplers, the mouth and nose. Erdal and Esmen (1995) present a

mathematical model of the head as a blunt sampler which concludes that for 200 μm particles the aspiration efficiency does not reach zero for wind velocities down to 0.5 m/s and breathing patterns with a tidal volume as low as 0.75 L.

The first study of the human head as a blunt sampler was conducted by Ogden and Birkett (1977, 1978). They used a tailor's dummy head on top of a box (as shoulders) placed in a wind tunnel to sample a test aerosol using a filter behind the nose or mouth. The particle sizes ranged from 5-30 μm and the sampling flow rates were 5, 20 and 40 L/min. The tests were conducted at two wind speeds, 0.75 and 2.75 m/s and at head orientations, with respect to oncoming wind, of 0°, 45°, 90°, 135°, and 180°. The results were reported as orientation-averaged over 360°. The results are summarized in Figure 3-2. Ogden and colleagues concluded that wind velocity, breathing pattern and nose *vs.* mouth breathing had little effect on inhalability.

In 1982, Armbruster and Breuer published the results of their study of inhalability as a function of particle size (Figure 3-3). They used a model of a human head, without torso, to determine inhalability for mouth and nose breathing for particles up to 60 μm. The wind velocities ranged from 1-8 m/s and the head orientations with respect to the direction of the wind were 0°, 90°, and 180°. Three breathing patterns were used to simulate a worker at "rest", "normal" and "hard" work conditions (minute

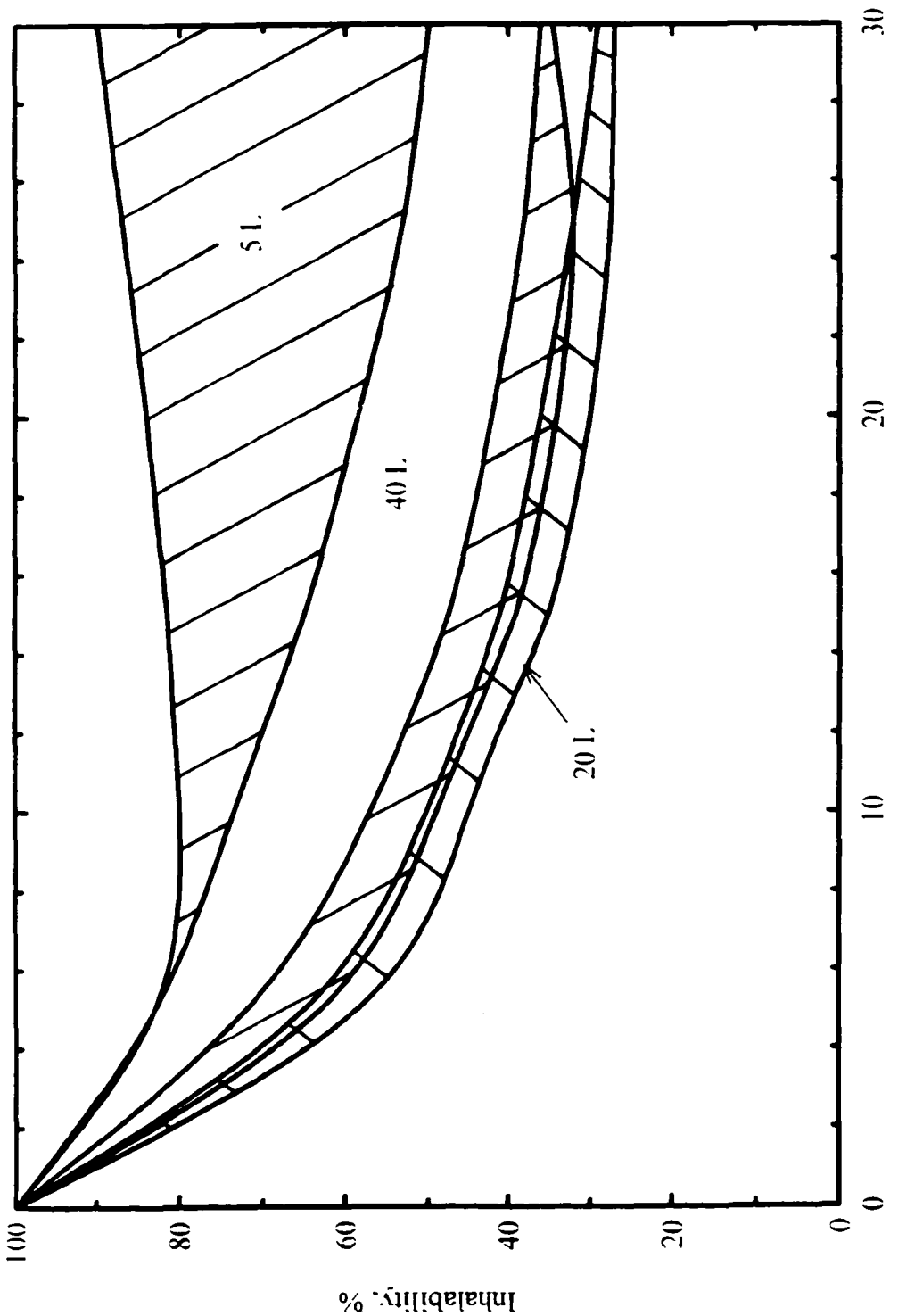

Figure 3-2: Inhalability results of Ogden and Birkett (1977) for three minute volumes (5, 20 and 40 L) at wind speeds of 0.75 and 2.75 m/s (adapted from Soderholm (1985).

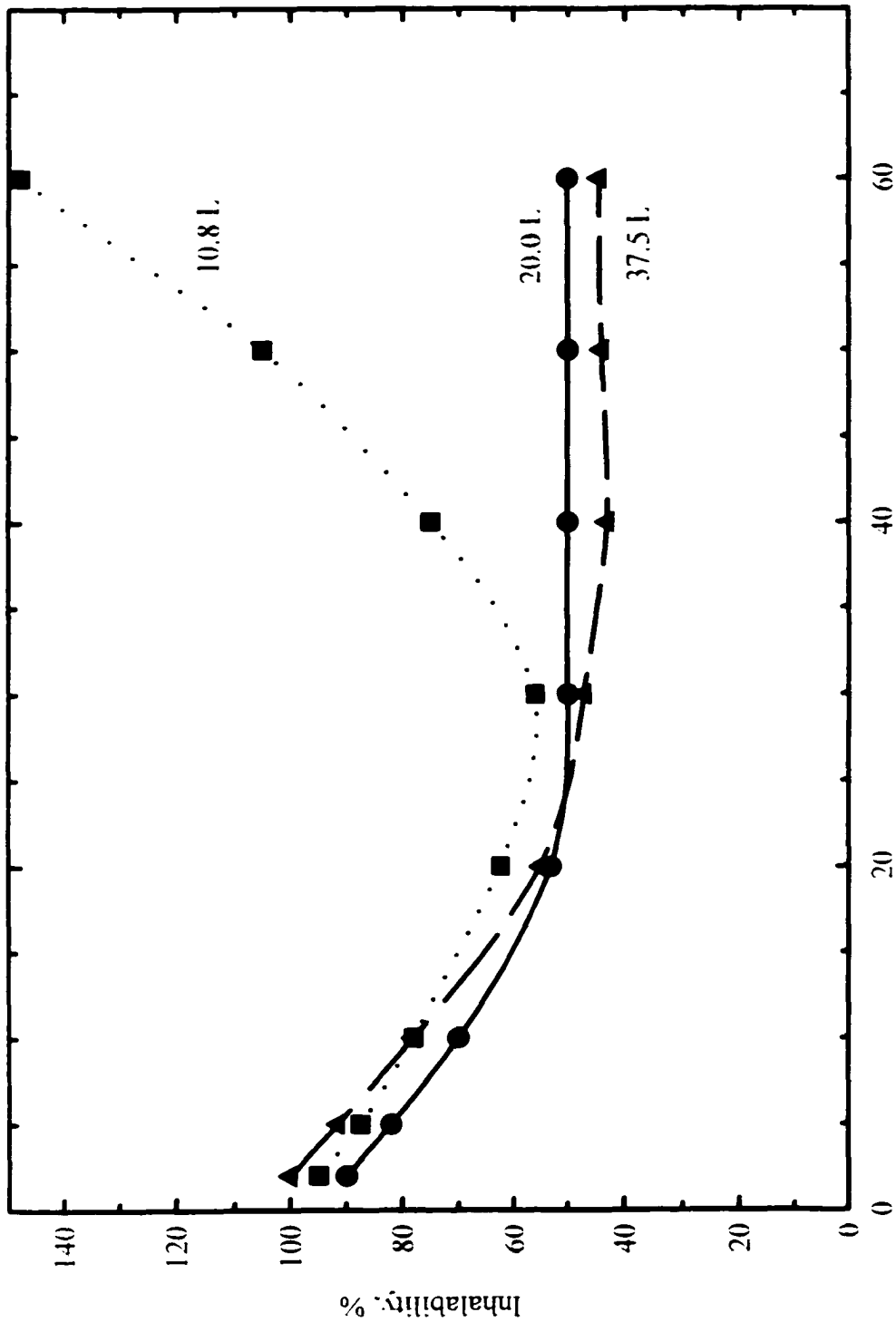

Figure 3-3: Inhalability results of Armbruster and Breuer (1982) for three minute volumes (10.8, 20 and 37.5 L) at wind speeds of 1, 2, 4, 6 and 8 m/s (adapted from Soderholm (1985).

volumes of 10.8, 20 and 37.5 L). The investigators also concluded that the main result was a relationship between particle size and aspiration efficiency (inhalability) and that wind velocity and breathing pattern had little effect on inhalability. The exception being at the high wind velocity condition, where particles with $d_a > 50$ μm were collected with greater efficiency than for wind speeds of 4 m/s or less.

Vincent and Mark (1982) used a full-size head and torso and narrowly graded aluminum oxide test aerosols to evaluate inhalability for particles up to 100 μm. The wind velocities used were 1, 2, and 4 m/s and the mannequin was either facing the wind or sequenced through five angle positions to provide an orientation-averaged measurement. Cyclic breathing at 20 L/min was used. This is comparable to a person at "normal" work condition. The results, summarized by Figure 3-4, confirmed that the main trend is due to the effect of particle size and found that wind velocity up to 4 m/s has little influence on the inhalability data. An important finding from this study was that the presence of the full-size torso made a notable difference in the air flow patterns and the measurements of inhalability.

The three studies presented above form the basis for what is generally accepted as the criterion for inhalability. The experimental conditions of the studies are outlined in Table 3-1. The work of Ogden and Birkett (1977) was used to develop the original ISO curve (ISO, 1981), while the other two studies were included in the development of the ACGIH curve (ACGIH, 1985). Both curves are shown in Figure 1-3. The

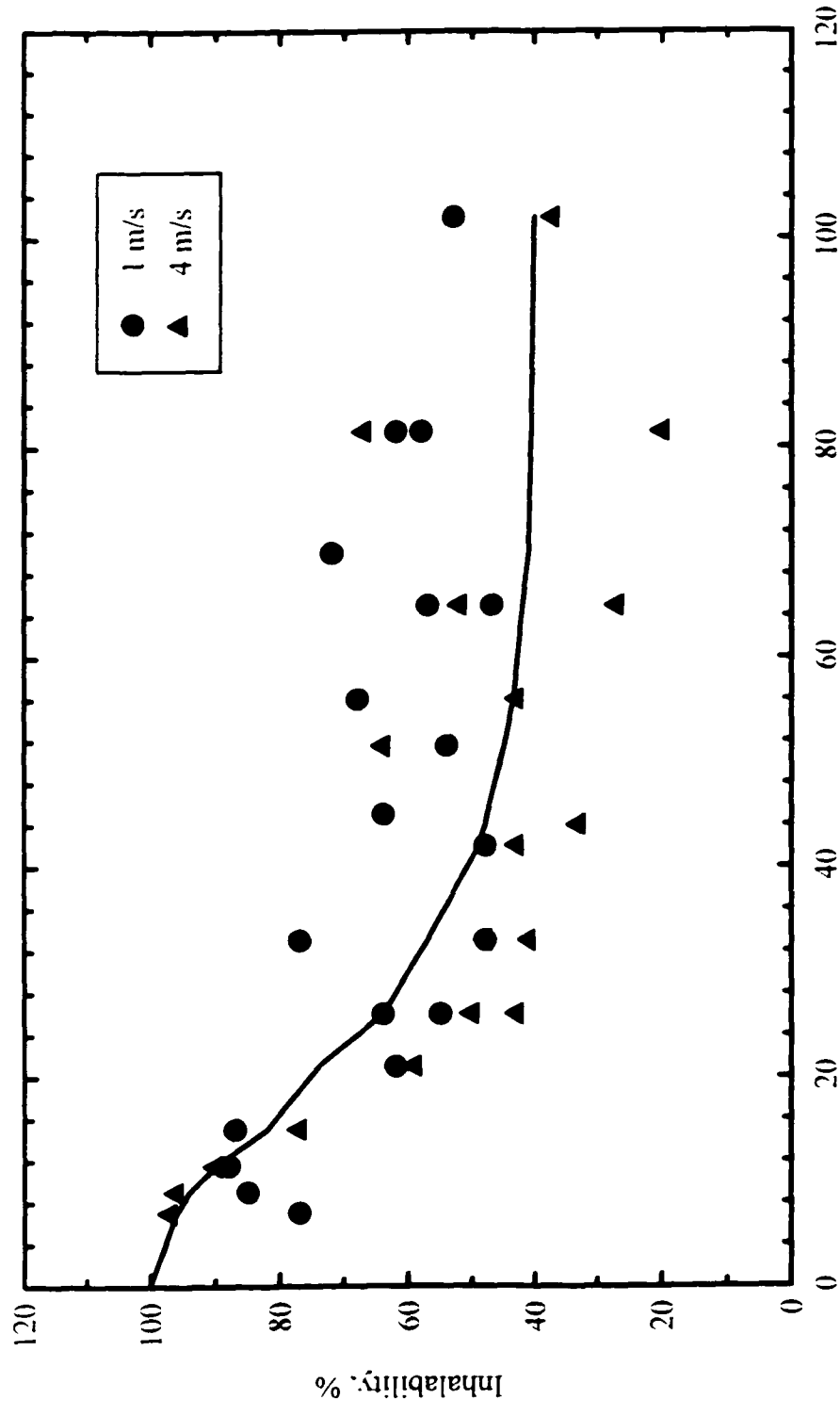

Figure 3-4: Inhalability results of Vincent and Mark (1982) for a minute volume of 20 L and at wind speeds of 1 and 4 m/s (adapted from Soderholm (1985).

original ISO criterion was based on an extrapolation of the available data to 0% for 185-μm particles. Because of the experimental design, primarily the use of a full-size torso and the largest range of aerodynamic diameters, the work of Vincent and Mark (1982) is the most useful and appropriate for defining IPM sampling criteria.

Table 3-1: Summary of Experimental Conditions for the Three Studies used to develop the IPM Criterion

Study	Experimental Set Up	Particle Sizes (μm)	Wind Velocities (m/s)	Orientation (degrees)	Minute Volume (L)
Ogden and Birkett (1977)	• dummy head on a box • 0.5 m^2 WT • monodisperse 2(ethylhexyl)-sebacate	5-30	0.75, 2.75	0, 45, 90,135, 180 results reported as orientation-averaged	5, 20, 40
Armbruster and Breuer (1982)	• dummy head • 0.5 m^2 WT • coal dust - sized after collection	up to 60	1, 2, 4, 6, 8	0, 90, 180 results reported as orientation-averaged	10.8, 20, 37.5
Vincent and Mark (1982)	• full-size head and torso • 3.75 m^2 WT • graded aloxite	up to 100	1, 2, 4	0, 45, 90, 135, 180 results reported as orientation-averaged	20

The currently accepted inhalability criterion is defined for particles less than 100 μm and indicates no effect due to wind velocity or breathing pattern. The curve does not

distinguish between mouth and nose inhalability, a potential source of significant difference. A worker at "rest" is likely to breathe through the nose, while a worker doing heavy labor probably uses up to 50% mouth breathing. A switch from nose to mouth breathing changes the position, orientation, flow rate, and sampling velocity of the effective sampler. Combined with the complex airflow patterns around a human body and head, these changes are anticipated to have an effect on inhalability.

3.2 Experimental

The primary goal of this research is to expand the available knowledge concerning the inhalability of large particles (10-150 μm) and the factors that influence inhalability. The study was designed to provide information about the effect of wind velocity and breathing pattern on the inhalability of particles over the range of 7-141 μm. It also investigated the difference between nose and mouth inhalability for particles in the indicated size range. The effects of the following five parameters were evaluated:

1. particle size: 7, 17, 22, 37, 52, 82, 116, and 141 μm,
2. wind velocity: 0.4, 1.0, 1.6 m/s,
3. head orientation with respect to oncoming wind,
4. nose and mouth breathing, and
5. breathing pattern: minute volumes of 14.2, 20.8, and 37.3 L.

3.2.1 Particle Size

The test dust was narrowly graded aluminum oxide (Al_2O_3) optical powder (General Abrasives/Treibacher, Inc., Niagara Falls, NY). In some cases, the bulk material was used as received, but most of the dusts used were either sieved using USA standard test sieves (Fisher Scientific Co., USA or Gilson Co., Inc., Worthington, OH) and a Gilson sieve shaker, model SS8-R (Gilson Co., Inc., Worthington, OH) or separated using a centripetal classifier (Vortec Products Co., Long Beach, CA). Nine sizes of test dust were used during the study. The size range was 7 - 141 μm with mass median aerodynamic diameters of 7, 17, 22, 37, 52, 82, 116, and 141. These represent narrowly distributed, but not monodisperse, particles.

3.2.1.1 Determination of Particle Size

When investigating particle size, there are a number of size distributions of interest. For example, the distribution of number, mass, or surface area can all provide useful information and can be expressed as a concentration. It is easy to imagine how each of these parameters could be linked to a health outcome. The distribution of particles is generally characterized by a median size, the size for which half of the distribution is larger and half of the distribution is smaller. Particle sizes in an aerosol are usually lognormally distributed and the spread in sizes is described by the geometric standard deviation (GSD). Aerosols can be either monodisperse or polydisperse. A monodisperse aerosol is one in which all of the particles are the same size. A polydisperse aerosol contains particles of different sizes. For practical purposes, an

aerosol with a GSD less than 1.35 can be considered sufficiently narrow for these studies.

The median size can be reported as a physical diameter or it can be linked to the behavior of the particles in air by using aerodynamic diameter, d_a. Particles with the same aerodynamic diameter can differ in size, shape and density, but they will all exhibit the same motion in air. Aerodynamic diameter, because of its direct relation to particle behavior, is used to characterize nearly all particle phenomena, including inhalability and sampling efficiency. Most commonly, the particles in an aerosol are characterized by their mass median aerodynamic diameter (MMAD).

The ideal particle is a sphere with a density of 1000 kg/m^3; this is called a standard density particle. For such a particle, the aerodynamic diameter is the same as the physical diameter. The aluminum oxide (Al_2O_3) particles used in this study are non-spherical and the density is 3960 kg/m^3. Using the physical diameter, d_p, and a dynamic shape factor, χ, the aerodynamic diameter can be calculated with

$$d_a = d_p\left(\frac{\rho_p}{\rho_0 \chi}\right)^{\frac{1}{2}} \qquad (3.2)$$

where ρ_p is the density of aluminum oxide and ρ_0 is standard density.

An AO Spencer optical microscope (American Optical Company, Buffalo, NY) capable of 100× magnification was used to determine the physical diameter of the test dusts. A micrometer-calibrated Porton graticule was used to size a minimum of 400 particles from each test dust. This allowed determination of the count median physical diameter (CMPD) and the GSD for each test dust.

Typically, Equation 3.2 is used to convert the physical diameters to aerodynamic diameters which provide the count median aerodynamic diameter (CMAD). MMAD can then be calculated from CMAD and GSD using the Hatch-Choate conversion equation:

$$MMAD = CMAD \exp\left(3 \ln^2 GSD\right) \tag{3.3}$$

This relatively simple process was not available for determining MMAD because the dynamic shape factor, χ, was unknown for Al_2O_3.

Dynamic shape factor can be determined if physical diameter, aerodynamic diameter, and particle density are known. A direct method for evaluating aerodynamic diameter is to measure the settling velocity, V_{TS}, of individual particles. Particle settling is an aerodynamic process and, therefore, related to aerodynamic size by the following equation:

$$V_{TS} = \frac{\rho_p d_p^{\,2} g}{18\eta} \tag{3.4}$$

where g is gravitational force, 9.81×10^{-1} m/s^2, and η is the viscosity of air, 1.81×10^{-5} Pa·s. Direct comparison of d_a and d_p for individual particles allows calculation of χ because

$$\chi = \frac{\rho_p}{\rho_0}\left(\frac{d_p}{d_a}\right)^2 \tag{3.5}$$

Attempts were made to measure V_{TS} for individual particles by dropping them down a glass tube (4-mm ID) illuminated with a 0.95 mW helium-neon laser (Spectrophysics, Palo Alto, CA). The descent through a given distance was timed using a stopwatch. This approach proved problematic because particles that were large enough to isolate and manipulate, those with $d_p > 70$ µm, settled too quickly for manual timing. Particles small enough to settle slowly, $d_p < 40$ µm, were too difficult to isolate and manipulate.

Left without traditional methods of determining aerodynamic diameter, an alternative method was required. Since the measurement of settling velocity is normally simple and uses primary standards, it is a choice method. The problem was that the easy-to-handle particles settled too quickly. By filling the settling tube with water, the viscosity of the fluid is increased and the particles settle more slowly which allows manual timing of their descent. The measured settling velocity is a hydrodynamic process and can be related to aerodynamic diameter by calculation.

Individual particles were isolated under 40× power of the optical microscope and their shape and physical diameter were recorded. Then, the particle was transferred to an illuminated vertical settling tube (a 100-ml graduated cylinder) filled with water and its travel time between two points was measured with a stopwatch. Water temperature was monitored during each measurement because it affects viscosity. This procedure was repeated for 51 particles with d_p in the range of 70 to 109 μm.

The hydrodynamic settling velocity, $V_{TS.H2O}$ is determined by

$$V_{TS.H_2O} = \frac{dx}{dt} \tag{3.6}$$

where dx is the distance traveled and dt is the time for travel. The hydrodynamic settling velocity can be used to determine the diameter of a spherical particle, d_s, with the same $V_{TS.H2O}$.

$$d_s = \left(\frac{18\eta_{H_2O} V_{TS.H_2O}}{\left(\rho_p - \rho_{H_2O}\right) g} \right)^{\frac{1}{2}} \tag{3.7}$$

where η_{H2O} is the viscosity of water (see below),

ρ_p is the density of the particle, 3960 kg/m^3,

ρ_{H2O} is the density of water, 1000 kg/m^3, and

g is the force of gravity, 9.81 m/s^2.

The viscosity of water is highly dependent on the water temperature. Tabulated values (η_T) obtained from the CRC Handbook of Physics and Chemistry (1983) were calculated using the empirical equation:

$$\log_{10}\frac{\eta_T}{\eta_{20}} = \frac{1.3272(20-T) - 0.001053(T-20)^2}{T+105} \qquad (3.8)$$

where η_{20} is accepted to be 1.002×10^{-3} Pa·s. Water viscosity ranged from 8.904×10^{-4} Pa·s (25 °C) to 9.548×10^{-4} Pa·s (22 °C).

All of the particles evaluated had a Reynold's number when settling in air, Re_{air}, greater than 0.5 (0.617-10.462), which is outside the Stoke's region and makes calculation of $V_{TS,air}$ and d_a more difficult. The difficulty arises because of a shift in the relationship between particle settling velocity and particle size from $V_{TS} \propto d_a^2$ to $V_{TS} \propto d_a^1$. As outlined by Hinds (1999), $V_{TS,air}$ is calculated using an iterative process or by using the following equations:

$$V_{TS,air} = \left(\frac{\eta_{air}}{\rho_g d_p}\right)\exp\left(-3.070 + 0.9935J - 0.0178J^2\right) \qquad (3.9)$$

where η_{air} is 1.81×10^{-5} Pa·s and ρ_g is the density of air, 1.20 kg/m^3. J is determined using the product of the coefficient of drag, C_D, and Re^2:

$$J = \ln\left[C_D(Re)^2\right] = \ln\left(\frac{4\rho_p\rho_g d^3 g}{3\eta^2}\right) \qquad (3.10)$$

Similarly, aerodynamic diameter, d_a, is calculated using:

$$d_a = \left(\frac{\eta}{\rho_g V_{TS,air}} \right) \exp\left(1.787 - 0.577H + 0.0109H^2\right) \qquad (3.11)$$

where

$$H = \ln\left(\frac{C_D}{Re}\right) = \ln\frac{4\rho_0 \eta g}{3\rho_g^2 \left(V_{TS,air}\right)^3} \qquad (3.12)$$

The calculated values of count median aerodynamic diameter (CMAD) can be compared to the values of count median physical diameter (CMPD) and the average ratio is used as a scaling factor. The Hatch-Choate conversion equation (Equation 3.3) can then be used to calculate MMADs for the test dusts.

Table 3-2: Aluminum Oxide Test Dust Particle Size Information

CMD[1], μm	CMAD[2], μm	GSD[1]	MMAD[3], μm
4.4	6.2	1.27	7
9.2	12.9	1.36	17
14	19.6	1.21	22
20	28.0	1.35	37
29	40.6	1.34	52
41	57.4	1.27	68
55	77.0	1.16	82
75	105.0	1.20	116
96	134.4	1.13	141

[1] determined by optical microscopy
[2] CMAD = CMD × scaling factor (1.4)
[3] MMAD = CMAD exp(3 ln^2 GSD)

The average ratio of CMAD to CMPD was 1.404 for d_p in the range of 70 to 109 μm. The results of this procedure correlate well with aerodynamic size measurements made by an Aerosizer instrument (Amherst Process Instruments, Inc., Hadley, MA). Table 3-2 lists the results for the nine test dusts used in the solid particle inhalability and sampler performance studies.

3.2.2 Wind Velocity

Most work environments have air velocities that are generally below 2 m/s. This is the reason measurements of inhalability and sampler performance are conducted at low velocity conditions. There are notable exceptions, such as, outdoor work or high-velocity particles either carried in a jet or generated by a mechanical process, such as, grinding. Vincent *et al.* (1990) developed an expression for inhalability at wind velocities greater than 4 m/s (Equation 1.3).

During the design phase of this study, 1 - 4 m/s was the accepted range for indoor workplace wind velocities. Three wind velocities were investigated: 0.4, 1.0 and 1.6 m/s. Recent studies (Berry and Froude, 1989; Baldwin and Maynard, 1998) indicate that indoor work environments have wind velocities lower than the velocities investigated in early studies of inhalability. They found that air velocity in most workplaces is less than 0.3 m/s and typically less than 0.1 m/s.

3.2.3 Head Orientation with Respect to Wind Direction

This study investigated two head orientations with respect to the oncoming wind: facing-the-wind (0°) and orientation-averaged (360°). A review of blunt sampler theory (Vincent, 1989) confirms the conceptual notion that a sampler facing the wind will collect large particles with better efficiency than when the sampler is oriented at angles other than 0° with respect to the oncoming wind. The facing-the-wind condition provides the upper limit for aspiration efficiency and the orientation-averaged condition by equally weighting the aspiration efficiencies associated with all angles from 0° through 360° is more representative of typical exposures. The IPM criterion is based on orientation-averaged data collected at set angles, not during continuous rotation. The mannequin used in this study completes one full rotation during a 16.95-minute sampling period. The facing-the-wind sample runs were 8.00 minutes. The duration of the sampling period was selected to ensure adequate dust collection for gravimetric analysis.

3.2.4 Nose and Mouth Breathing

Sampler orientation and sampler inlet are anticipated to effect inhalability (Vincent, 1989). It is easy to imagine that the open mouth, with its larger area and axial orientation, will collect large particles more efficiently than the nostrils, which are smaller and require the oncoming air to make a 90° turn for sampling. This is complicated by the flow of air around and near the torso and head. Air streams

approaching the torso must diverge and compress to allow the air to get past the obstruction. This results in lateral, vertical, and horizontal motion of the air. In the immediate vicinity of the mouth or nose the streamlines converge to enter the mouth or nose. Turbulence and eddies form and the airflow and movement of aerosol particles becomes difficult to predict. The complexity of air and particle motion near the nose and mouth make it impossible to model inhalability with current technology.

Further complicating the issue is that workers at low exercise tend to breathe through their nose. As the level of exercise increases, workers begin to also breath through their mouth. The relative proportions of nose and mouth breathing have been studied (James *et al.*, 1994), but are not a concern of this project. This investigation evaluates exclusive nose and exclusive mouth breathing only. In the present study, inhalability for 100% nose breathing was compared to inhalability for 100% mouth breathing at one wind velocity (1.0 m/s) and one breathing pattern (20.8 /min). The goal was to determine the difference in inhalability due to mouth or nose breathing.

3.2.5 Breathing Pattern

A cam-driven mechanical breathing machine (Nelson *et al.*, 1972) was used to simulate breathing rates associated with "rest", "moderate", and "heavy" work conditions (Silverman *et al.*, 1951) with inspiratory minute volumes of 14.2, 20.8 and 37.3 liters respectively. These correspond to work rates of 0, 208, and 622

kg·m/min (5, 35, and 105 Watts). Table 3-3 shows the minute volume, respiration rate, work rate and tidal volume for each of the three conditions. A single piston is used for minute volumes of 14.2 and 20.8 L, but two pistons are required to provide sufficient respiratory volume for 37.3 L/min. Valve-regulated hoses, one for inhalation and one for exhalation, connected the nose or mouth sampler to the breathing machine.

Table 3-3: Work Rate, Respiration Rate, Minute Volume and Tidal Volume for the Selected Breathing Patterns.

Work Rate (Watts)	Work Rate (kg·m/min)	Respiration Rate (min^{-1})	Minute Volume (Liters)	Tidal Volume (Liters)
0	0	19.6	14.2	0.72
35	208	21.2	20.8	0.98
105	622	23.0	37.3	1.62

Previous studies of inhalability have also used cyclic sampler flow to simulate human breathing; however, this is the first study designed to allow exhalation back through the mannequin nose or mouth. Consider the exhaled breath of a worker exposed to large particles and facing the wind. Inhaled particles have been removed by deposition mechanisms and a jet of clean air is exhaled into the flow field in the immediate vicinity of the mouth or nose just prior to the next inhalation. The airflow and eddies near the sampler (mouth or nose) are changed and the aerosol in the vicinity of the samplers has also been diluted by mixing with the clean exhaled air. This effect can modify measurements of inhalability, and thus exhalation through the mouth or nose should be included in the experimental set up to optimize the

simulation of human breathing. There was some concern that the exhalation air could dislodge collected particles from the filter and sampler probes. An evaluation of sample loss due to exhalation indicated negligible loss of particles from the sample filter or sampler inlet.

3.2.6 Test Strategy

With three replications of each set of conditions, there were 36 experimental runs for each particle size. Nine particle sizes required a minimum of 324 runs. For each particle size and breathing rate, the runs were sequenced randomly. Table 3-4 shows the combinations tested. After the initial runs were completed, bad data were discarded and the runs repeated. Runs were repeated when there was experimental error due to malfunction of mechanical equipment or operational mistakes or when systematic error was indicated by a data set with a coefficient of variation greater than 0.3. New data replaced discarded data for analysis. Altogether, 450 experimental runs were performed, meaning that just over one-fourth of the runs were repeated.

Table 3-4: Combinations of Sample Parameters for the Inhalability Study.

Mouth/ Nose	Particle Sizes	Minute volumes	Wind velocities	Orientations	Replications	Total
mouth	9	1	3	2	3	162
mouth	9	2	1	2	3	108
nose	9	1	1	2	3	54
Total						324

3.2.7 Description of the Mannequin

A full-size, full-torso fiberglass mannequin (Silvestri Co., Los Angeles, CA) was used for the study (Figure 3-5). The face (Model SM701) is a size that represents overlapping dimensions for men and women (Douglas, 1978). The face is 22.5 cm long (nasion-menton length) by 13.4 cm wide (bizygomatic diameter). The mouth opening is a 30 mm x 6-mm oval with an area of 1.6 cm^2 (Kuo, 1993). The nasal openings are 7 mm x 10-mm ovals. The mouth and nasal openings are connected to their respective 47-mm filter holders by copper tubing that was shaped to a close fit with the openings. All particles that collect inside the copper tubes are included in the sample. The back of the mannequin's head is removable to allow insertion of the 47-mm filter holders within the cavity (Figure 3-6). The back of the head is replaced and a wig is fitted on the mannequin during sampling. The mannequin was painted with conductive paint (EMI/RFI Shield Coating, distributed by McMaster-Carr, Santa Fe Springs, CA) and its surface grounded.

3.3 Results and Discussion

Inhalability was determined as the ratio of the mass concentration measured by the mannequin sampler to the true wind tunnel aerosol concentration determined by isokinetic samplers located in the test section. An isokinetic sampler was positioned 0.3 m to either side and above the mouth of the mannequin. At this distance, the samples are collected from an undisrupted aerosol stream. The isokinetic samplers were constructed from 25-mm in-line stainless steel filter holders (Gelman Sciences,

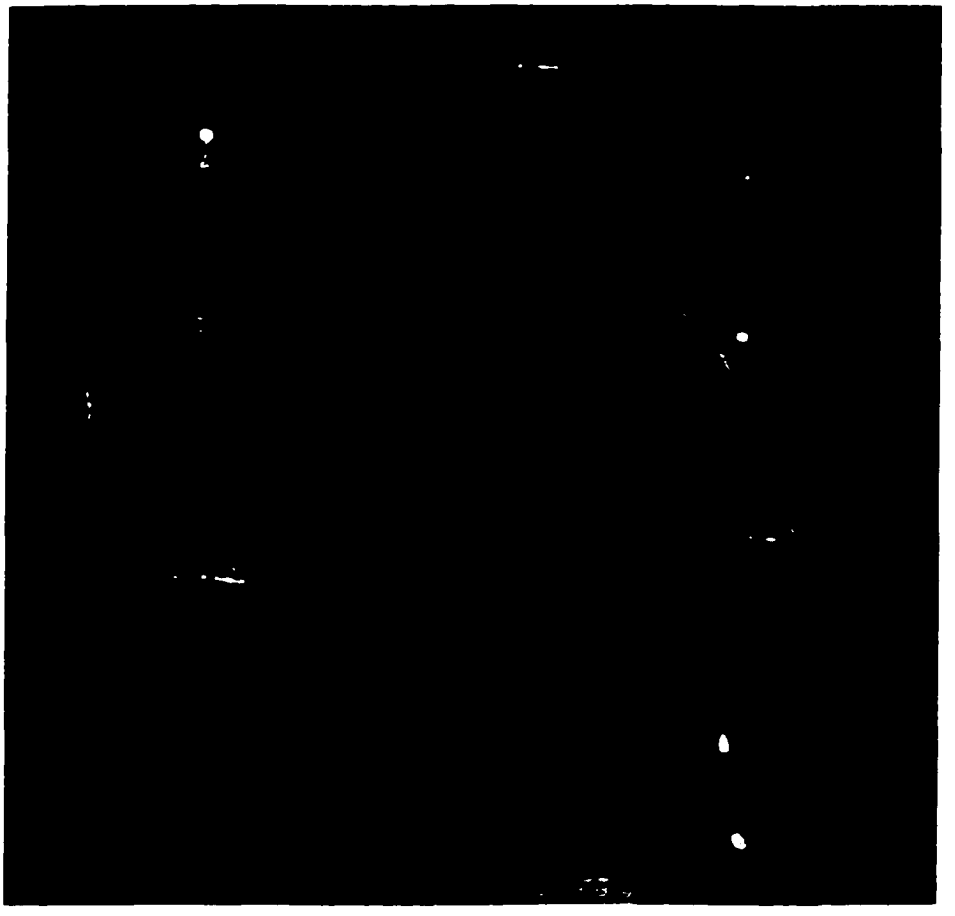

Figure 3-5: The mannequin and location of (a) the isokinetic samplers and (b) the personal samplers.

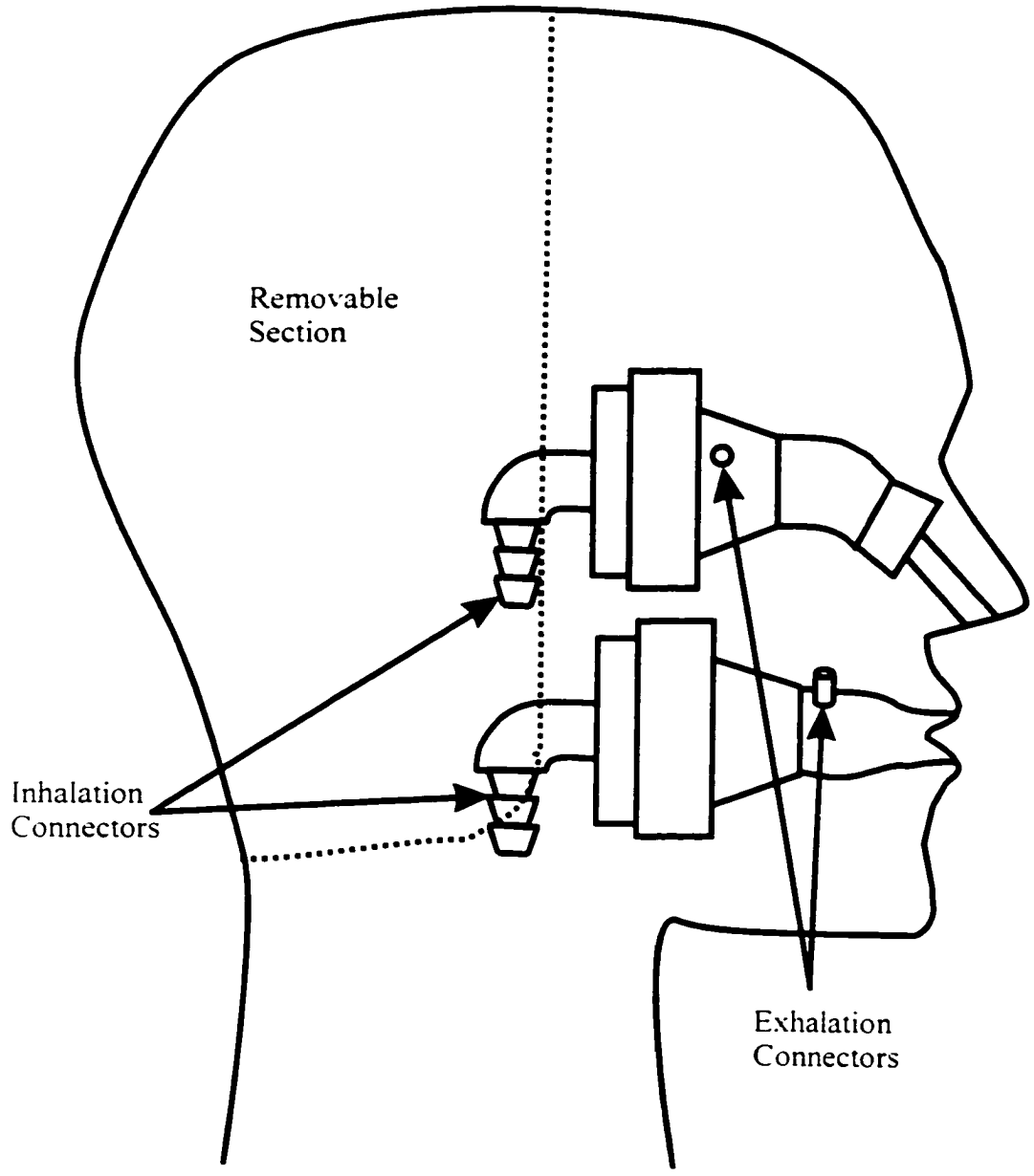

Figure 3-6: Diagram of mannequin head.

Inc., Ann Arbor, MI, P/N 1209) fitted with 8.5-mm ID brass probes which extend 32-mm from the face of the filter holder. The probes were filed to give a sharp edge at the inlet. Sampling flow was provided by house vacuum and controlled by metering valves. Rotameters (Dwyer Instruments, Michigan City, IN) reading 10 L/min full scale were calibrated with a spirometer and then used to monitor the airflow through the isokinetic samplers.

Mass concentration was determined by gravimetric analysis of the filters. The ratio of total mass collected to volume of air sampled is reported as mass concentration. Care was taken to ensure that all of the dust entering the sampler was included in the sample. Dust particles that settled inside the probe or on the filter holder wall were gently brushed, using a fine-bristled artist brush, onto the filter prior to weighing. The precision of the Cahn electrobalance (model C-25 or C-35) was 0.01 mg. For the isokinetic samplers, the average mass gain was used to calculate true concentration in the wind tunnel. For the largest particles ($d_a > 68$ μm), only the two side isokinetic samplers were used to determine wind tunnel concentration because the aerosol sampled by the top isokinetic sampler was not representative of the aerosol concentration in the vicinity of the mouth or nose due to particle settling. For 141-μm particles and a wind velocity of 0.4 m/s, sampling was not possible because nearly all the particles had settled below the level of the samplers.

3.3.1 Orientation-Averaged Inhalability for Mouth Breathing

The combined inhalability results for orientation-averaged mouth breathing are shown in Figure 3-7. Also shown is the accepted IPM criterion curve. The data show a similar shape to the IPM criterion, but exhibit lower inhalability for particles larger than 35 μm. While the IPM criterion plateaus at an inhalability of about 50% for particles larger than 50 μm, the data indicate a plateau at about 30% for particles larger than 75 μm. The data do not indicate that inhalability reaches zero at least for particles up to 141 μm.

The reason for the difference between the data and the IPM criterion is not evident, but there are some possible explanations. One potential cause is the difference in the methods used to determine orientation-averaged inhalability. A continuously rotating mannequin, like the one used in this investigation, provides a sample that is equally representative of all angles. Prior studies determined orientation-averaged inhalability as the simple average of results obtained from measurements at discrete angles, such as, 0°, 45°, 90°, *etc.* Since aspiration efficiency is much greater when the sampler is oriented in a narrow range of angles around 0°, the use of discrete angles may overestimate the contribution of the facing-the-wind condition. This would result in a higher value for large particle inhalability than for the continuous rotation method used in this research.

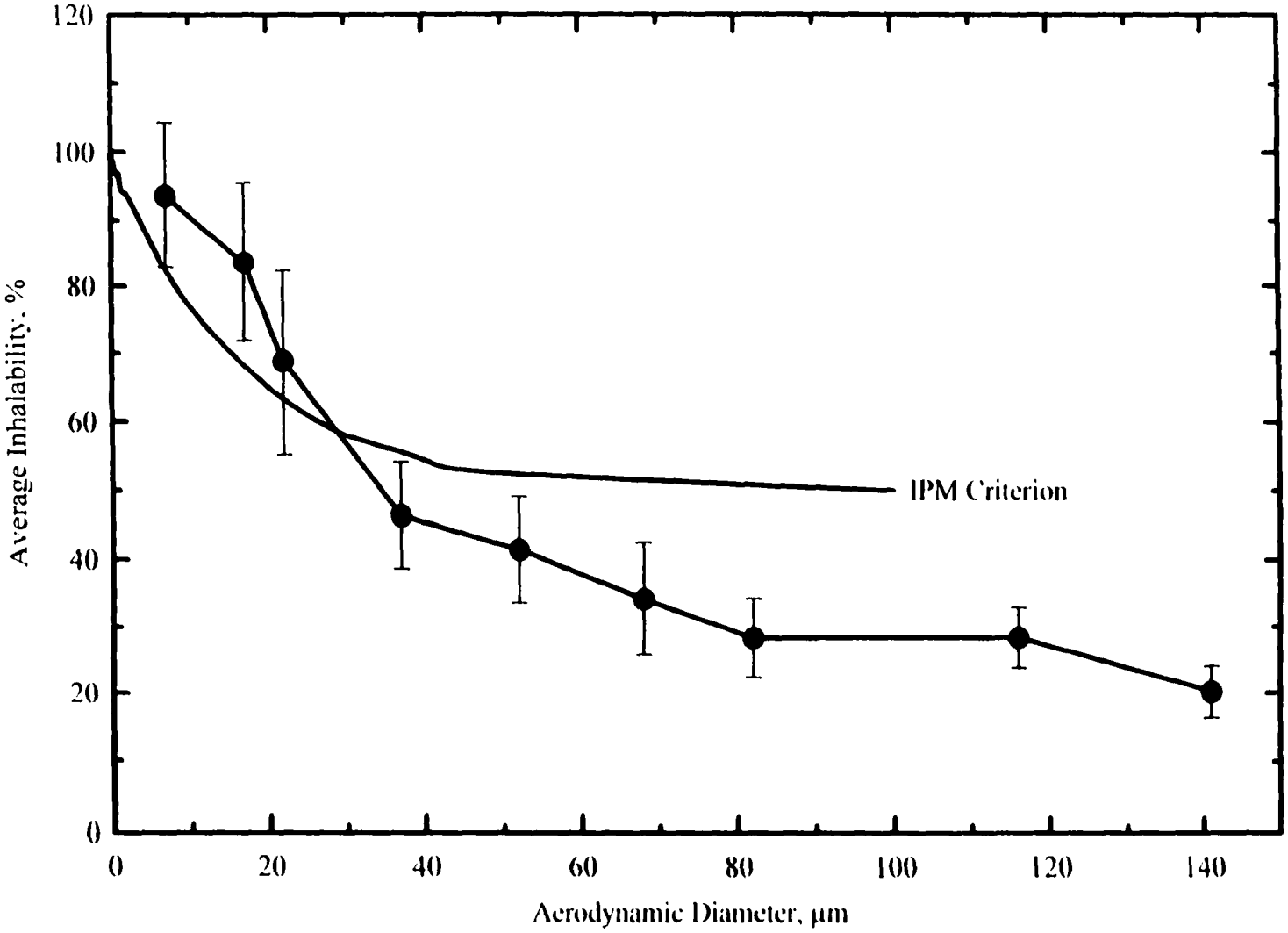

Figure 3-7: Inhalability for orientation-averaged mouth breathing, data for wind velocities and breathing patterns combined.

Another explanation is that previous studies did not neutralize the charge on the test particles. Vincent and Mark (1982) noted the accumulation of dust around the mouth of their mannequin. The dust could have been dislodged by incoming particles, inhaled, and included in their samples. This would, in effect, increase the observed values for inhalability. Because charged particles could have affected the results, care was taken during this work to ground all components of the test system and neutralize the charge on particles.

A third possibility is the difference in the breathing mechanism of the mannequins. Mannequins used in previous studies used only inhalation. The mannequin used in this study exhales through the mouth, or nose, as well. The exhalation of clean air creates a region in front of the sampler (mouth or nose) where the aerosol concentration is low. This could result in lower values for inhalability for the measurements reported here.

The fourth possibility is general and speaks to the notion that wind tunnel test systems for inhalability are complex and unique. Considering the specialized set up for individual test facilities, apparatus-specific variation may translate to differences in results. Comparisons between this system and other test systems were made. Several differences were noted, but none could be isolated as the cause of differences in results.

Figure 3-8 shows the same data as Figure 3-7, but includes lines indicating the theoretical large particle limit of relative inhalability for the three wind velocities have been added to the graph. The lines were developed using the assumptions that large particles travel in a straight line and this corresponds to an inhalability of 100% when the mannequin is facing the wind. If particle settling is neglected, the inhaled concentration, C_i, is:

$$C_i = \frac{mass\ inhaled}{volume\ inhaled} = \frac{C_m \times U \times A\cos\theta}{Q} \qquad (3.13)$$

where C_m is mass concentration, U is wind tunnel air velocity, A is mouth area, Q is sampler flow rate, and θ is the angle of the sampler (mouth) axis with respect to the oncoming wind. The relative inhalability, IF_{rel}, is the ratio of the inhaled concentration relative to that of the facing-the-wind condition. For continuous rotation:

$$IF_{rel} = \frac{\frac{1}{\pi}\int_0^{\pi} C_i(\theta)\, d\theta}{C_i(\theta = 0)} \qquad (3.14)$$

where IF_{rel} is 0 when $\theta \geq \pi/2$. For the largest particles at the lowest air velocities, the particles do not travel horizontally, so the inhaled concentration must be reduced by $\cos\phi$, where ϕ is the downward angle of the particle's straight-line trajectory resulting from settling:

$$\phi = \arctan\frac{V_{ts}}{U} \qquad (3.15)$$

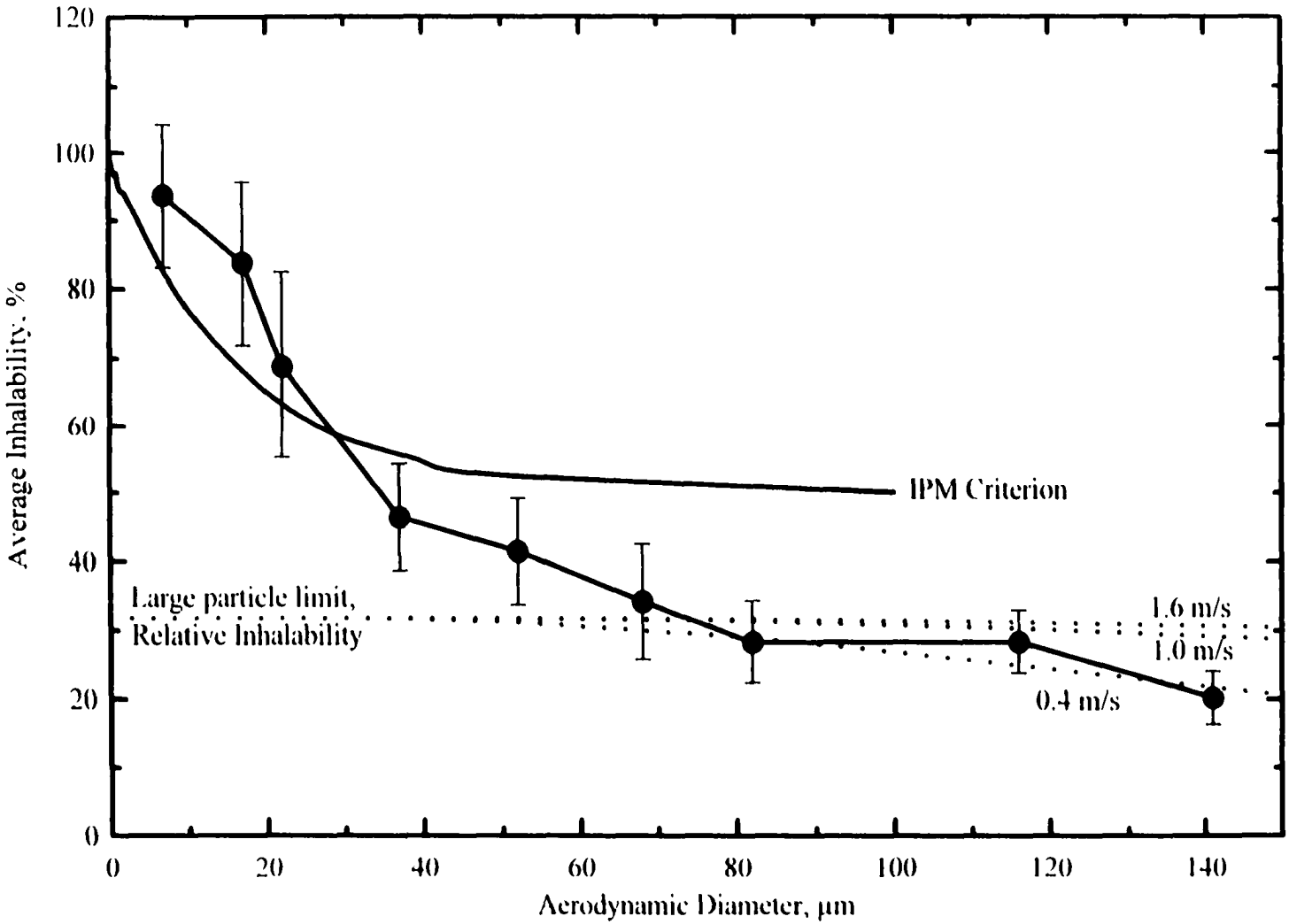

Figure 3-8: Large particle limit of Relative Inhalability and the inhalability curve for orientation-averaged mouth breathing.

Mouth inhalability results show good agreement with the theoretical large particle limits for particles with an aerodynamic diameter greater than 60 μm.

3.3.1.1 Effect of Wind Velocity on Orientation-Averaged Mouth Inhalability

The results for the effect of wind velocity on orientation-averaged mouth inhalability are presented in Figure 3-9. The data shown were collected at a respiratory minute volume of 20.8 L. The three curves are similar in shape and follow the same general trend. Appearance suggests that there is no effect due to wind velocity and statistical analysis confirms this decision. The data set passed tests for normal variance and equal variance, which allowed the use of a two-way analysis of variance (ANOVA). Sigma Stat (Jandel Corporation) scientific software was used for statistical analyses of data. The difference between the mean values for the nine particle sizes was barely significant ($p = 0.0469$). This finding agrees with previous studies, which concluded that wind velocities in the range of 1 - 4 m/s have little effect on orientation-averaged mouth inhalability.

3.3.1.2 Effect of Breathing Pattern on Orientation-Averaged Mouth Inhalability

The effect of breathing pattern on orientation-averaged mouth inhalability is shown in Figure 3-10. The data presented are for a wind velocity of 1.0 m/s. The curves are similar in shape and there is no clear systematic pattern. A two-way ANOVA finds that the variance due to changes in breathing rate is significant ($p = 0.00213$) and that there is little interaction between breathing rate and particle size ($p = 0.0405$).

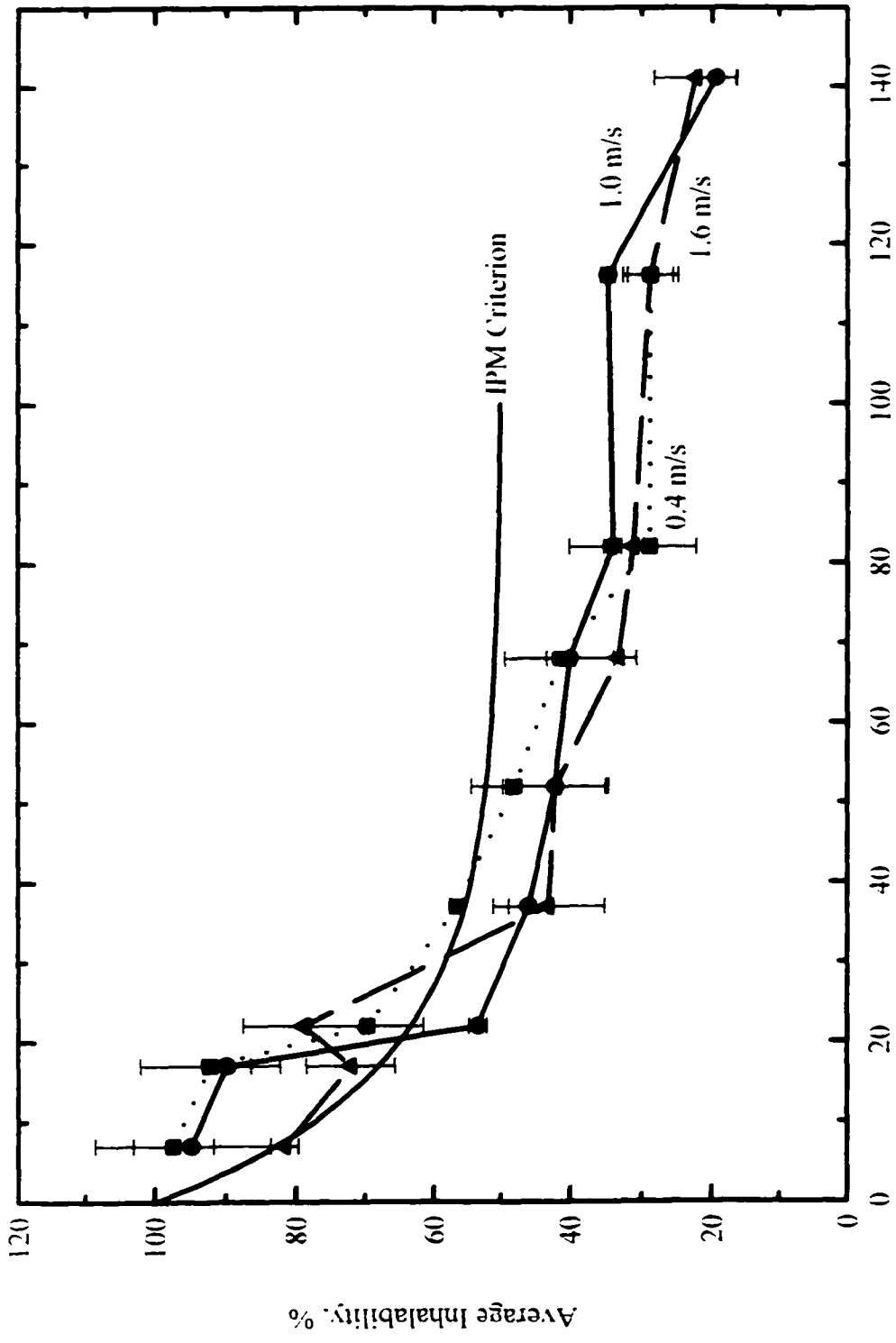

Figure 3-9: Effect of wind velocity on inhalability for orientation-averaged mouth breathing, minute volume = 20.8 L/min.

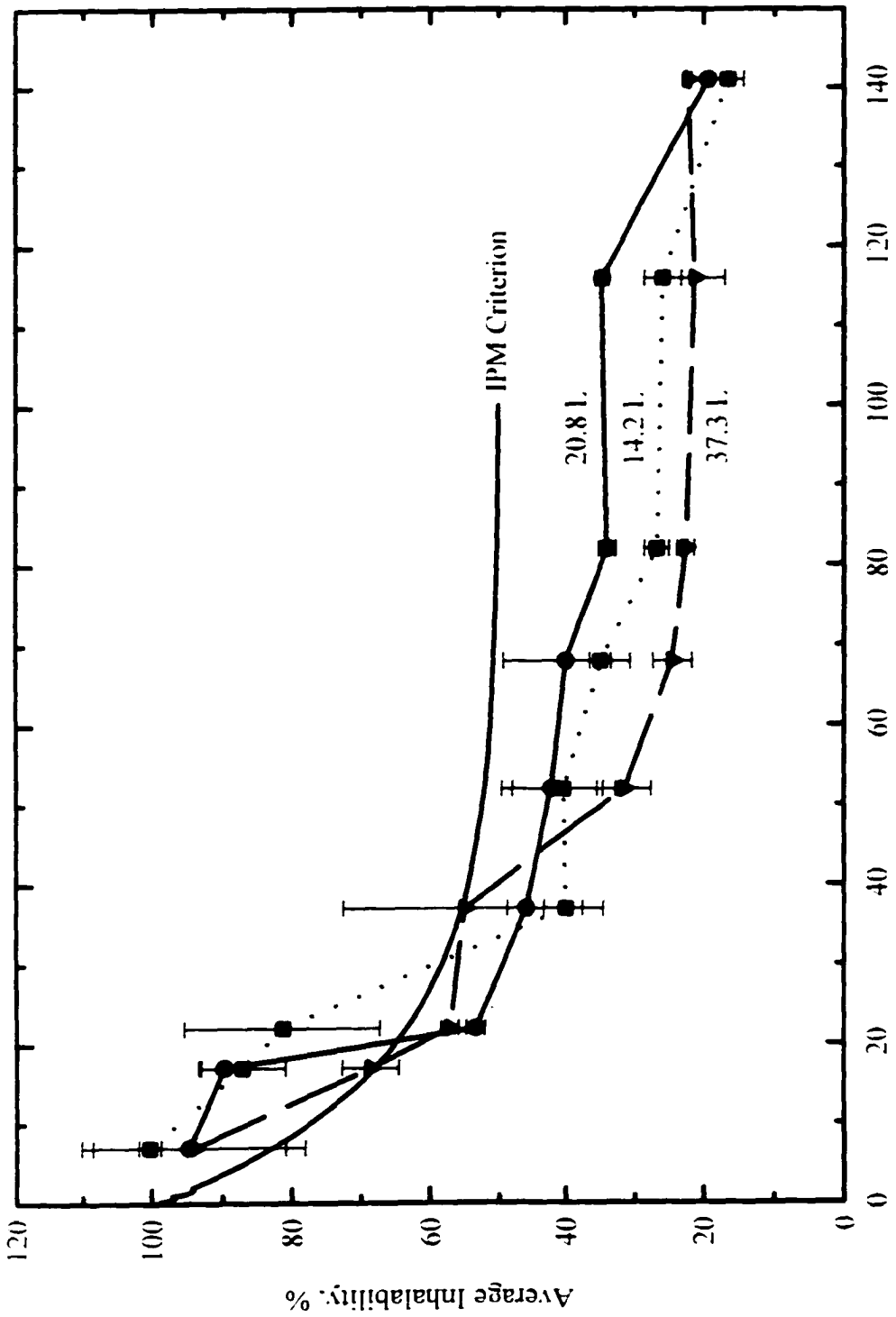

Figure 3-10: Effect of breathing pattern on inhalability for orientation-averaged mouth breathing, wind velocity = 1.0 m/s.

When comparing two curves at a time ($p < 0.05$), those for minutes volumes of 14.2 and 20.8 were not different, while those for 14.2 *vs.* 37.3 and 20.8 *vs.* 37.3 were Work by Ogden and colleagues (1977) found that the effect of breathing pattern was small and not particularly systematic; the data from this study confirm their finding. It is interesting to note that the middle breathing rate resulted in the highest inhalability. Perhaps, this is the result of differences in airflow pattern in the region near the mouth associated with variation in breathing rate.

3.3.1 Facing-the-Wind Mouth Inhalability

Figure 3-11 shows the combined data for facing-the-wind inhalability for mouth breathing. Inhalability plateaus at about 75% for particles between 20 and 115 μm and drops sharply to 50% for 140-μm particles. There are no previous studies for comparison and this represents the first evaluation of facing-the-wind inhalability for mouth breathing. For certain occupational environments this may be an important distinction. Large particle inhalability for workers facing into the oncoming wind is expected to be significantly higher than for workers exposed to omnidirectional airflow.

3.3.2.1 Effect of Wind Velocity on Facing-the-Wind Mouth Inhalability

The data for the effect of wind velocity on facing-the-wind mouth inhalability are illustrated in Figure 3-12. Again, the respiratory minute volume was 20.8 L/min. For particles larger than 70 μm, measured inhalability was greater with increased

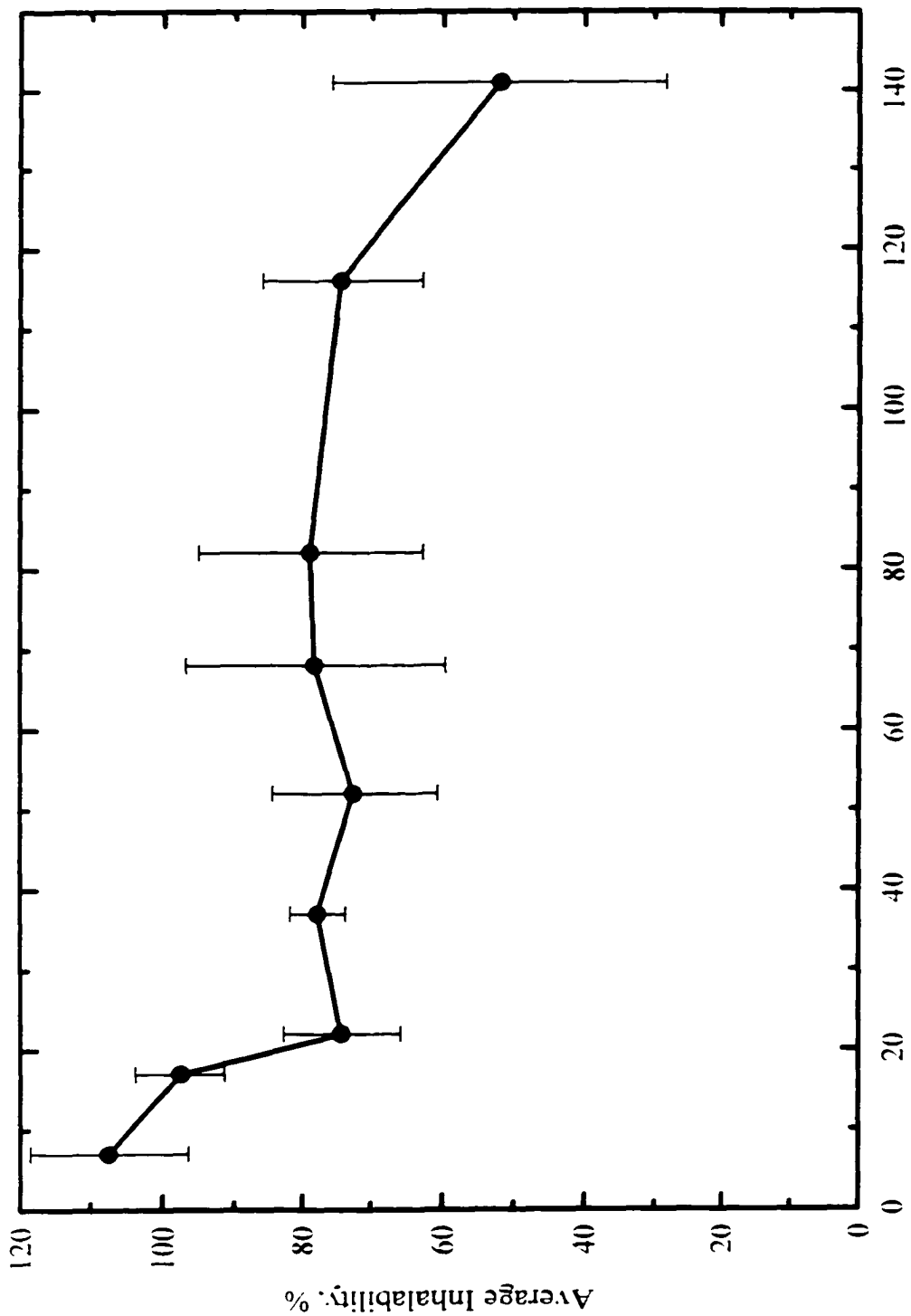

Figure 3-11: Inhalability for facing-the-wind mouth breathing, data for wind velocities and breathing patterns combined.

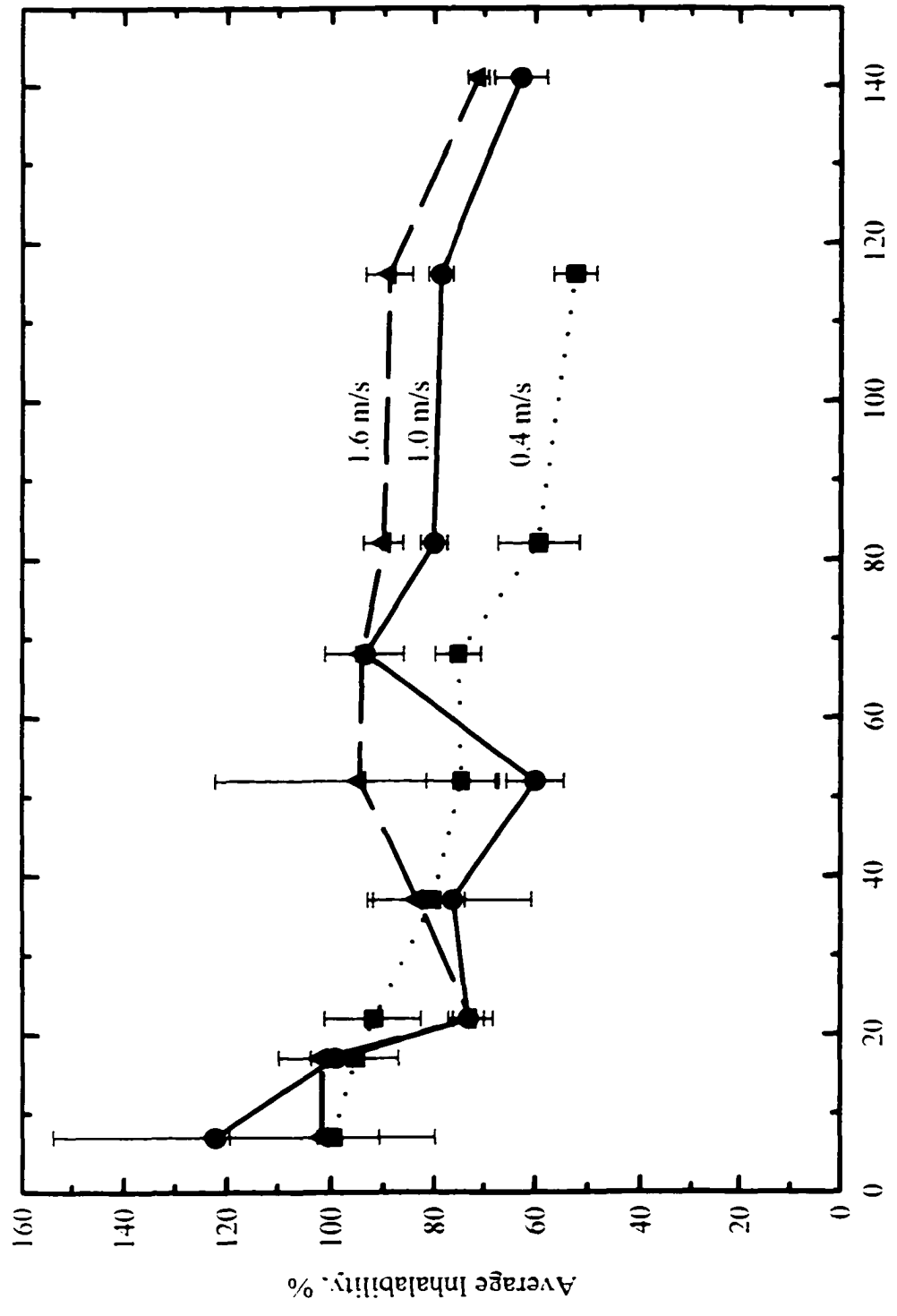

Figure 3-12: Effect of wind velocity on inhalability for facing-the-wind mouth breathing, minute volume = 20.8 L/min.

wind velocity. The results might be due to the competition between straight-line motion and settling for large particles. The effect appears to be systematic and a two-way ANOVA found a significant difference due to wind velocity ($p = 0.00440$); however, when two curves are compared at a time significant variation ($p < 0.05$) is found only between the lowest and highest wind velocity.

3.3.2.2 Effect of Breathing Pattern on Facing-the-Wind Mouth Inhalability

Figure 3-13 shows the effect of breathing pattern on mouth inhalability for facing-the wind conditions. Wind velocity was 1.0 m/s for all samples. In general, the results show no clear pattern and it is difficult to see any relationship between breathing pattern and inhalability. A closer look suggests that there may be some systematic effect for particles larger than 80 μm. A two-way ANOVA indicates that the effect of breathing rate is significant ($p = 0.0000925$) and that there is an interaction between breathing rate and particle size ($p = 0.00225$). Once more, this is the first study that attempts to evaluate the effect of breathing pattern for facing-the-wind conditions and there are no other investigations available for comparison.

3.3.3 Inhalability for Nose Breathing

Inhalability for orientation-averaged and facing-the-wind nose breathing is shown in Figure 3-14. Orientation-averaged nose inhalability drops quickly from more than 60% for particles smaller than 20 μm to a plateau at less than 10% for larger particles. Facing-the-wind nose inhalability drops from nearly 100% for 7-μm

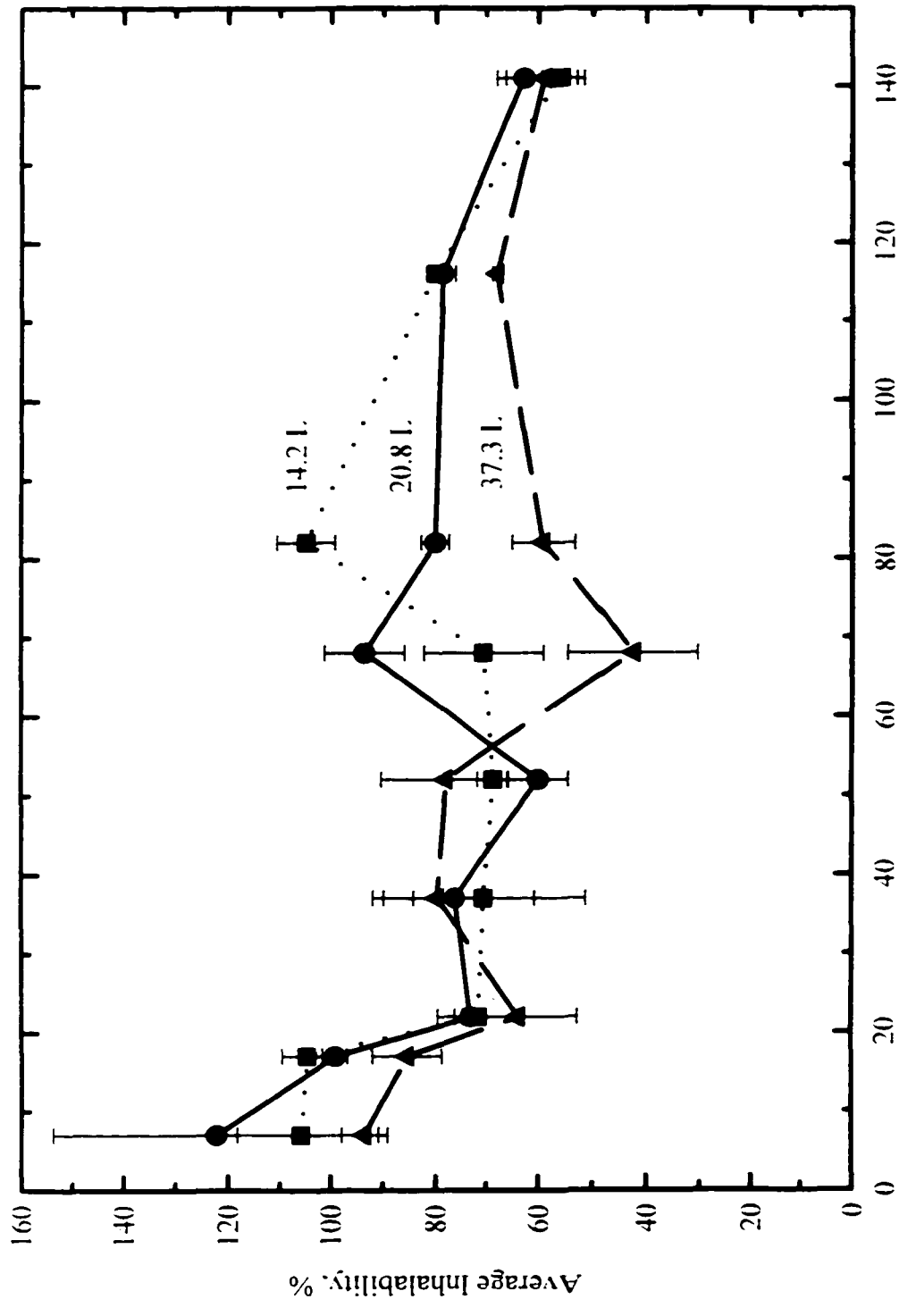

Figure 3-13: Effect of breathing pattern on inhalability for facing-the-wind mouth breathing, wind velocity = 1 m/s.

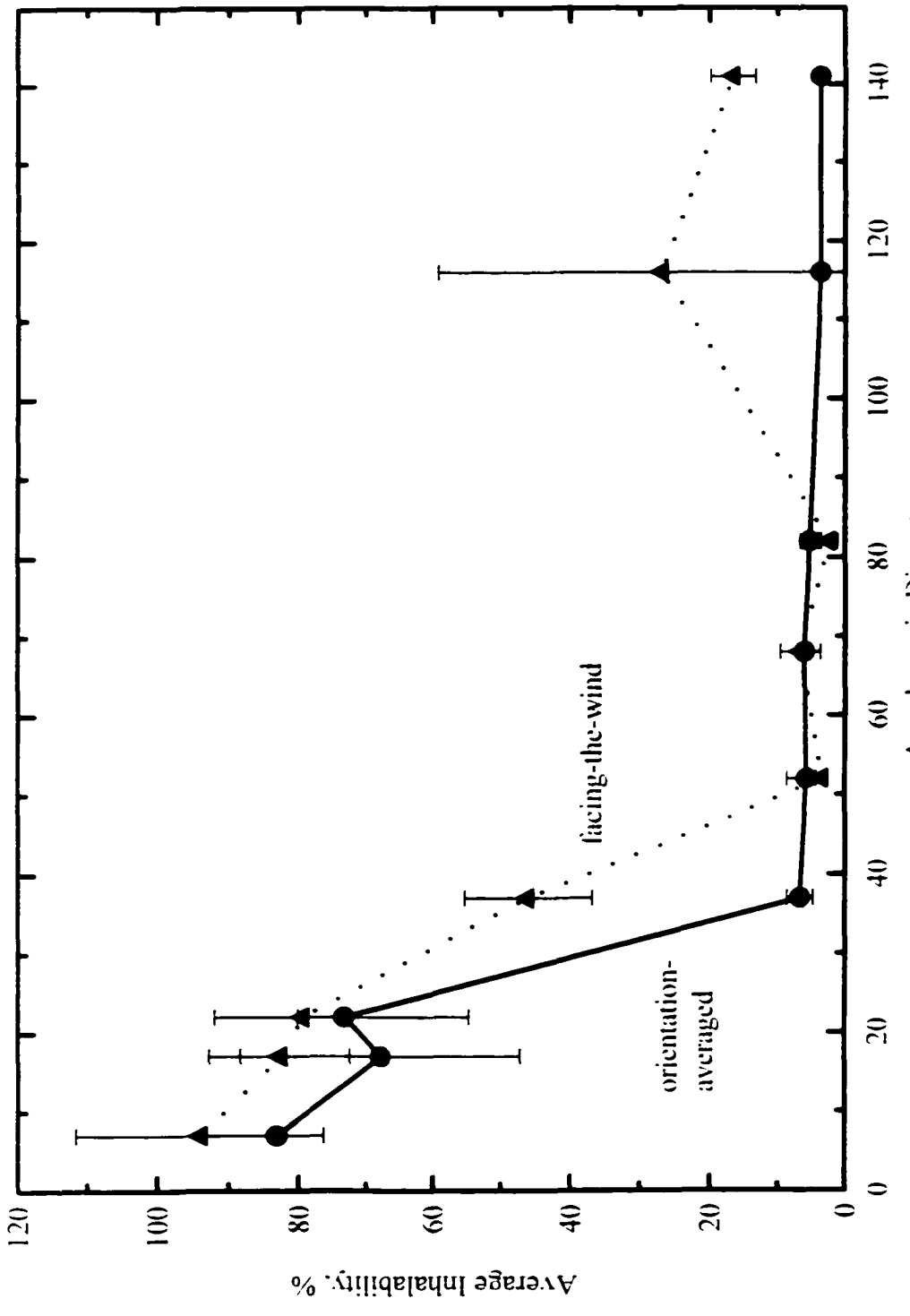

Figure 3-14: Inhalability for nose breathing.

particles to less than 10% for particles between 50 and 80 μm. For particles larger than 80 μm, there appears to be an increase in facing-the-wind nose inhalability, but the trend is not clear because of the large variability in the results for d_a = 116 μm.

For the range of particle sizes included in this study, inhalability for nose breathing does not appear to go to zero. This can be explained by the vertical motion of air, from the torso up toward the face, that can carry particles into the vicinity of the nose. This was the first study of nose inhalability and there are no published data for comparison.

3.4 Conclusion

In general, wind velocities in the range of 0.4 - 1.6 m/s and breathing patterns associated with minute volumes of 14.2 - 37.3 liters show little or no effect on measurements of mouth inhalability. Orientation with respect to wind direction has the greatest effect on inhalability and should be considered in reference to worker exposure monitoring. Facing-the-wind mouth inhalability is nearly twice that of orientation-averaged measurements for particles larger than 40 μm. This is an important difference for workers who face the oncoming wind and are exposed to large particles. It means that their exposure to particles larger than 40 μm could be double the value predicted by a sampler designed to match an orientation-averaged curve, like the current IPM criterion.

The inhalability curve found here shows a significant deviation from the IPM criterion. The source of the difference is unknown, but may be related to differences in experimental set up. This investigation took care to minimize sampling errors and have confidence in the data. Additionally, the curve has been extended beyond 100 μm to 140 μm. The results suggest that a revision of the current ACGIH/CEN/ISO IPM criterion is needed, if for no other reason than to include particles larger than 100 μm.

A common trend in all of the curves for mouth inhalability is the consistent decrease in inhalability for particles larger than 116 μm. Certainly, the loss is related to aerodynamic behavior of the particles. It may be related to a complicated interaction between particle physics and air motion in the region of the mouth. Possibly, it is a result of the competition between horizontal velocity and settling velocity. It is an interesting trend and warrants future investigation.

This was the first study to look specifically at the difference between orientation-averaged and facing-the-wind mouth inhalability. Figure 3-15 shows the effect of mannequin position on the combined results of mouth inhalability for all wind velocities and breathing patterns studied. Facing the wind inhalability is nearly twice that of orientation-averaged measurements for particles with an aerodynamic diameter greater than 40 μm. This is an important difference for workers who face the oncoming wind, such as, some machinists or forklift truck operators working

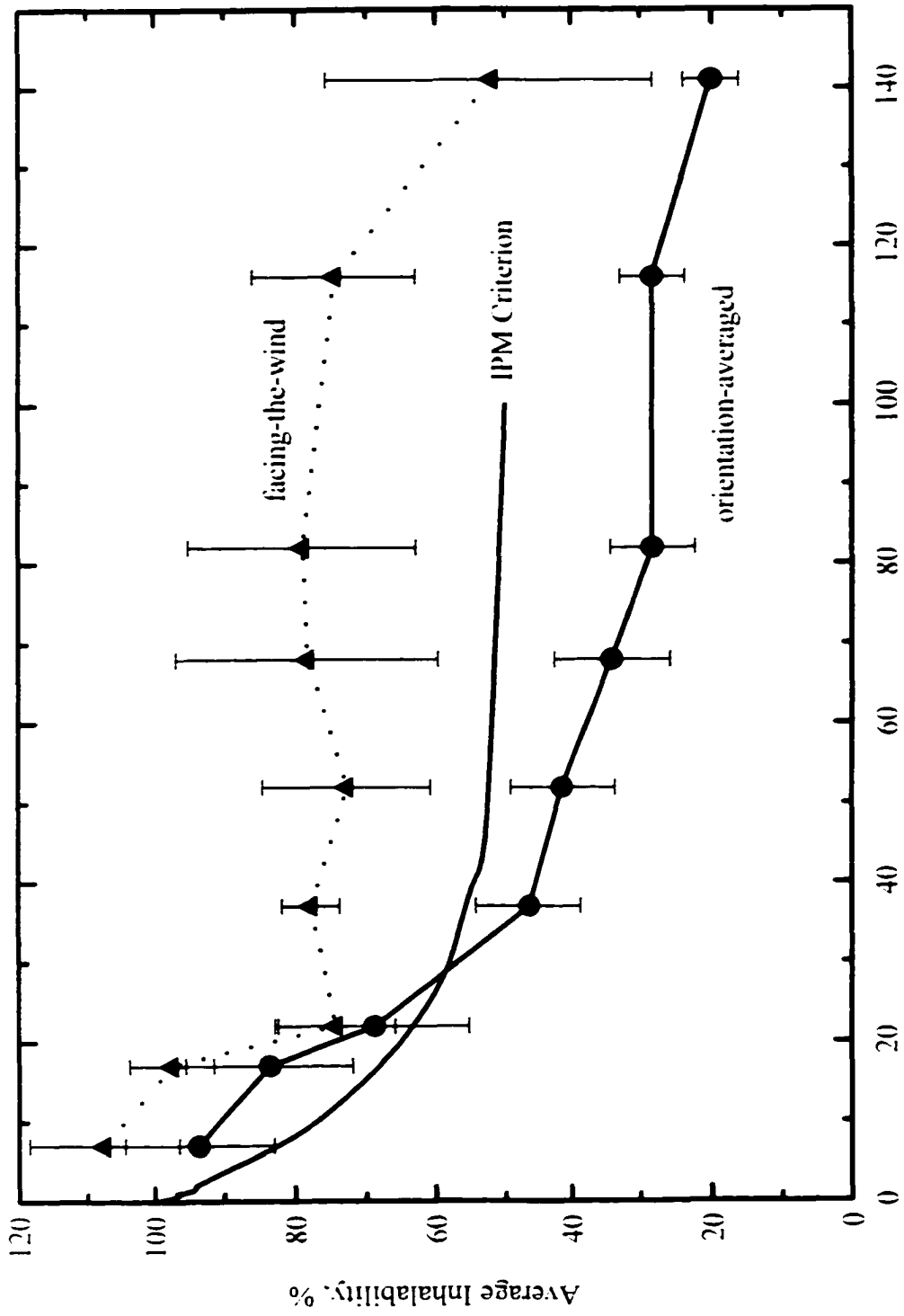

Figure 3-15: Inhalability for mouth breathing.

within an airflow field. It means that their exposure to particles larger than 40 μm could be double that predicted by a personal sampler designed to meet the accepted IPM criterion.

The inhalability curves for nose breathing are notably different than the IPM criterion. Personal sampling devices designed to meet the IPM curve will overestimate the exposure contribution of particles larger than 30 μm. While this is unlikely to result in overexposure to toxic aerosols, it may not provide an accurate representation of exposure for nose-breathing workers.

Chapter 4: Performance of Personal Inhalable Samplers

4.0 Introduction

Personal monitoring of employee exposures began as an improved way to assess potential hazards. Workers are generally exposed to localized sources of airborne contaminants and concentrations fall quickly with distance from the source. This is especially true for large particles. Consequently, the best location for placement of a sampler is within the breathing zone of the worker, where the sampled concentration should be representative of the exposure to the worker. This notion led to the development of small sampling devices that can be clipped to a collar or otherwise placed within 30 cm of the mouth and nose and attached to a light-weight, battery-powered, constant-flow pump, usually worn at the waist.

The body of a person wearing a personal sampler becomes, in effect, part of the sampler because it will affect air currents in the vicinity of the sampler, which affect the aspiration efficiency of the sampling device. Blunt sampler theory, reviewed by Vincent (1989), indicates that personal sampler performance will not be the same when worn attached to a worker compared to the performance when the sampler isolated from the body. It is for this reason that personal sampler performance should be tested on a full-size human mannequin.

In the US, airborne particles have been sampled as "total" dust using a 37-mm in-line filter cassette with a 4-mm inlet, except when respirable fraction sampling is required. A "total" dust sample was thought to be representative of the ambient aerosol concentration (Beaulieu *et al.*, 1980: Fairchild *et al.*, 1980), but this sampling method has been shown to undersample large particles and underestimate both the ambient concentration and the inhalable fraction (Buchan *et al.*, 1986). Side-by-side field comparisons of 37-mm in-line "total" dust samplers and IOM inhalable samplers have been conducted (Vinzents, 1988; Notø *et al.*, 1996; Wilsey *et al.*, 1996). All have found that the concentration measured by the inhalable sampler is greater than that measured by the "total" dust sampler. In general, the larger the particles, the larger the difference in measured concentration, indicating that the 37-mm in-line filter cassette undersamples large particles. A comparison study performed in a lead smelter (Spear *et al.*, 1997) found that the ratio of sampling efficiency for the IOM to that of the 37-mm cassette ranged from 1.39 to 2.14 for lead and 1.29 to 2.12 for cadmium.

4.1 Background

The establishment of particle size-selective criteria has created a need for personal sampling instruments that will accurately measure the aerosol fractions. Several designs for inhalable samplers have come to the fore; these include the CIP-10 (Courbon *et al.*, 1983), the Institute of Occupational Medicine (IOM) inhalable sampler (Mark and Vincent, 1986), the GSP sampler, and the PERSPEC sampler

(Prodi *et al.*, 1986) among others. In turn, this has created a need for the evaluation of inhalable sampler performance. A very small number of studies have focused on the development and characterization of inhalable samplers (Mark and Vincent, 1986; Chung *et al.*, 1987; Vincent and Mark, 1990). Most notably, Kenny *et al.* (1997) evaluated eight different samplers using wind speeds of 0.5, 1 and 4 m/s and particle sizes ranging from 7 - 100 μm. In general, these studies found that only one of the currently available devices shows reasonable agreement with the IPM criterion, the IOM (Institute of Occupational Medicine) personal sampler, developed by Mark and Vincent (1986). The IOM personal sampler is the most commonly used device in the US for measuring the inhalable fraction of coarse dusts.

4.2 Experimental

The use of the UCLA low-velocity wind tunnel and a full-size, full-torso mannequin for the inhalability study presented an opportunity for a simultaneous evaluation of personal inhalable samplers. The samplers listed below were tested under the same wind velocity and mannequin orientation conditions described in Chapter 3 for the inhalability study. The goal of the present study was to evaluate the performance of the eight samplers listed below over the full range of particle sizes and to investigate and compare the effect of various inlet sizes and sampler positions. The IOM has a 15-mm inlet and, when properly attached to a worker's lapel, faces forward. The 37-mm in-line cassette commonly used for "total" dust sampling has a 4-mm inlet and faces roughly 60° to 70° below the horizontal plane.

The eight samplers evaluated were the:

1. 37-mm in-line cassette with 4-mm inlet positioned downward, the
2. 37-mm in-line cassette with 4-mm inlet positioned forward, the
3. 37-mm open face cassette (32-mm inlet) positioned downward, the
4. 37-mm open face cassette (32-mm inlet) positioned forward, the
5. 37-mm in-line cassette with 8-mm inlet positioned forward, the
6. 37-mm in-line cassette with 16-mm inlet positioned forward, the
7. IOM personal sampler, and the
8. Marple personal cascade impactor, inlet and final stage only.

The samplers evaluated in this study were either positioned forward, like the proper alignment of an IOM sampler, or positioned downward, as is the case for a 37-mm "total" dust sampler worn by a worker. In order to position the samplers fashioned from 37-mm cassettes to face forward, a brass backing plate was designed with a clip for attachment to the lapel.

The 37-mm cassettes (SKC, Inc., Eighty-Four, PA, Catalog No. 225-2) are made of polystyrene and the IOM personal sampler (SKC, Inc., Eighty-Four, PA, Catalog No. 225-70) is made of conductive plastic. 37-mm cassettes with 4-mm inlets were used to construct the 37-mm samplers with 8-mm and 16-mm inlets. Automotive body repair paste (Dynatron/Bondo® Corp., Atlanta, GA, P/N 310) was used to fill the top of the cassette. Then, an inlet hole of the appropriate size was drilled in the center

and a lathe was used to create a 3-mm lip around the inlet. Figure 4-1 shows the different samplers and the brass backing plate.

The inlet of the Marple personal cascade impactor was selected for evaluation because it is a device that is commonly used to determine the particle size distribution of personal exposures (Lodge and Chan, 1986). The 26-mm circular inlet is covered by a faceplate that causes the air stream to diverge before entering the sampler. It is useful to evaluate the ability of the inlet to match the inhalability criterion

During each experimental run, two personal samplers were attached to the lapel on either side of the front of the mannequin's torso (refer to Figure 3-5). The sampling devices were connected with Tygon® tubing to SKC Airchek Model 224-PCXR4 personal sampling pumps (SKC, Inc., Eighty-four, PA). The pumps were operated at 2.0 L/min. The sampling strategy for the inhalability study allowed collection of at least 24 measurements for each sampler. Two samplers, the IOM and the 37-mm in-line facing down, were evaluated at all three wind velocities (0.4, 1.0, and 1.6 m/s), while the remaining samplers were evaluated at 1.0 m/s only. The performance of all eight samplers was measured for both orientation-averaged and facing-the-wind conditions.

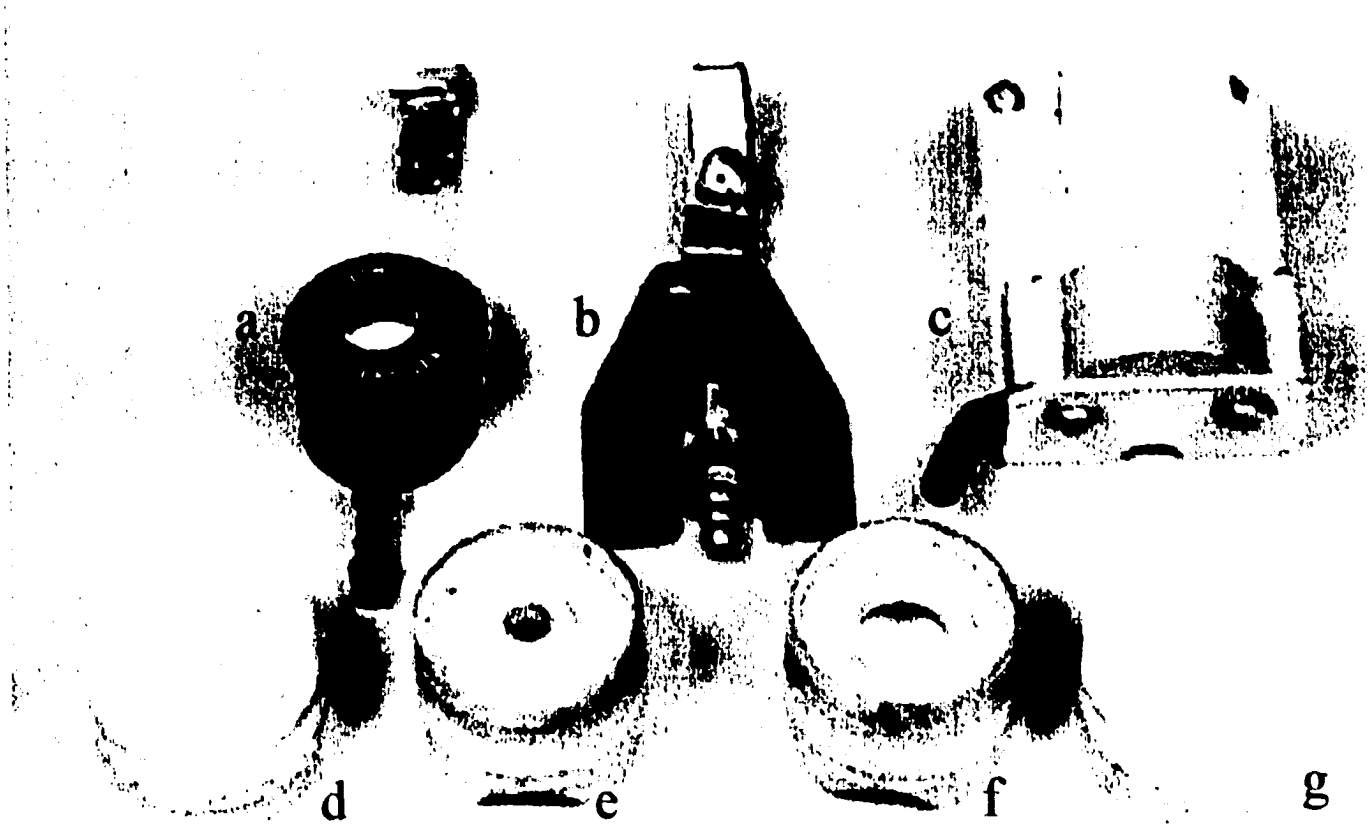

Figure 4-1: Personal samplers: (a) IOM sampler, (b) backing plate for 37-mm cassettes, (c) Marple personal cascade impactor, (d-g) 37-mm in-line cassettes with inlets of 4, 8, 16, and 32 mm.

The performance of each sampler was evaluated by its aspiration efficiency, E_f. Aspiration efficiency is the ratio of the aerosol concentration measured by the sampler, C_f, to the true wind tunnel concentration, C_o, measured by the isokinetic samplers. The relationship is expressed as:

$$E_f = \frac{C_f}{C_o} \tag{4.1}$$

The aspiration efficiency as a function of particle size can then be compared to the IPM criterion to determine the ability of the sampler to match the curve. The better the agreement between the sampler curve and the IPM curve, the more likely the sampler is a good candidate for monitoring worker exposure to inhalable particles.

4.3 Results and Discussion

The results for aspiration efficiency as a function of particle size for each of the eight sampler options are shown in Figures 4-2(a) through 4-2(h) for both orientation-averaged and facing-the-wind positioning. The IPM criterion is included on each of the graphs for comparison.

4.3.1 Performance of the Eight Samplers

The traditional "total" dust sampler (Figure 4-2(a)) shows a similar trend in aspiration efficiency for both orientation conditions with the orientation-averaged results lower than those for facing-the-wind. The orientation-averaged results

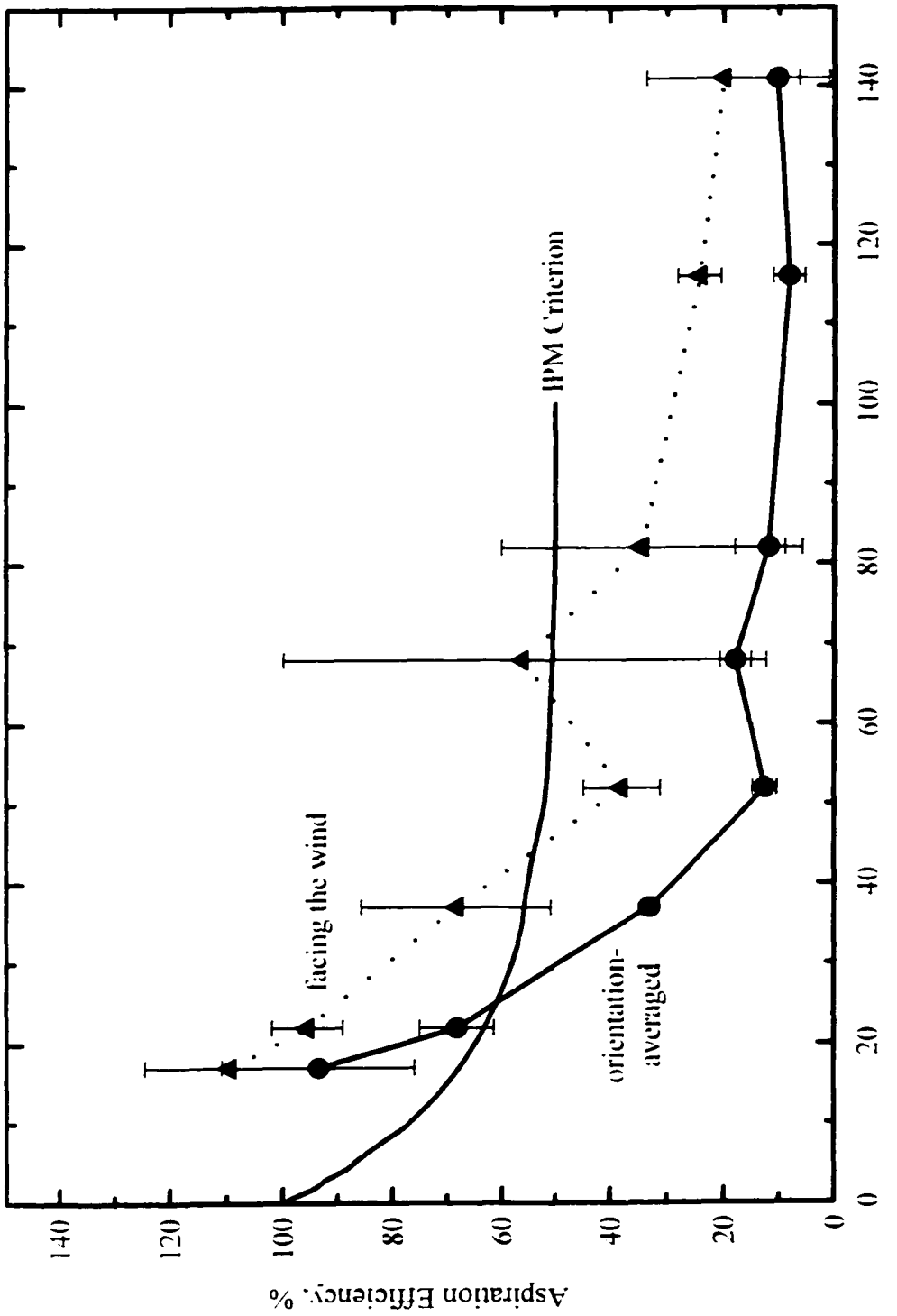

Figure 4-2(a): Performance curves for the 37-mm in-line cassette with a 4-mm inlet, positioned downward.

plateau at about 15% for particles larger than 50 μm. For particles larger than 40 μm the curve is notably lower than the IPM criterion. The results confirm the findings of previous studies, which found that the "total" dust sampling method commonly used in the US underestimates the contribution of large particles. Figure 4-2(b) shows the results for the same sampler when faced forward. The aspiration efficiency is reasonably close for both orientations with respect to wind direction. There is no systematic difference in the effects.

An open face (32-mm inlet) cassette when faced down, as is the case with most monitoring for occupational exposure, does not appear to be a good choice for sampling inhalable particles (Figure 4-2(c)). Aspiration efficiency seems to be independent of wind direction, but the device oversamples particles smaller than 50 μm while undersampling particles larger than 70 μm. Figure 4-2(d) illustrates the aspiration efficiency when the open face cassette is positioned forward. There is tremendous oversampling of particles larger than 50 μm with a more than six-fold increase in the orientation-averaged collection of 116-μm particles compared to the extrapolated IPM criterion curve. There is a rapid drop in aspiration efficiency from just over 300% for 116-μm particles to about 10% for particles with an aerodynamic diameter of 141 μm. The reason for this is unclear. One possible explanation is that 141-μm particles may have enough inertia to bounce off the filter and be lost from the sample, while 116-μm particles adhere to the filter.

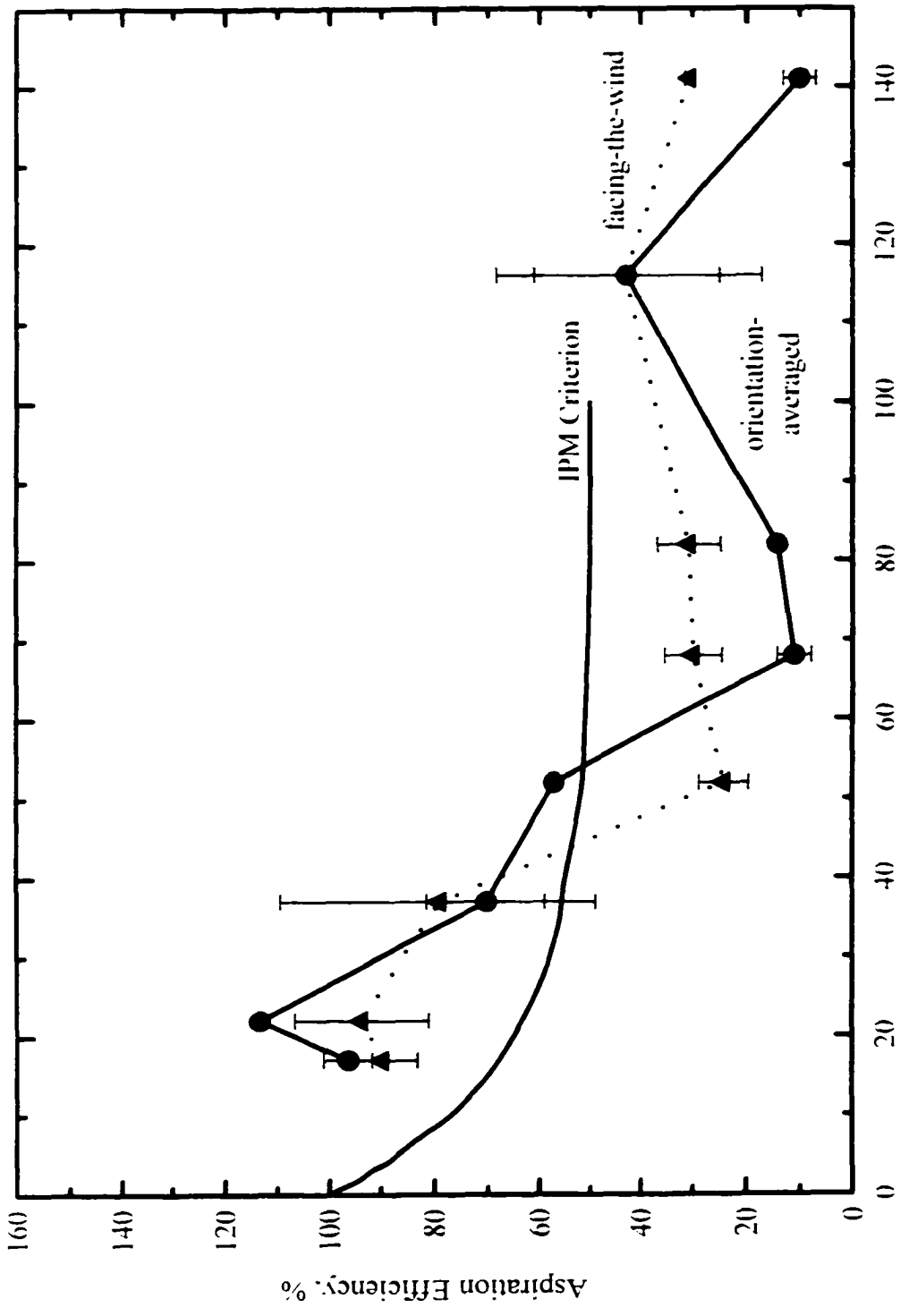

Figure 4-2(b): Performance curves for the 37-mm in-line cassette with a 4-mm inlet, positioned forward.

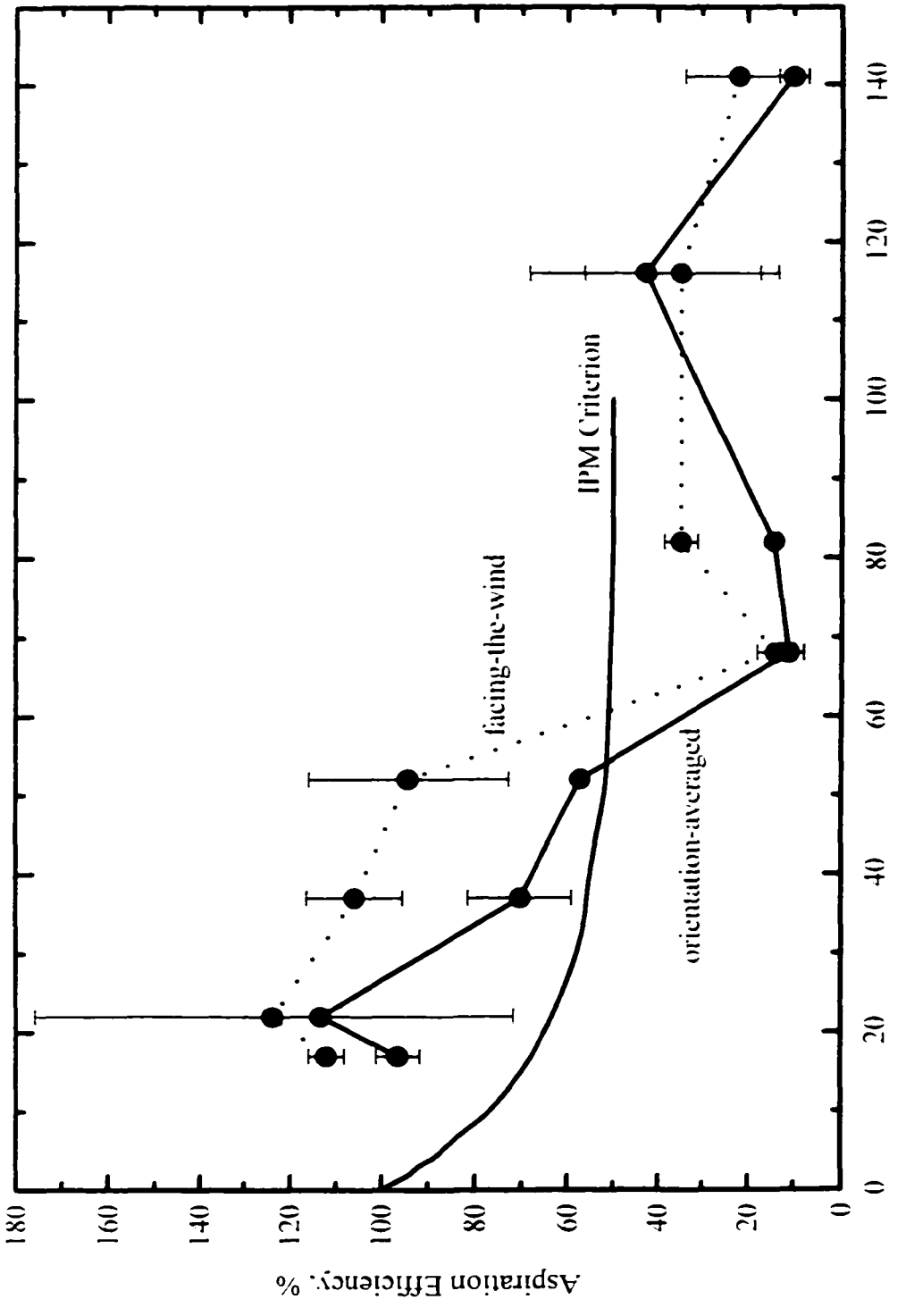

Figure 4-2(c): Performance curves for the 37-mm in-line cassette with a 32-mm inlet (open face), positioned downward.

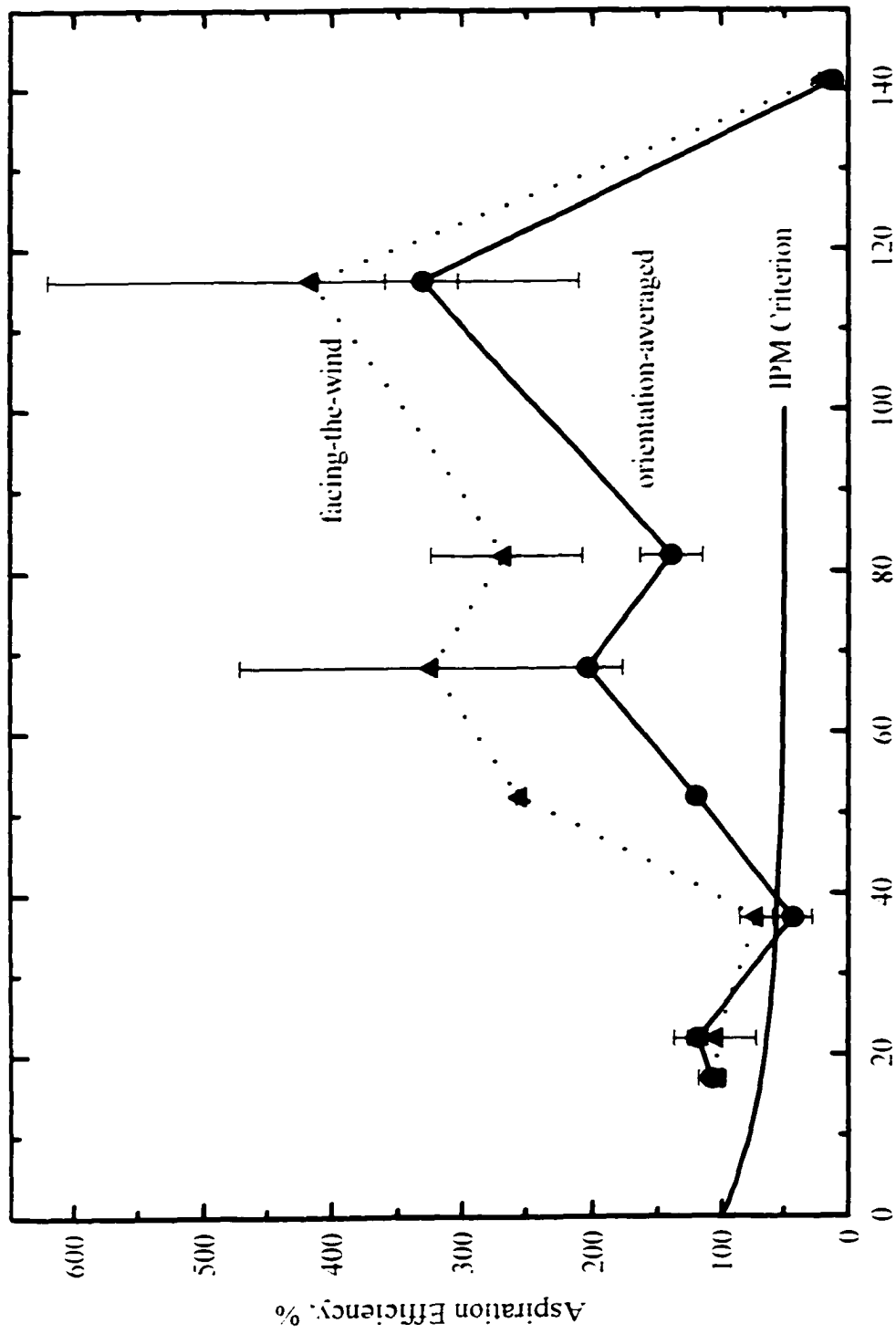

Figure 4-2(d): Performance curves for the 37-mm in-line cassette with a 32-mm inlet (open face), positioned forward.

The IOM personal inhalable sampler shows very good agreement with the IPM criterion for orientation-averaged measurements (Figure 4-2(e)). The data are consistent with those published by other investigators (Mark and Vincent, 1986; Kenny *et al.*, 1997). The extension of the efficiency curve beyond 100 μm shows a plateau at about 75%. The facing-the-wind data indicate that the sampler overestimates the contribution of particles larger than 50 μm and that the effect becomes increasingly pronounced with an increase in particle size.

Figure 4-2(f) shows the performance of the Marple personal cascade impactor. The orientation-averaged results show good agreement with the IPM criterion for particle sizes out to 70 μm. The results for the facing-the-wind condition generally overestimate the concentration of large particles. There is a divergence in the data sets that increases with increasing particle size.

For a 37-mm cassette fitted with an 8-mm inlet and positioned forward, the trend in aspiration efficiency data for orientation-averaged sampling is similar to that for facing-the-wind measurements (Figure 4-2(g)). The orientation-averaged data show a fairly good fit to the inhalability criterion. When the size of the inlet is increased to 16-mm, as shown in Figure 4-2(h), the device oversamples particles larger than 70 μm for orientation-averaged sampling. The facing-the-wind condition exhibits an increase in the general aspiration efficiency trend for the very largest particles, 141 μm.

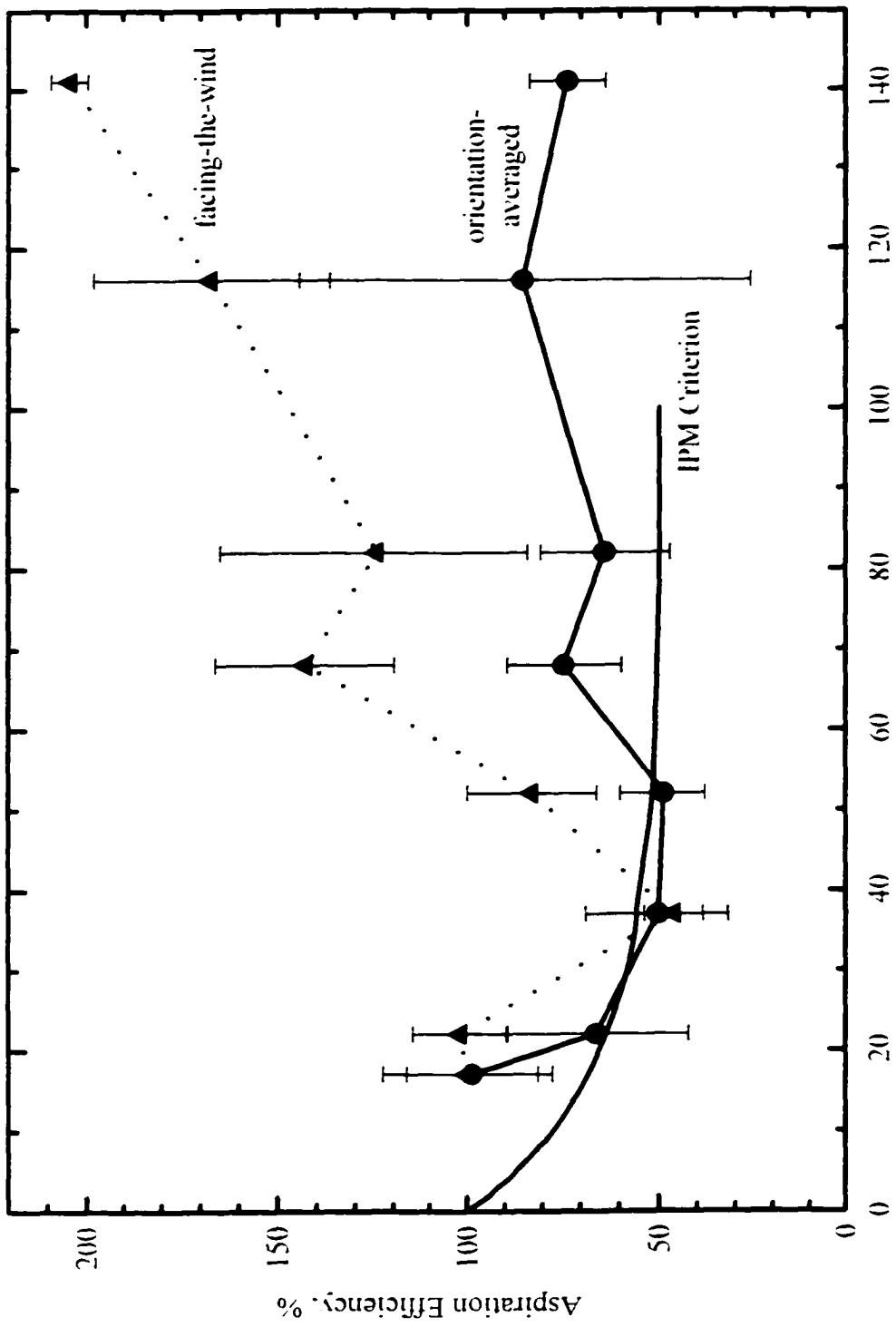

Figure 4-2(e): Performance curves for the IOM personal inhalable sampler.

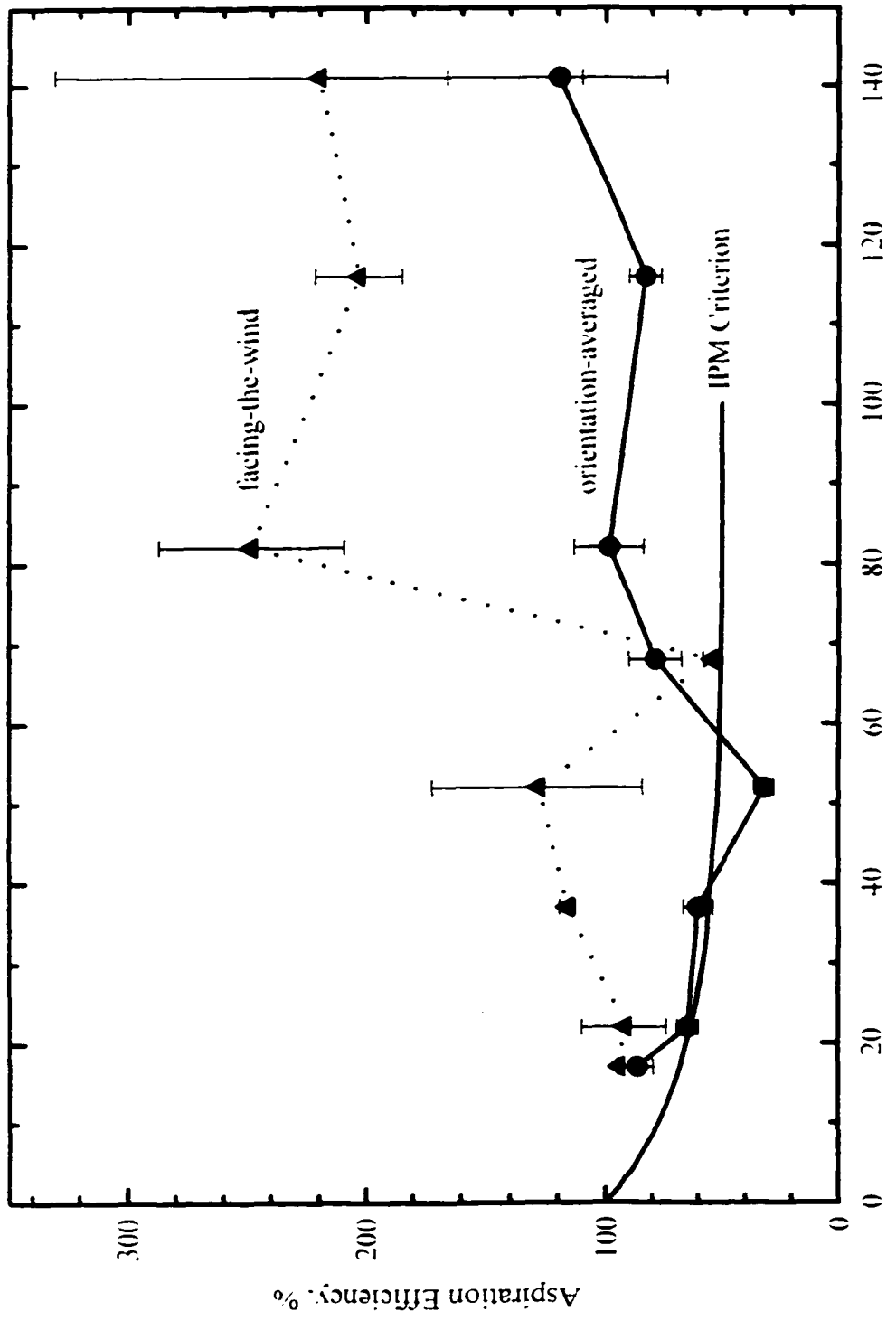

Figure 4-2(f): Performance curves for the Marple personal cascade impactor.

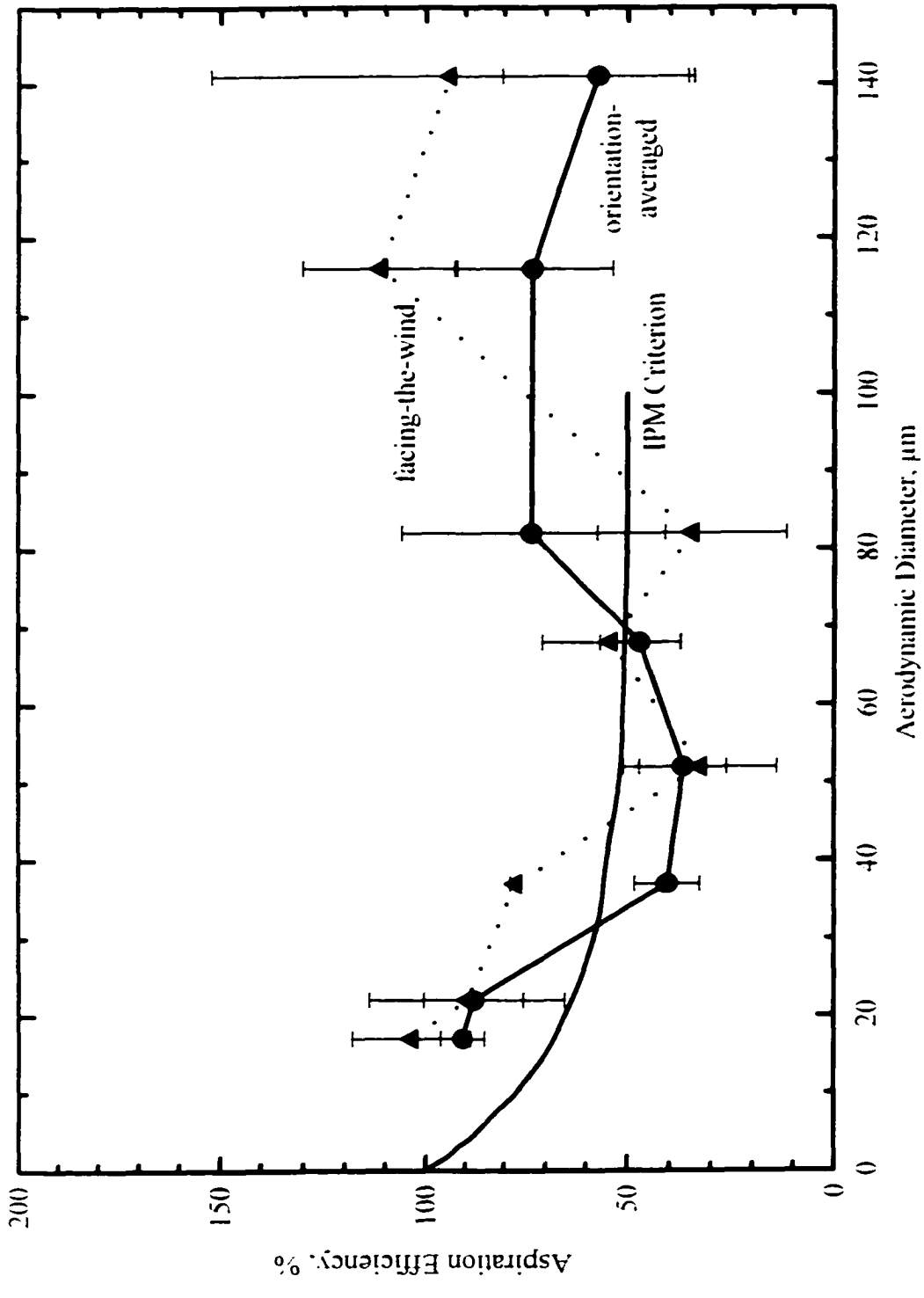

Figure 4-2(g): Performance curves for the 37-mm in-line cassette with an 8-mm inlet, positioned forward.

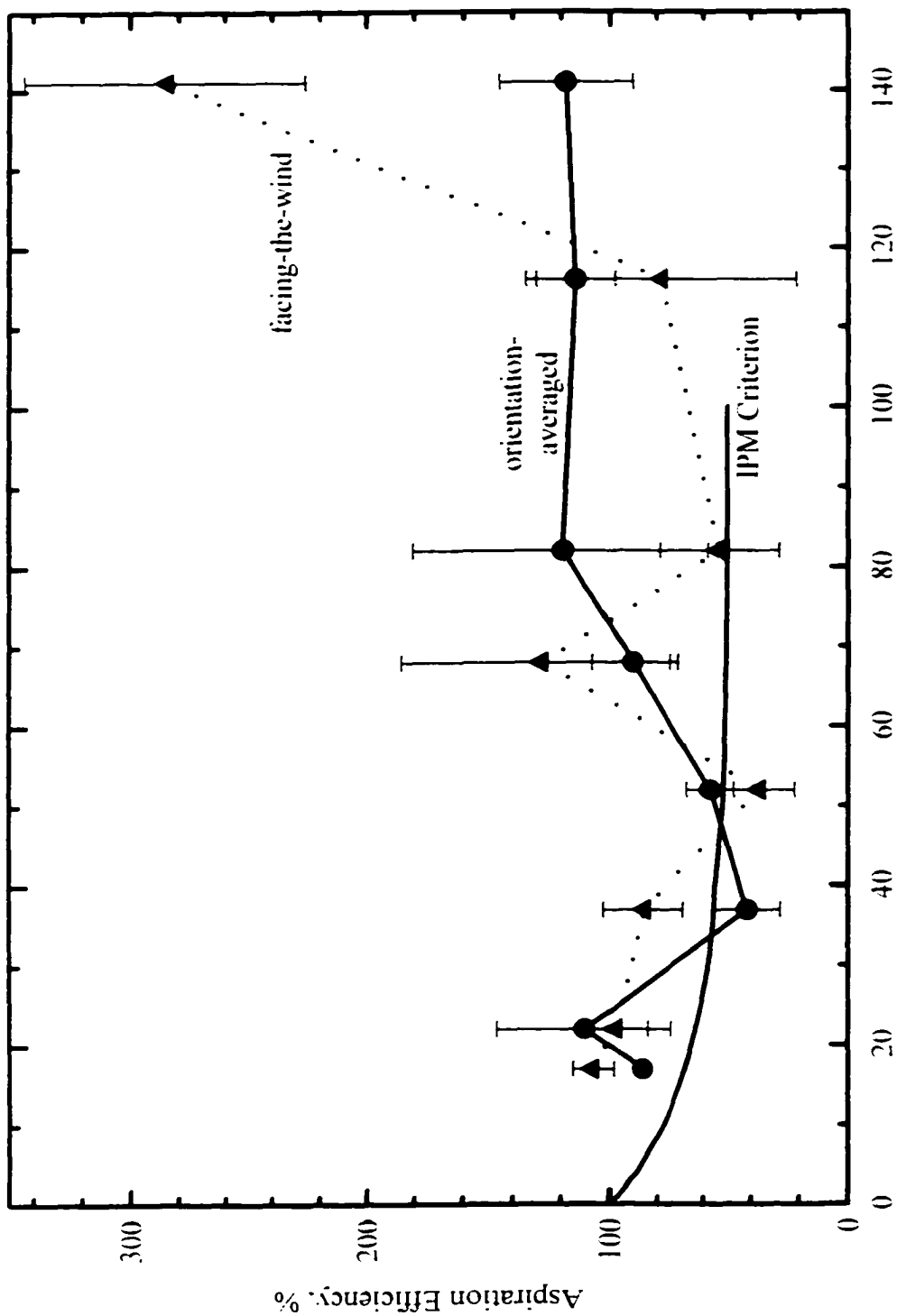

Figure 4-2(b): Performance curves for the 37-mm in-line cassette with a 16-mm inlet, positioned forward.

4.3.2 Effect of Wind Velocity

The data indicate that wind velocity, in the range of 0.4 - 1.6 m/s, has no effect on orientation-averaged performance for the 37-mm "total" dust sampler (Figure 4-3). When the same sampler faces the wind, there appears to be systematic effect for particles between 60 and 100 μm; aspiration efficiency is lower for lower wind velocities. Above 100 μm, the trend may reverse. The data are not clear (Figure 4-4).

The effect of wind velocity on orientation-averaged performance of the IOM is given in Figure 4-5. The effect appears to be systematic; the lower the wind velocity, the higher the aspiration efficiency for a given particle size. At 0.4 m/s, there is noticeable deviation from the IPM criterion. The sampler performance curve closely matches low air velocity inhalability results published by Aitken *et al.* (1999) for a respiratory rate of 20 L/min, suggesting that the IOM sampler may also be appropriate for monitoring worker exposure to inhalable particles less than 100 μm when wind velocities are low. When the IOM sampler faces into the wind during sampling, as shown in Figure 4-6, the effect of wind velocity is unclear and may be obscured by wide variation in the data.

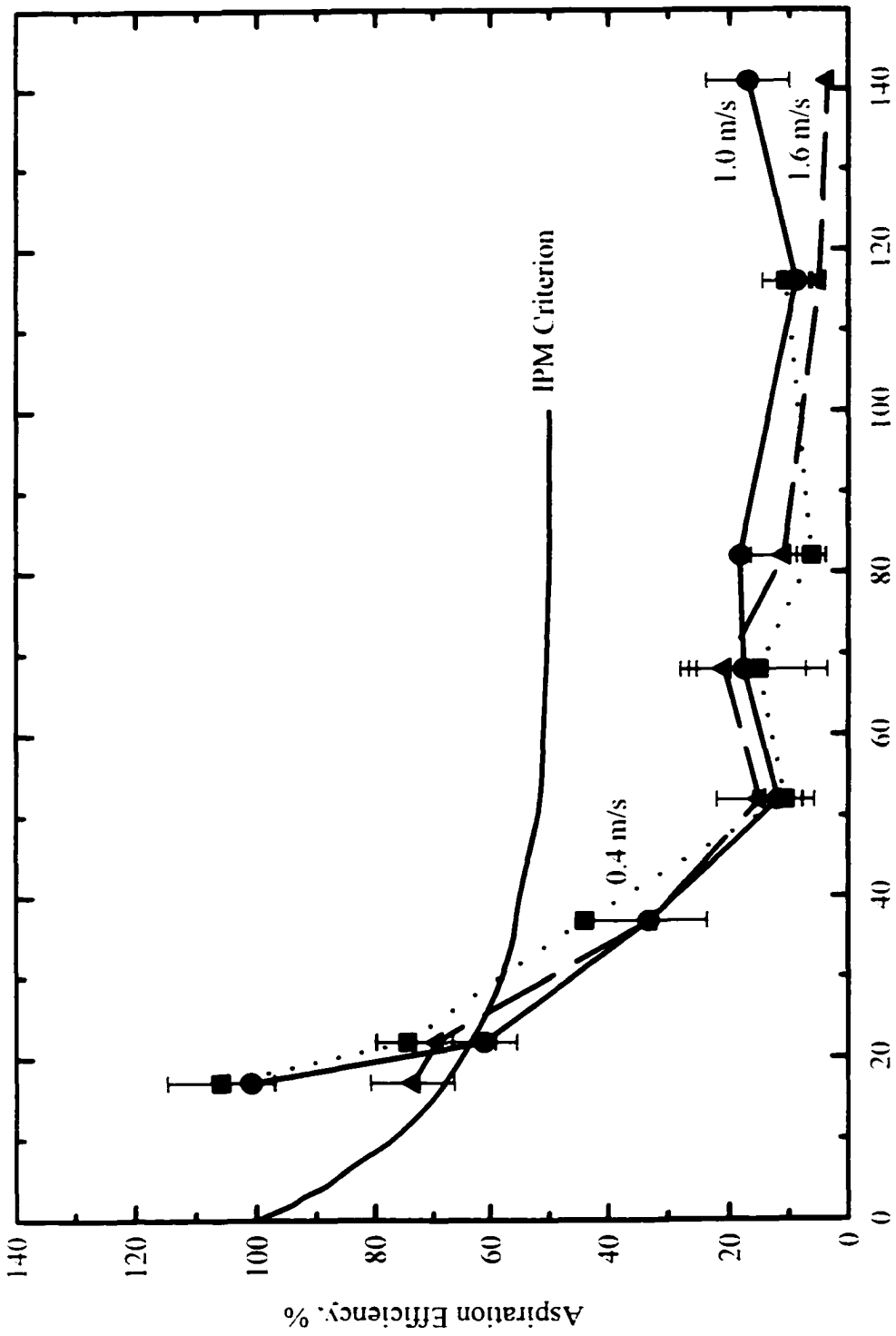

Figure 4-3: Effect of wind velocity on orientation-averaged performance of the 37-mm in-line cassette with a 4-mm inlet, positioned downward.

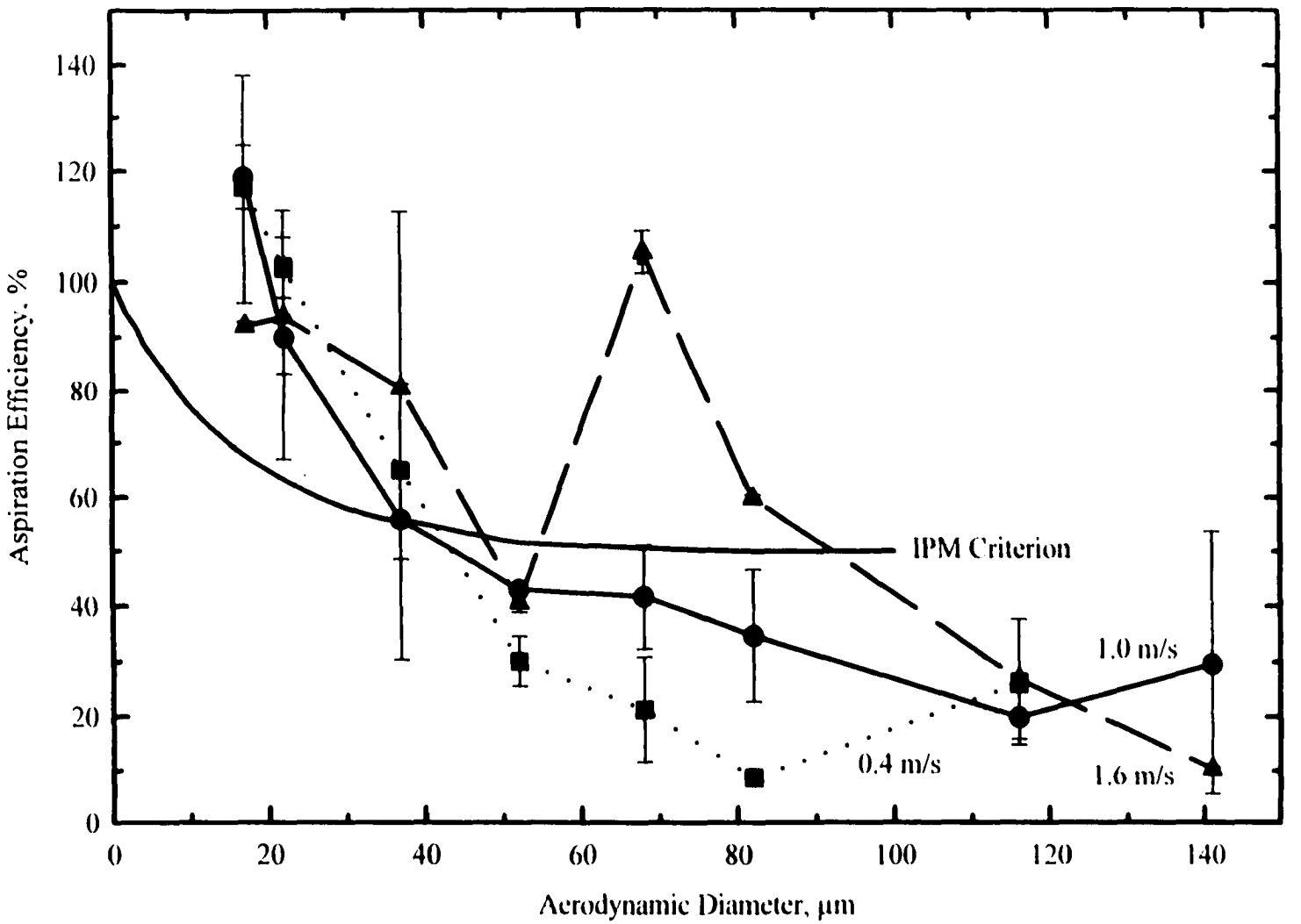

Figure 4-4: Effect of wind velocity on facing-the-wind performance of the 37-mm in-line cassette with a 4-mm inlet, positioned downward.

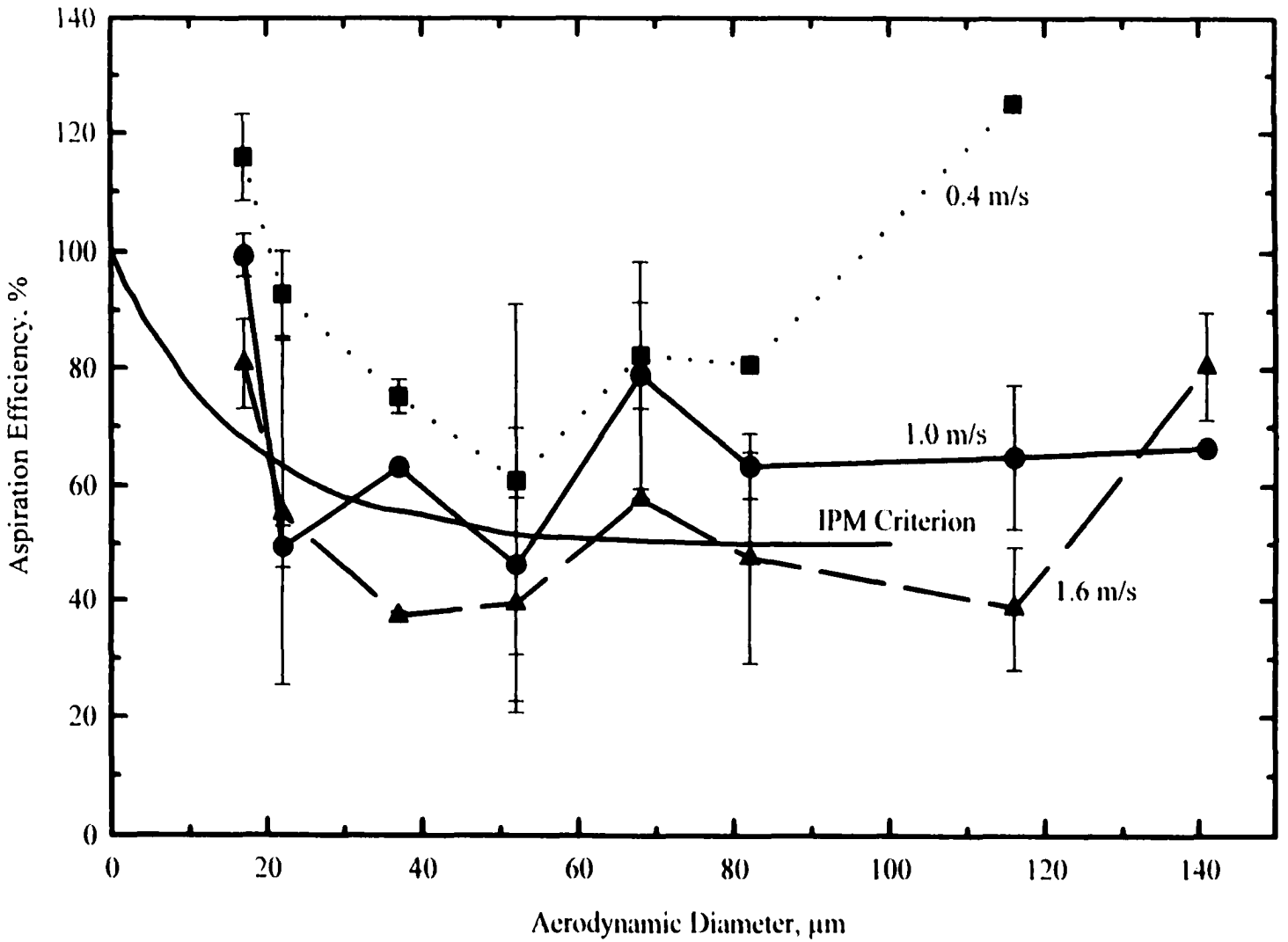

Figure 4-5: Effect of wind velocity on orientation-averaged performance of the IOM personal inhalable sampler.

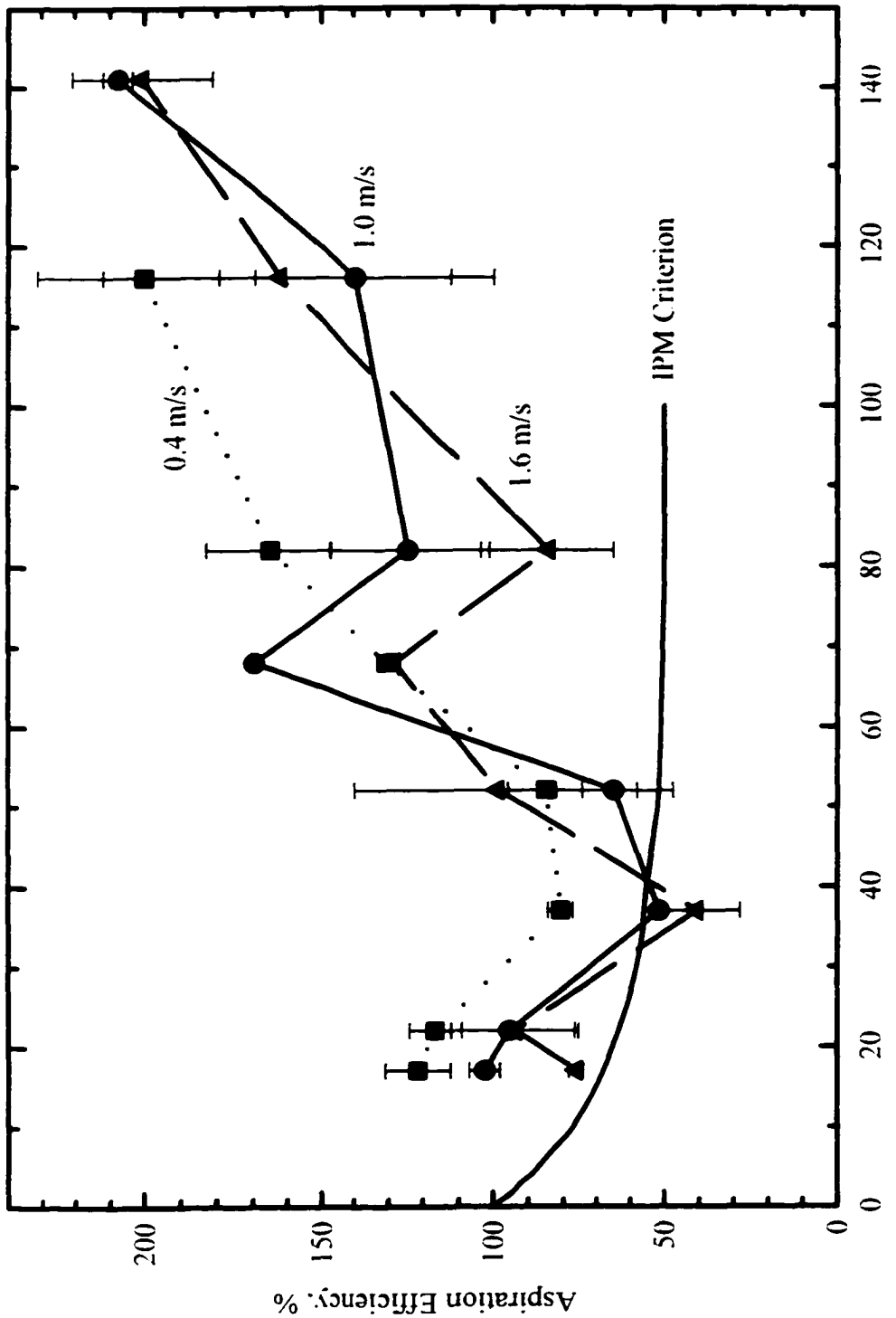

Figure 4-6: Effect of wind velocity on facing-the-wind performance of the IOM personal inhalable sampler.

4.3.3 Effect of Sampler Position

Figures 4-7 and 4-8 show the difference in orientation-averaged performance, as a function of sampler positioning for the 37-mm cassette with a 4-mm inlet and the open face, or 32-mm inlet, cassette. Both inlets show higher aspiration efficiency for the facing forward position. For the 4-mm inlet, there is decreasing aspiration efficiency with increasing particle size in either position. As particle size increases, the 32-mm inlet generally shows increasing efficiency when facing forward and decreasing efficiency when facing down.

An interesting result is the rapid increase in facing-the-wind aspiration efficiency for 116 and 141-μm particles observed for samplers with a large, unobstructed, forward-facing inlet. This includes the IOM sampler, the 37-mm cassette with 16-mm inlet and the open face (32-mm inlet) cassette. The effect may be explained by the inertia of the particles, which causes them to be "thrown" into the sampler instead of following the air stream. These samplers are sub-isokinetic and it is expected that they will collect additional particles. The quick drop in aspiration efficiency between particle sizes 116 μm and 141 μm for the open face (32-mm) sampler may be explained by particle bounce as mentioned earlier.

4.3.4 Effect of Inlet Size

Another noteworthy trend for forward-facing samplers is that there appears to be a systematic effect related to inlet size for orientation-averaged measurements. The

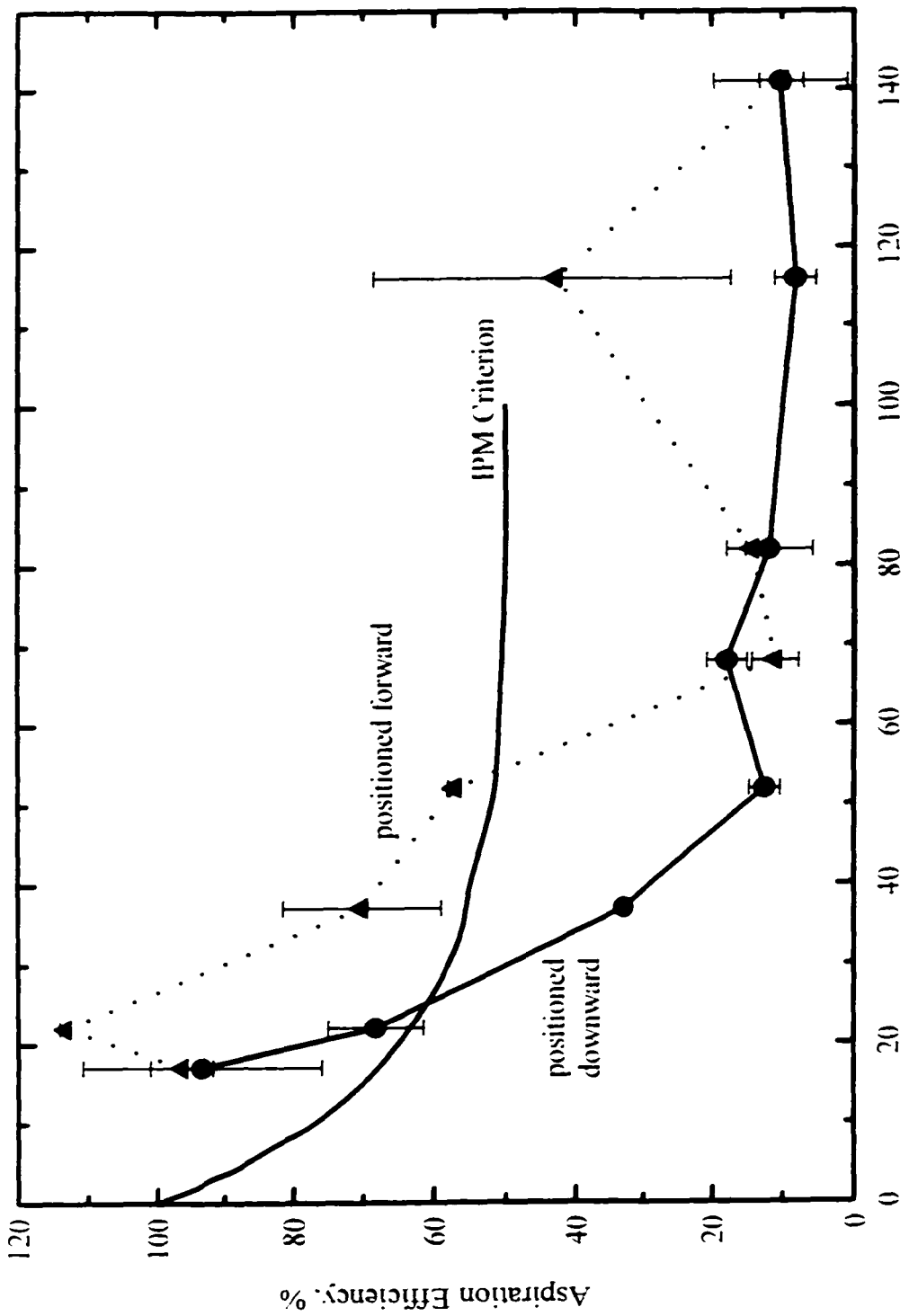

Figure 4-7: Effect of sampler position on orientation-averaged performance of the 37-mm in-line cassette with a 4-mm inlet.

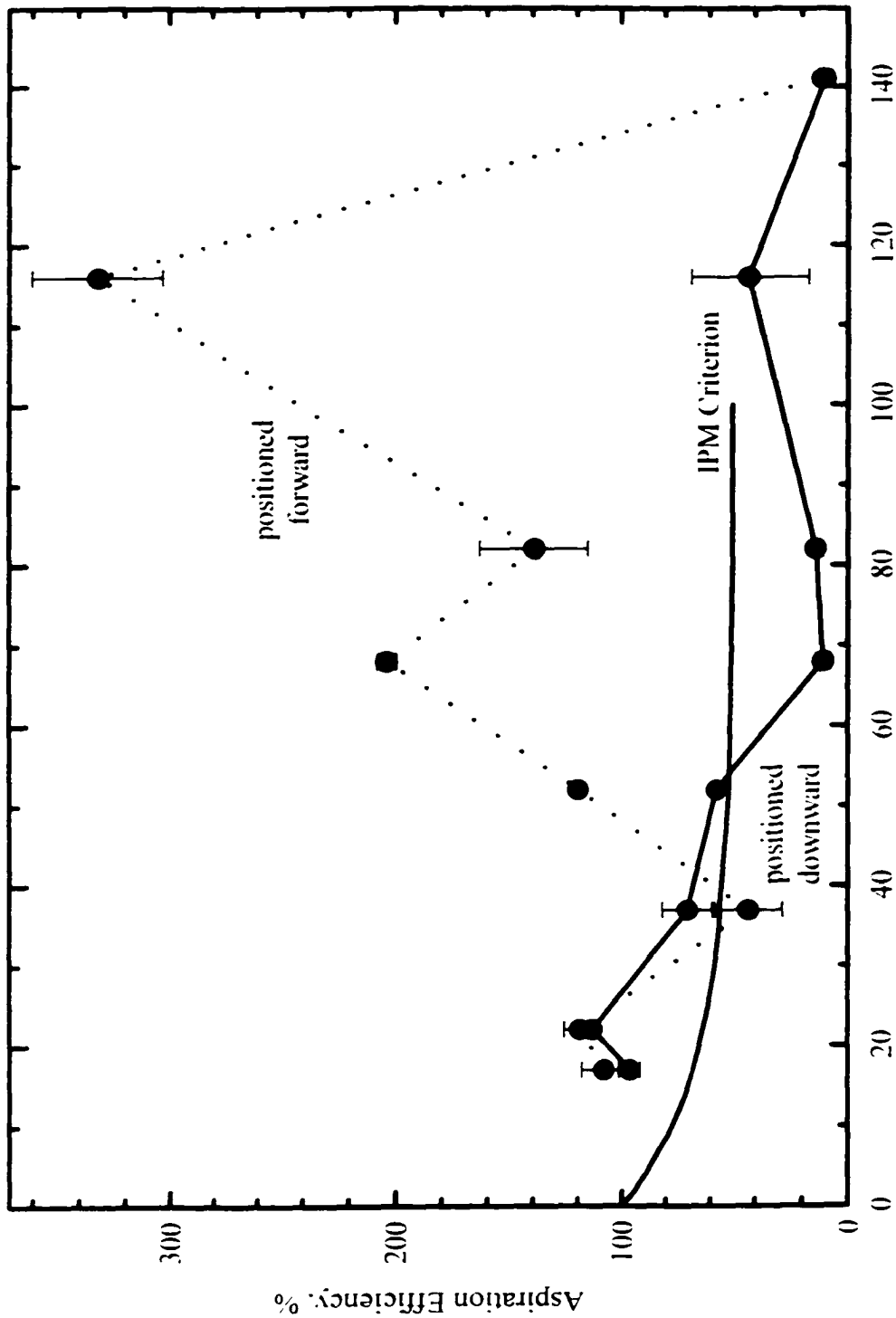

Figure 4-8: Effect of sampler position on orientation-averaged performance of the 37-mm in-line cassette with a 32-mm inlet (open face).

effect is illustrated in Figure 4-9. For particles larger than 70 μm, aspiration efficiency increases with increased inlet diameter. This may be explained by the straight-line motion of large particles and the influence on sampling when the mannequin moves through a narrow range of angles around 0°.

4.3.5 Oversampling of 7-μm Particles

A troublesome trend in the orientation-averaged data for all the samplers is seen in the measured aspiration efficiency for particles with an aerodynamic diameter of 7 μm. All of the values are above 100% with some as high as 170%. This is counter-intuitive because an overestimation of concentration is not anticipated for small particles. Small particles are agile enough to react quickly to changes in airflow direction and should be sampled with near 100% efficiency. The presence of a torso behind the sampler may cause a stagnation point in the region of the samplers which, in effect, produces a calm air sampling situation (May, 1967). Under calm air conditions, aspiration efficiency is also expected to be 100% for a wide range of particle sizes (Yoshida *et al.*, 1978; Breslin and Stein, 1975).

The observed trend is believed to be an artifact related to the experienced difficulty of delivering dust of this size to the wind tunnel. A review of the raw data and laboratory notes showed that measured wind tunnel dust concentrations were significantly lower for 7-μm particles than for other particle sizes. During the runs, care was taken to ensure that bridging did not occur in the dust feeders, meaning that

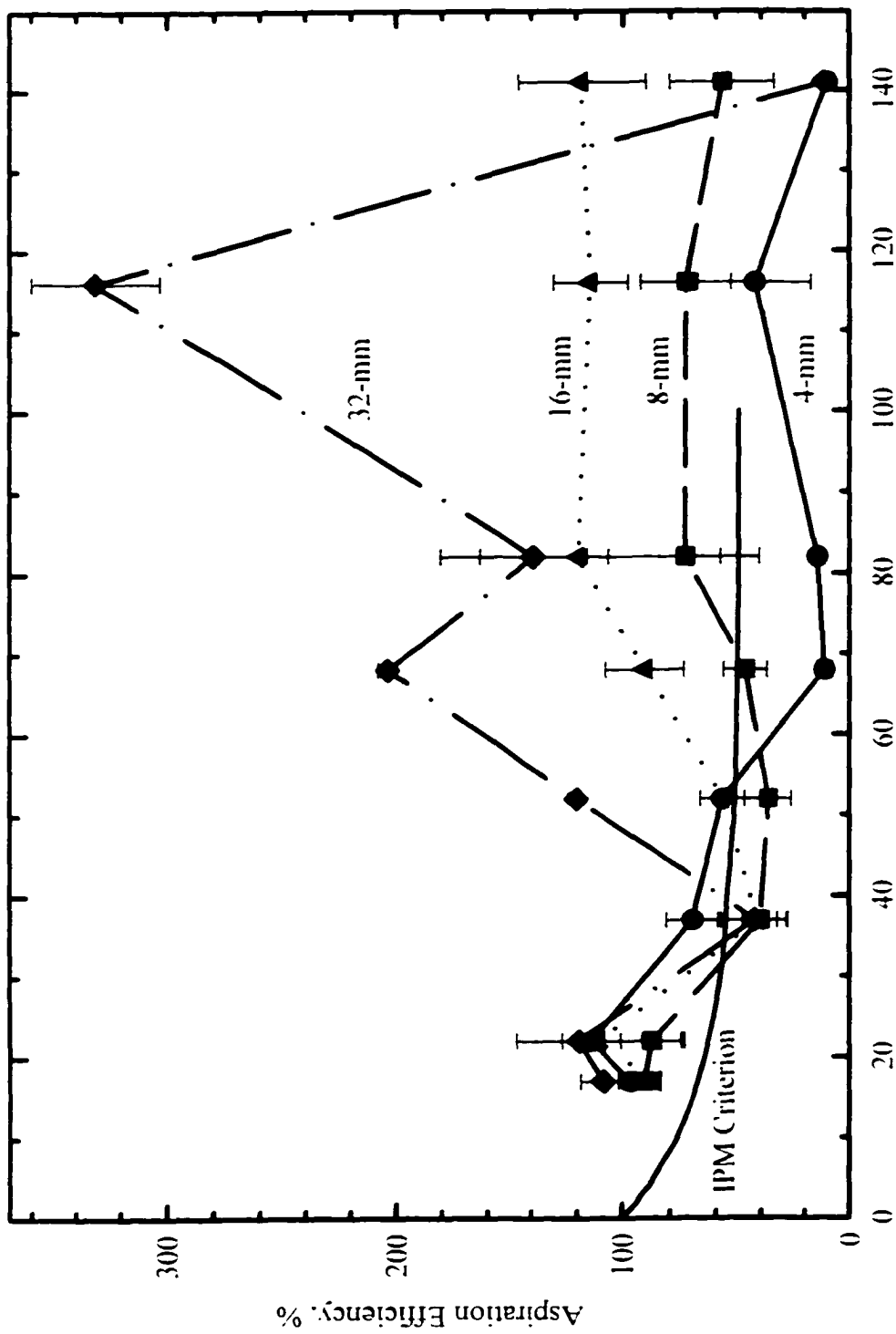

Figure 4-9: Effect of inlet size on orientation-averaged performance of the 37-mm in-line sampler when positioned forward.

insufficient dust supply cannot explain the lower measured concentrations. Additionally, there were notations that "chunks" were observed on the personal sampler filters and that dust build up was seen in the delivery nozzles. Again, this was seen only for d_a = 7 μm. This supports the notion that much of the dust deposited in the supply system and was resuspended as large, agglomerated particles with aerodynamic diameters larger than 150 μm. A bimodal distribution of particle sizes, especially one with a ten-fold difference between the modes, is likely to have resulted in a stratified aerosol concentration in the test section. The personal samplers may have been collecting "clumps" as well as individual particles while the isokinetic samplers, located 10 cm above the personal samplers, may have been collecting only 7-μm particles. This explains the observed oversampling of 7-μm particles without disqualifying the results for other particle sizes or the results of the inhalability study.

4.3.6 Comparison to the IPM Criterion

Figure 4-10 shows the orientation-averaged aspiration efficiency, as a function of particle size, for the three samplers that had the best agreement with the IPM criterion curve. The samplers included in the graph are 1) the IOM personal inhalable sampler, 2) the 37-mm cassette with a 4-mm inlet, facing forward and 3) the same cassette with an 8-mm inlet. One would expect that the performance of these three devices is similar because they are similar in geometry. In general, the

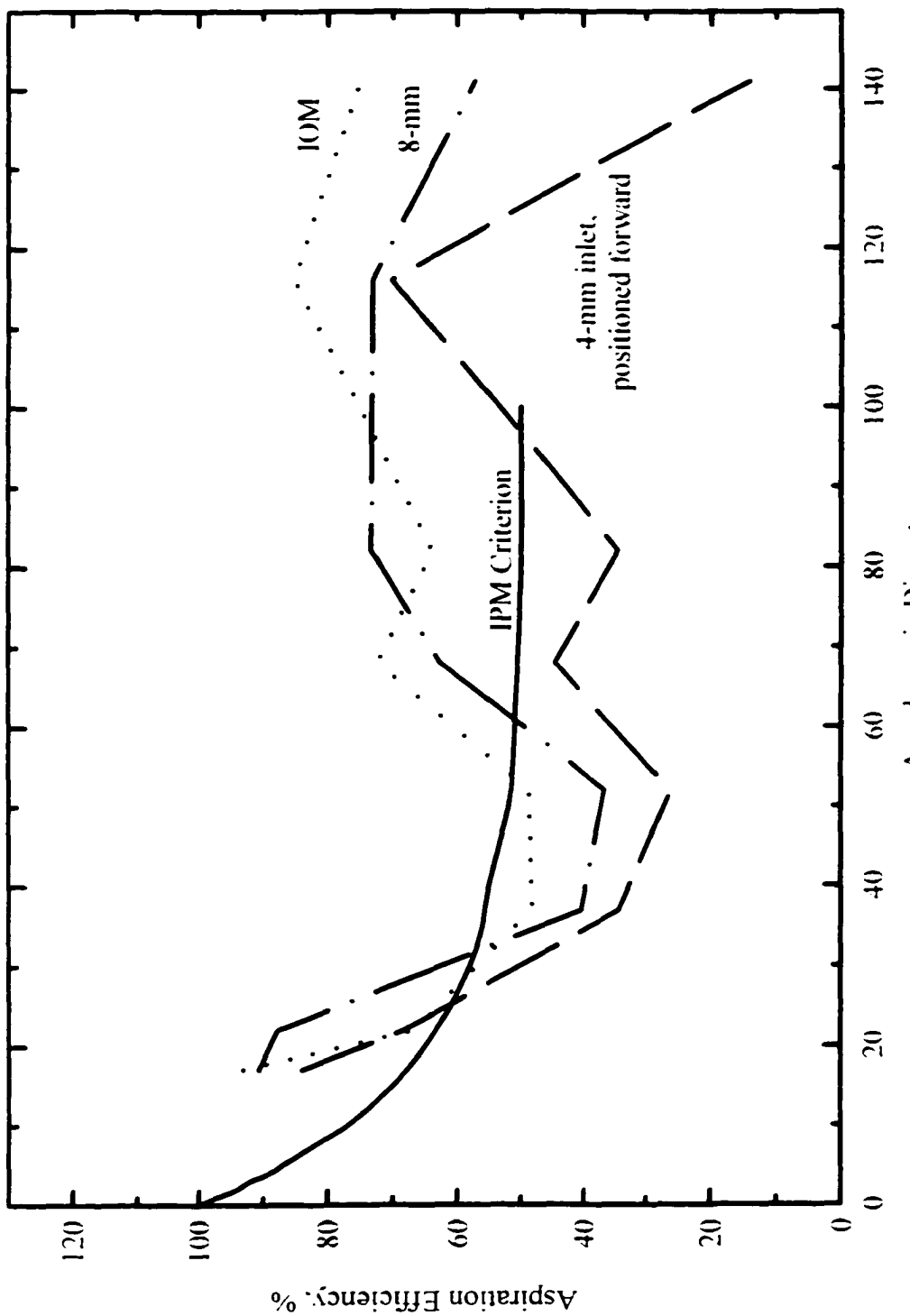

Figure 4-10: Three samplers showing best agreement with the IPM criterion.

IOM and the forward-facing 37-mm cassette with an 8-mm inlet show closest agreement with the inhalability criterion.

4.4 Conclusion

The UCLA low velocity wind tunnel provided an acceptable test system for the evaluation of personal inhalable sampler performance. Clumping of the test dust complicated the sampling of the smallest particles and the data for 7-μm particles were discarded because they were unreliable. Dust particles of larger sizes did not share this phenomenon and the data were usable. Future use of this test system for evaluating the aspiration efficiency of small solid particles will require redesign of the dust delivery system to prevent clumping of small particles.

The IOM personal inhalable sampler was found to have good agreement with the inhalability criterion for particles with aerodynamic diameters less than 100 μm. This confirms the findings of previous studies. This research also indicates that a modified 37-mm cassette with an 8-mm inlet closely approximates the IPM curve when the device faces forward. It appears that there is a range of inlet sizes, somewhere between 4 and 16 mm, which will provide good results as long as the sampler is positioned forward.

The performance curves for the three samplers with the closest agreement to the orientation-averaged mouth inhalability curve from the inhalability study (Chapter 3)

are shown in Figure 4-11. The IOM sampler provides a good fit only for particles smaller than 50 μm. In general, none of the samplers evaluated offer a reasonable match to the orientation-averaged mouth inhalability results of this research.

The 37-mm in-line filter cassette with a 4-mm inlet shows good agreement with the inhalability curve for orientation-averaged nose breathing when the device faces downward (Figure 4-12). The similarity between the geometry of the nose, which has small inlets that face down, and the sampler is apparent and probably accounts for the close agreement.

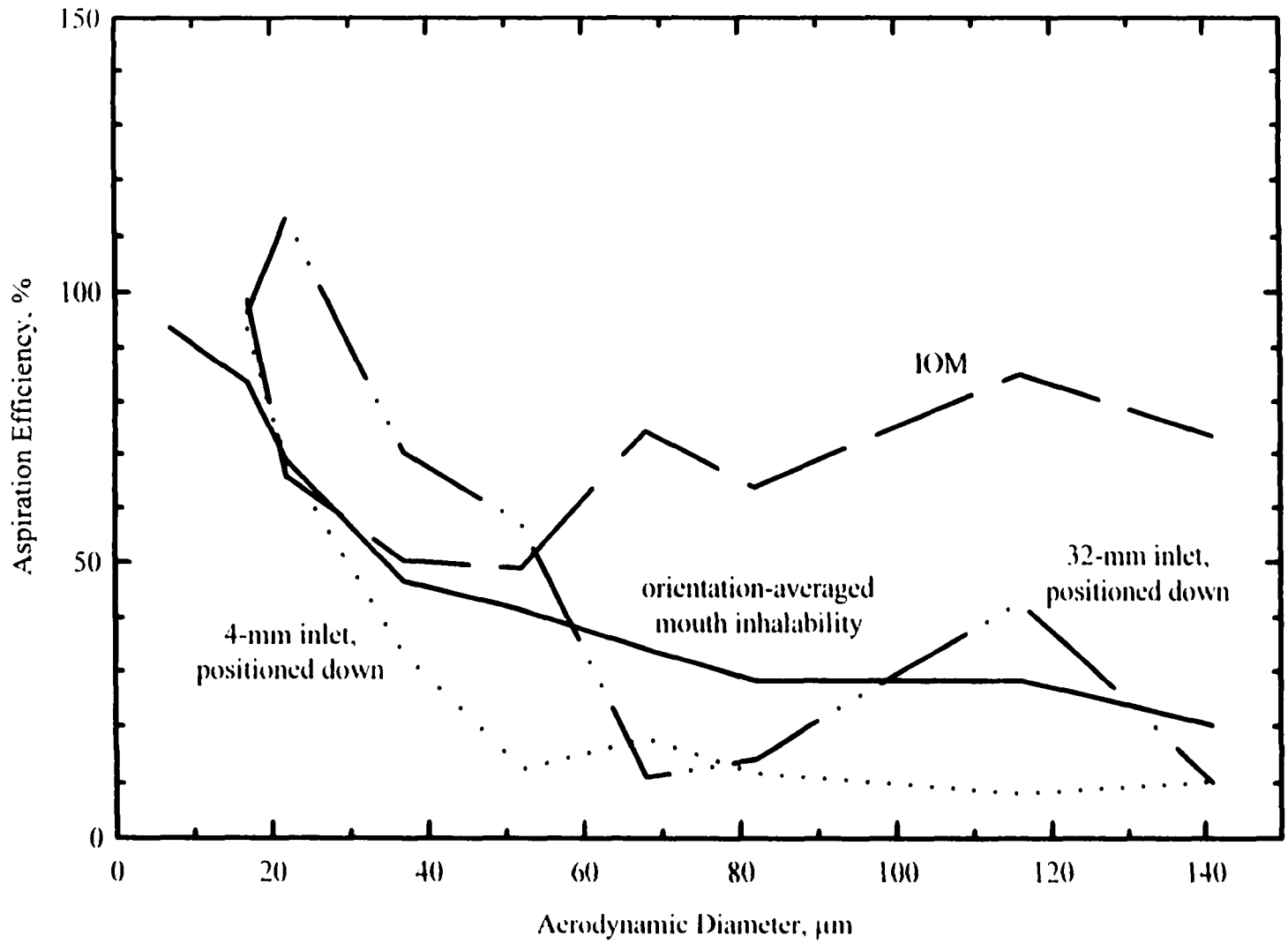

Figure 4-11: Three samplers showing best agreement with orientation-averaged mouth inhalability from this research.

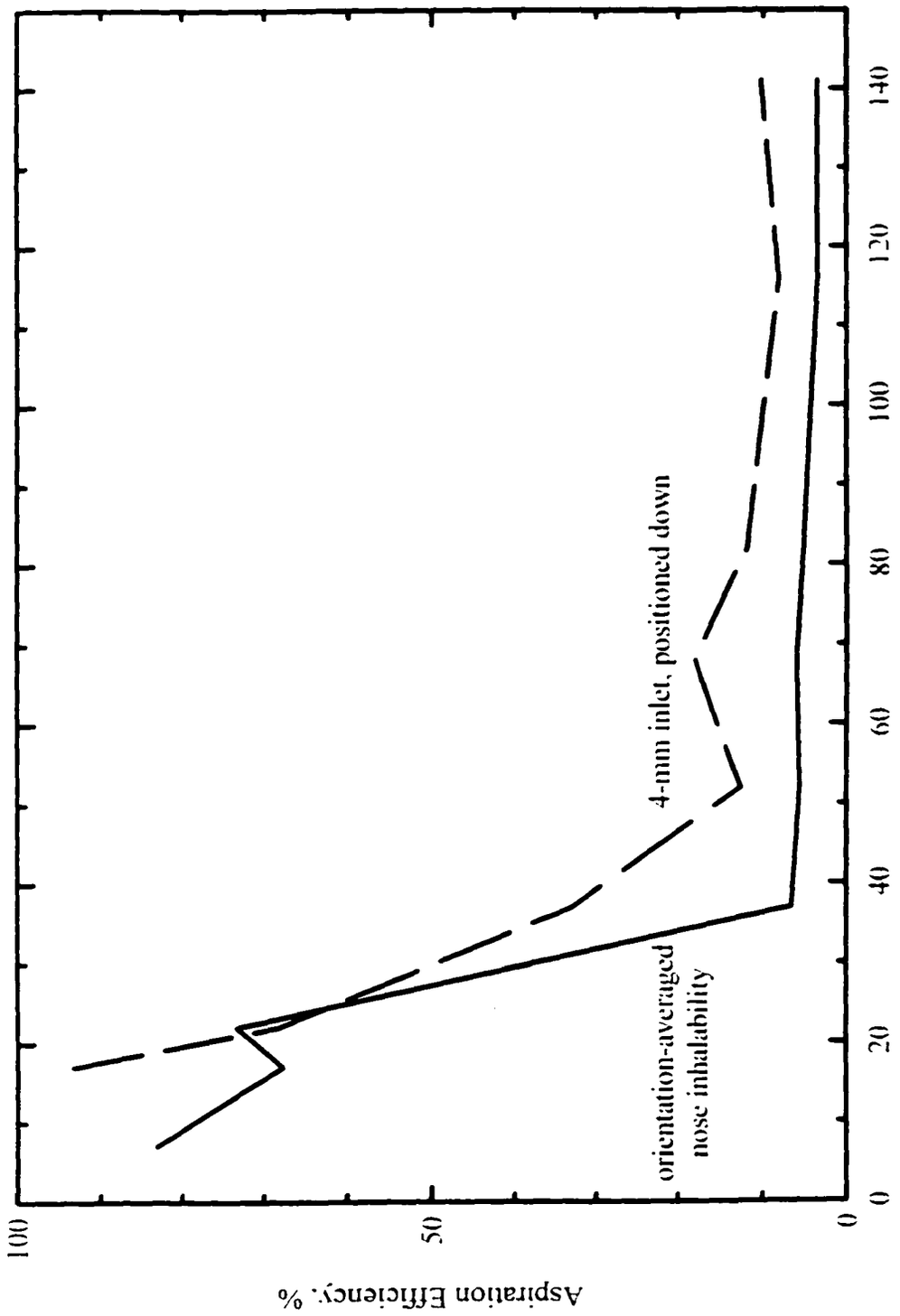

Figure 4-12: Sampler showing best agreement with orientation-averaged nose inhalability from this research.

Chapter 5: Inhalability of Large Liquid Particles

5.0 Introduction

The wind tunnel described in Chapter 1 and, in abbreviated form, the experimental design presented in Chapter 3 was used to examine the inhalability and sampling of large liquid particles. With the exception of the 1977 study by Ogden and Birkett, previous investigations of particle inhalability have been conducted using solid particles. The movement of solid and liquid particles of the same aerodynamic size is expected to be the same. So why is there interest in repeating the study with liquid particles?

While similarly-sized solid and liquid particles have the same aerodynamic behavior, the differences in their materials give them different physical properties. Under the right conditions a solid particle will bounce off of a hard surface, while a liquid particle will stick to that surface. A particle in an airstream that will carry it into the inlet of the mannequin's mouth or nose will be sampled. Solid particles just outside this airstream may strike the lip, nose or cheek of the mannequin and slide or bounce into the sampled airstream. This could result in collection of particles that otherwise would not enter the sampler. Another potential phenomenon was described by Vincent and Mark (1982); they noticed a build up of dust on the face, including the lips, of the mannequin. A particle striking the lips could possibly resuspend the

collected dust or knock it into the mouth. Again, this would result in the collection of particles not originally included in the sampled air volume.

5.1 Background

The phenomenon of particle bounce is described in papers by Dahneke (1971) and Cheng and Yeh (1979); Hinds (1999) presents a discussion of adhesive forces. When a solid particle strikes a hard surface at low velocity, the particle loses kinetic energy by plastic deformation and other contact effects. If the rebound energy remains sufficient to exceed the adhesive force between the surfaces, the particle will bounce. If not, it will stick. Once adhered to the surface, force is required to remove the particle. Particle material, size and velocity, in addition to the hardness of the contact material, affect particle bounce. Bounce is more likely to occur for large particles, high velocities, and hard surfaces. The particle material and the range of particle sizes and wind velocities used in the solid particle inhalability study were ideal for bounce to occur.

The mannequin used for these inhalability studies is made of fiberglass and the face is a hard surface. Kuo (1993) found that for particles larger than 30 μm, nearly all the particles bounced off the surface of the mannequin face. When a particle strikes the soft, moist skin of a human face it adheres instead of bouncing. To mimic the effect of skin either the mannequin face can be coated with grease or liquid particles

can be used in the test aerosol. In either case, particles striking the face of the mannequin are anticipated to stick with near 100% efficiency.

The primary purpose of this study was to investigate inhalability for large liquid particles and to compare the results to those for solid particles. The results of the study are also used to evaluate the possibility of particle resuspension from the sample filter during exhalation.

5.2 Experimental

The experimental conditions evaluated represent a subset of those studied for solid particle inhalability. All experiments were conducted at an inspiratory minute volume of 20.8 L/min. The conditions evaluated were:

1. particle sizes: 22, 50, 80 and 122 μm,
2. wind velocity: 0.4, 1.0, 1.6 m/s,
3. mannequin position: facing the wind or continuous rotation, and
4. nose and mouth breathing.

5.2.1 Particle Generation

Four sizes of particles were used during the study: 22, 50, 80 and 122 μm. The particles were generated using a TSI Model 3450 vibrating orifice aerosol generator (VOAG) (TSI Inc., St. Paul, MN). A VOAG uses the instability and natural tendency for break up of a cylindrical liquid stream to form particles (Berglund and

Liu, 1973). Left to its own, a liquid jet will break up in an uncontrolled process that results in particles of differing sizes. However, by applying a controlled disturbance of the stream, it is possible to generate particles that are uniform in size (Berglund and Liu, 1973). The TSI Model 3450 VOAG employs a piezoelectric crystal to produce a periodic disturbance of the stream, usually in the range of 5 - 200 kHz.

The frequency of jet disturbance, f, and the liquid flow rate, Q, through the orifice are used to calculate the diameter of the liquid droplet, d_d:

$$d_d = \left(\frac{6}{\pi} \frac{Q}{f} \right)^{\frac{1}{3}} \tag{5.1}$$

The droplets are then dispersed and diluted by mixing with air and allowed to shrink as the volatile materials evaporate. The diameter, d_p, of the remaining particles is a function of the concentration of non-volatile materials, C, in the test solution:

$$d_p = C^{\frac{1}{3}} d_d \tag{5.2}$$

A benefit of using a VOAG to generate the test aerosol is that the particles are spherical and monodisperse. It is only necessary to correct for density to obtain the aerodynamic diameter, d_a:

$$d_a = d_p \left(\frac{\rho_p}{\rho_{std}} \right)^{\frac{1}{2}} \tag{5.3}$$

where ρ_p is the density of the solute (894 kg/m^3 for oleic acid) and ρ_{std} is standard density, 1000 kg/m^3.

Varying the concentration of non-volatile materials in the test solution generates different particle sizes. Altering the disturbance frequency or the liquid feed rate also affects the particle size. Table 5-1 shows the values used for each of these parameters for the particle sizes used in this research.

Table 5-1: Parameters used for Liquid Particle Generation

d_a, μm	Orifice diameter, μm	Vibration frequency, kHz	Liquid feed rate, cm^3/min	Non-volatile fraction, %
22	20	4.995	0.147	15.3
50	50	24.49 – 24.51	0.584 – 0.608	19.0
80	50	24.49 – 24.51	1.070 – 1.098	43.1
122	100	58.47	2.201 – 2.292	14.8

The liquid sprayed through the orifice was a solution made of a non-volatile solute in a volatile solvent. The test solutions used in this study contained oleic acid, methanol and uranine, and acetone (Fisher Chemicals, Fair Lawn, NJ). The uranine was first dissolved in methanol and then mixed with the appropriate proportions of oleic acid and acetone. Acetone served as the solvent, while the other materials were considered non-volatile. Methanol is volatile, but it was not expected to evaporate

significantly in the short time (< 2 s) between droplet generation and particle collection.

The original aerosol delivery system was altered to accommodate the VOAG. The orifice cap was removed from its normal position on the equipment case and placed on the aerosol delivery manifold in the wind tunnel in place of the dust delivery nozzles. The syringe pump that is standard equipment for the TSI VOAG was replaced with an Ismatech IPC peristaltic pump (Ismatech SA, Glattburg, Switzerland). This was necessary to provide uninterrupted flow of the test solution. Wherever possible, Teflon® tubing and fittings were used. Silicone tubing was used for applications that required more flexibility, such as, the feed tube in the peristaltic pump. Figure 5-1 is a photograph showing the components of the liquid particle generation system.

5.2.2 Sample Analysis

The aerosol output of the VOAG is small compared to that of the three dust generators used for the solid particle study, so it was impractical to use gravimetric analysis to determine the sampled concentrations. Uranine, a disodium salt of fluorescein, was used as a fluorescent tag for the particles. It is easily detected at 10 ppb (parts per billion). Each particle contains a known amount of uranine, making is easy to calculate air concentration by comparing measured values of fluorescence to a standards curve. Pre-cut polyvinyl chloride (PVC) filters with a pore size of 5 μm

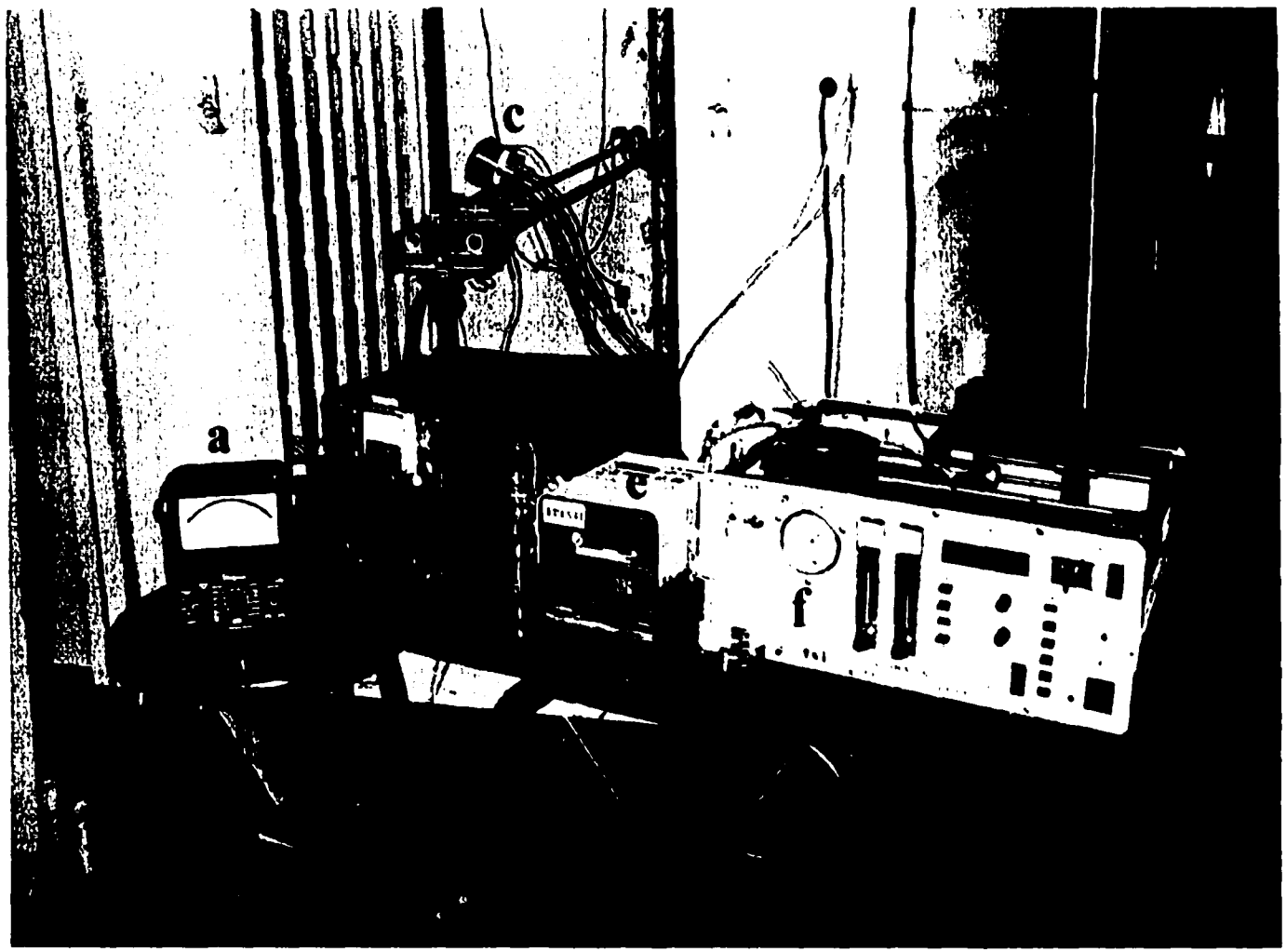

Figure 5-1: Liquid particle generation system, showing (a) Simpson multimeter, (b) power supply, (c) vibrating orifice mounted on aerosol delivery manifold, (d) test solution reservoir, (e) peristaltic pump, and (f) TSI VOAG (used for frequency generation and metering of aerosol dispersion air supply).

(SKC, Inc., Eighty-Four, PA) were used to collect the samples. The samples were desorbed from the filters and diluted as required using a buffer solution containing boric acid and borax. The recipe for the buffer solution was:

Part A: 12.40 g boric acid in 1000 mL of water

Part B: 19.05 g sodium borate in 1000 mL of water

Buffer: 50 mL Part A, 59 mL Part B; dilute the mixture to 200 mL

Particles that settled inside the sampler before reaching the filter were collected using a cotton swab and added to the desorption vial. The buffer (pH = 8.5 - 9.0) was needed because fluctuations in pH can effect the fluorescence measurements. Fluorescence was measured using a Perkin-Elmer Model 650-40 Fluorescence Spectrophotometer equipped with a xenon lamp powered by a Perkin-Elmer Model 150 Power Supply. The excitation wavelength was set to 493 nanometers (nm) with a slit width of 10 nm and the emission wavelength was 522 nm. The emission slit was adjusted to provide optimal fluorescence readings.

5.2.3 Particle Charge

Because the liquid particles were mechanically generated and dispersed, it was anticipated that they would collect charge during the aerosolization process. Measurements of particle charge found that a 60-μm particle carries +17,700 charges. It was possible to reduce the charge on the particles to - 643 (- 3.5% of the original charge) by applying a small voltage across the exit nozzle of the aerosol

generator. An Ambitrol Model 4005 power supply (Power Designs, Inc., New York), monitored using a Simpson Model 260 multimeter (Simpson Electric Co., Elgin, IL), was used to supply voltage in the range of ± 0.35 V to the exit nozzle. Before each experimental run, the particle charge was minimized using the Faraday-cup sampler and electrometer described in Chapter 2.

5.3 Results and Discussion

Inhalability was calculated as the ratio of the number concentration measured by the mouth or nose sampler to the number concentration determined by the isokinetic samplers. The value for the isokinetic sampler located above the mannequin head was excluded for 80 μm particles and wind velocities of 0.4 and 1.0 m/s and for 122 μm particles at all three wind velocities. In these cases, the concentration measured by the top isokinetic sampler was not representative of the concentration in the vicinity of the mouth or nose because nearly all the particles had settled below the level of the sampler. This was also observed in the solid particle inhalability study (Chapter 3).

5.3.1 Orientation-Averaged Mouth Inhalability

Figure 5-2 shows the results for orientation-averaged mouth inhalability for liquid particles and solid particles. Each of the curves represents the combined data for the three wind velocities evaluated. Also shown is the IPM criterion curve. The solid particle and liquid particle curves have the same general shape, but for particles

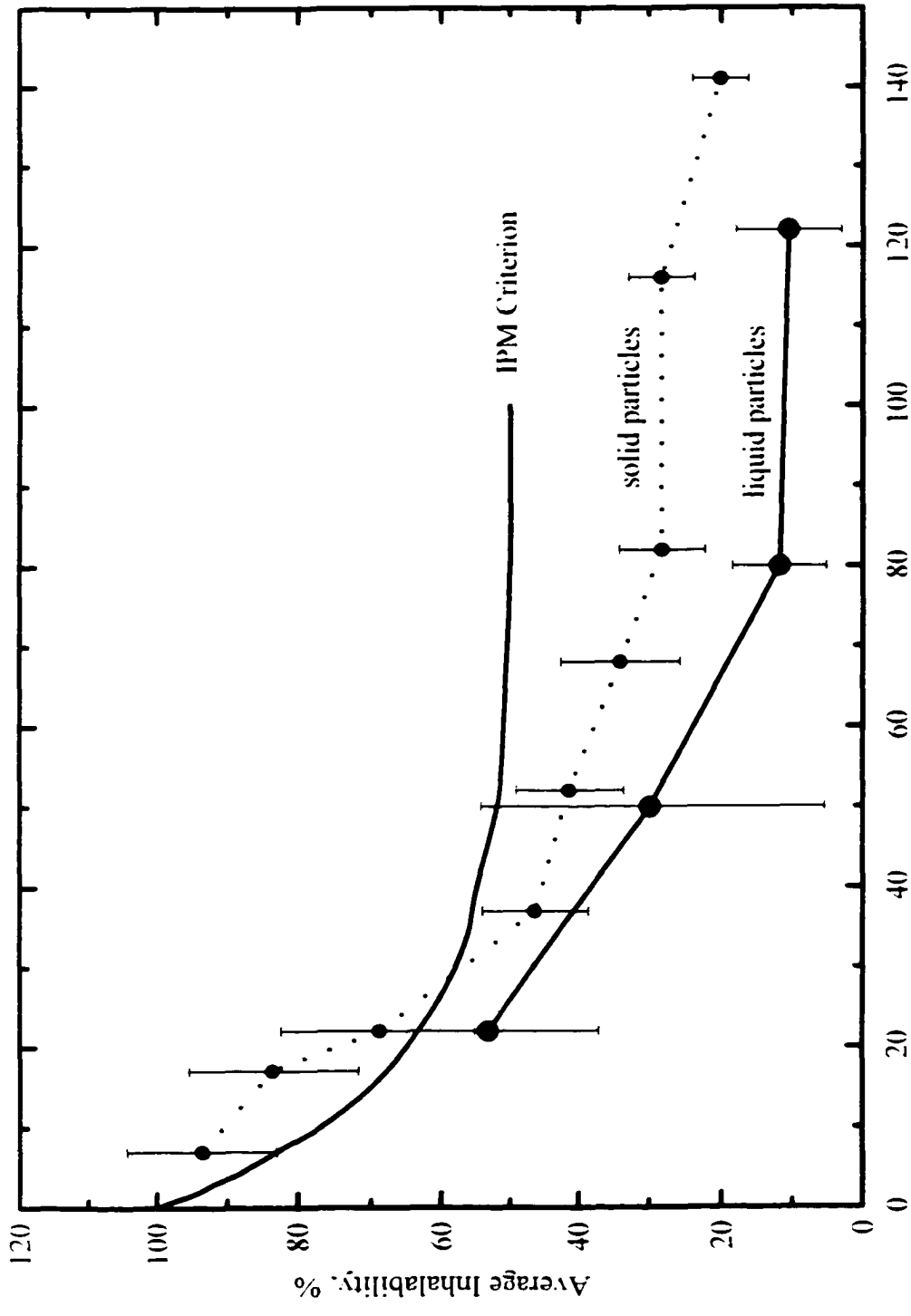

Figure 5-2: Inhalability for orientation-averaged mouth breathing, combined data for three wind velocities.

larger than 50 μm, the two curves are different. Each curve plateaus for particles larger than 80 μm, but the measured inhalability for liquid particles larger than 80 μm is 50 - 70% lower than the measured inhalability for solid particles larger than 80 μm. Compared to the IPM criterion, the measured liquid particle inhalability for mouth breathing is one-half the value for 50-μm particles and one-fifth the value for particles larger than 80 μm. The results suggest that particle bounce had a significant effect on the measurement of solid particle orientation-averaged mouth inhalability, especially for particles larger than 50 μm.

5.3.1.1 Effect of Wind Velocity on Orientation-Averaged Mouth Inhalability

The effect of wind velocity on orientation-averaged mouth inhalability for liquid particles is shown in Figure 5-3. Inhalability is increased at the lowest wind velocity (0.4 m/s). Measurements of liquid particle inhalability are not significantly different ($p = 0.0140$) at wind velocities of 1.0 and 1.6 m/s. The increase in inhalability at 0.4 m/s is especially pronounced for particle sizes less than 50 μm. The results confirm the notion that bounce is more likely to occur as particle size and wind velocity increase.

5.3.2 Facing-the-Wind Mouth Inhalability

Figure 5-4 shows the results for facing-the-wind mouth breathing for liquid particles and solid particles. For particles larger than 50 μm, the difference in measured inhalability becomes significant. For particles with an aerodynamic diameter of 80

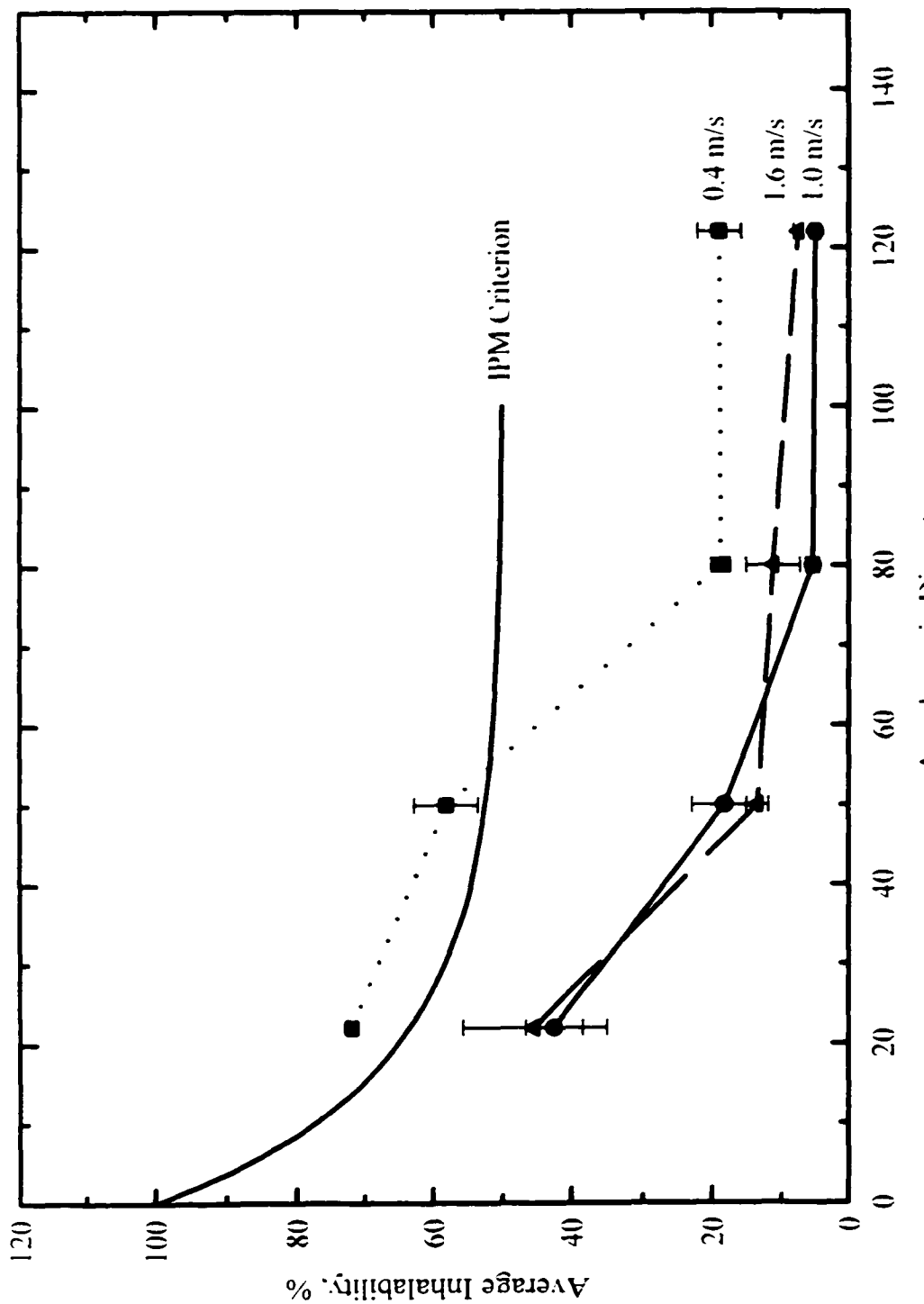

Figure 5-3: Effect of wind velocity on orientation-averaged inhalability for mouth breathing.

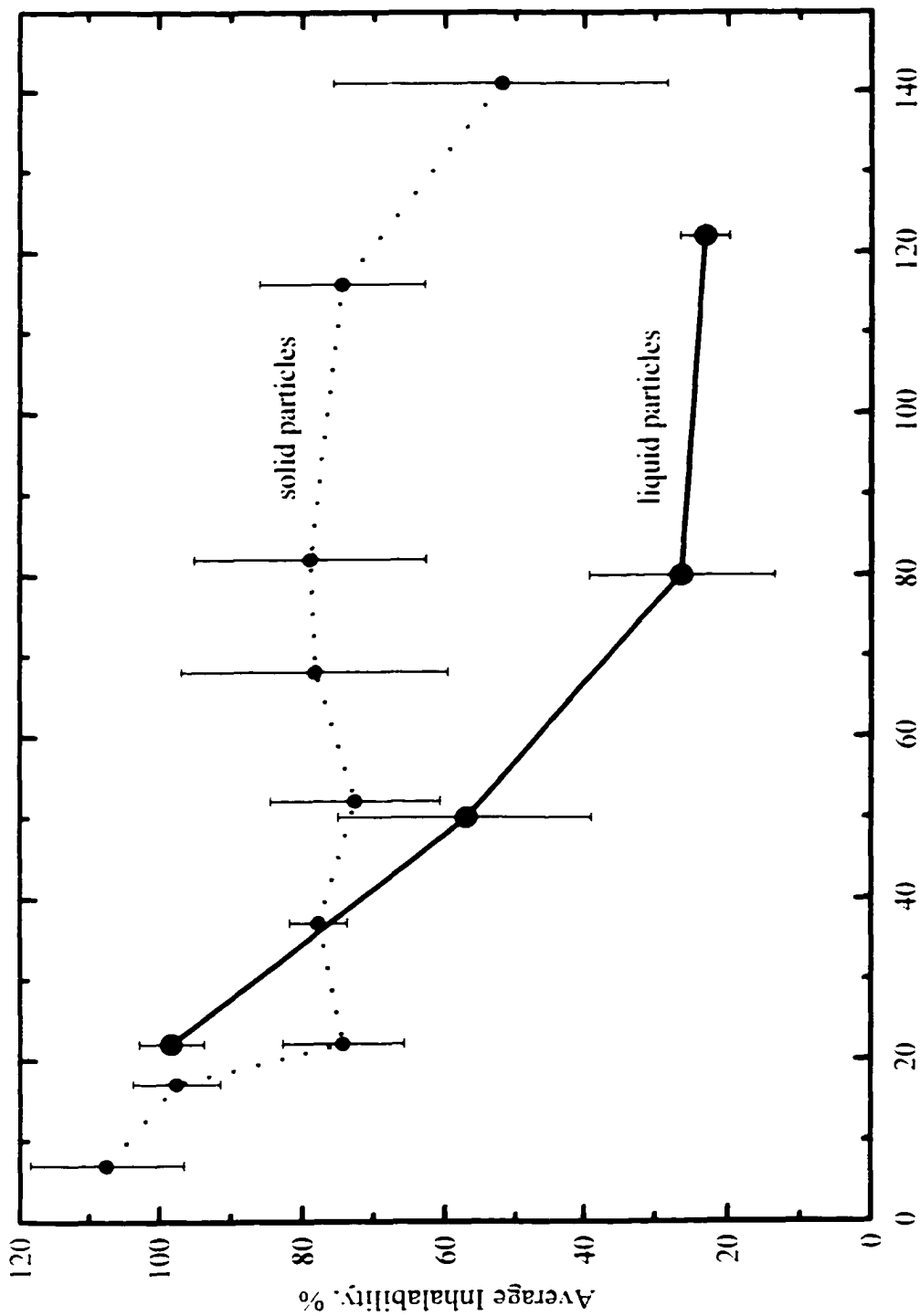

Figure 5-4: Inhalability for facing-the-wind mouth breathing, combined data for three wind velocities.

μm, the measured inhalability for liquid particles was approximately 25% of the measured inhalability for solid particles. Another noticeable difference is in the shape of the two curves. The curve for solid particles plateaus at 20 μm, while the liquid particle curve shows a plateau at about 80 μm. The results indicate that for d_a greater than 50-μm particle bounce has a significant effect on measured inhalability for facing-the-wind mouth breathing.

5.3.2.1 Effect of Wind Velocity on Facing-the-Wind Mouth Inhalability

The effect of wind velocity on liquid particle inhalability for facing-the-wind mouth breathing is shown in Figure 5-5. The three curves have the same general shape and trend. There may be some difference at the lowest wind velocity (0.4 m/s) for 50-μm particles, but it was not statistically significant ($p = 0.291$). Wind velocity (0.4 -1.6 m/s) does not affect measured inhalability.

5.3.3 Nose Inhalability

Figure 5-6 shows the measured inhalability for liquid particles when breathing through the nose. For particles with an aerodynamic diameter of 22 μm, the orientation-averaged inhalability is about 10% and the facing-the-wind inhalability is 75%. As particle size increase, the orientation-averaged results decrease until they plateau between 1 and 2% for particles between 80 and 122 μm. The facing-the-wind inhalability curve declines steeply to converge with the orientation-averaged inhalability curve at 80 μm. The orientation-averaged results indicate that nose

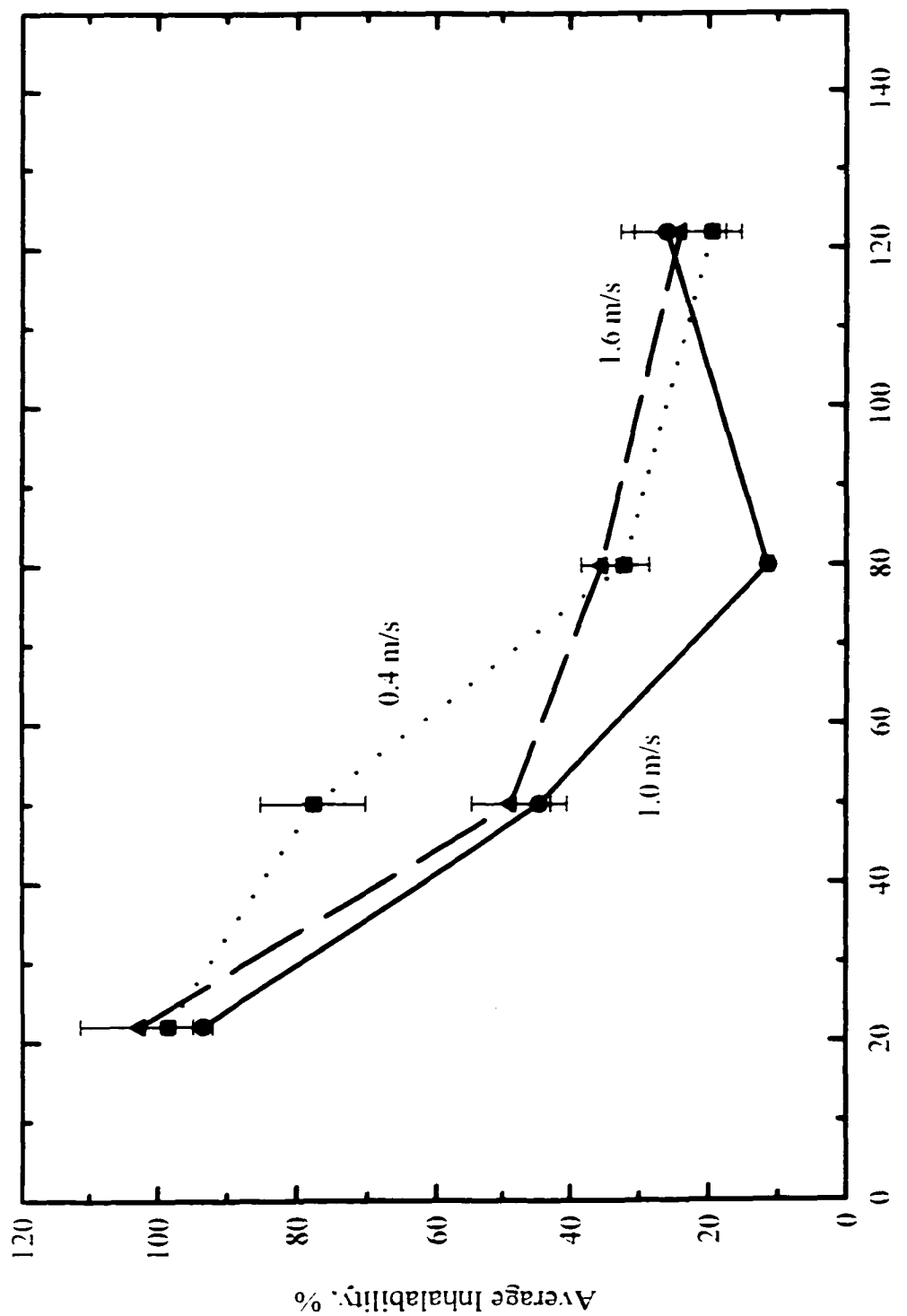

Figure 5-5: Effect of wind velocity on facing-the-wind inhalability for mouth breathing.

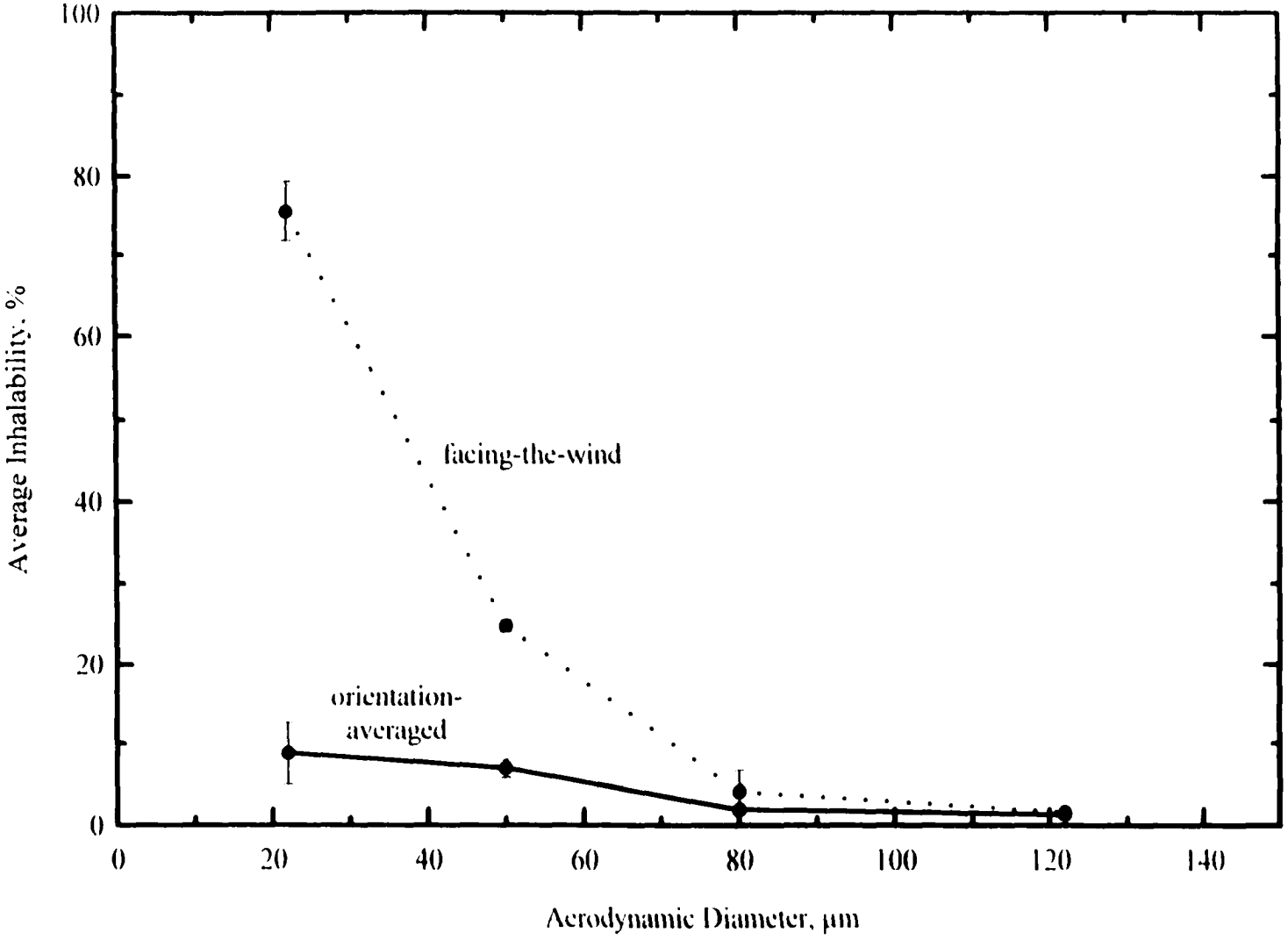

Figure 5-6: Liquid particle inhalability for nose breathing.

inhalability is 10% for 20-μm particles and it is theoretically indicated that very small particles are inhaled with 100% efficiency. The data do not indicate for which particle size orientation-averaged nose inhalability begins to drop; however, it is reasonable to assume that the decline is steep and that the size at which 50% of the particles are inhaled is less than 20 μm.

Figure 5-7 is a copy of Figure 3-14 showing nose inhalability for solid particles. A comparison of Figures 5-6 and 5-7 shows that the liquid particle and solid particle inhalabilty curves are similar for the facing-the-wind condition. However, there is significant difference between the orientation-averaged inhalability curves. The nose inhalability for solid, 20-μm particles is 70%, seven-times higher than for liquid particles of the same size. For solid particles, the inhalability plateau occurs when particles are 35 μm. A comparison of the orientation-averaged curves for solid and liquid particles suggests that particle bounce affects measured nose inhalability for particles smaller than 35 μm.

5.4 Conclusion

The results of the liquid particle inhalability study provide information that is interesting and useful, particularly when compared to the results of the solid particle inhalability study and the IPM criterion. The data sets from the present research strongly suggest that particle bounce has a significant influence on measured mouth

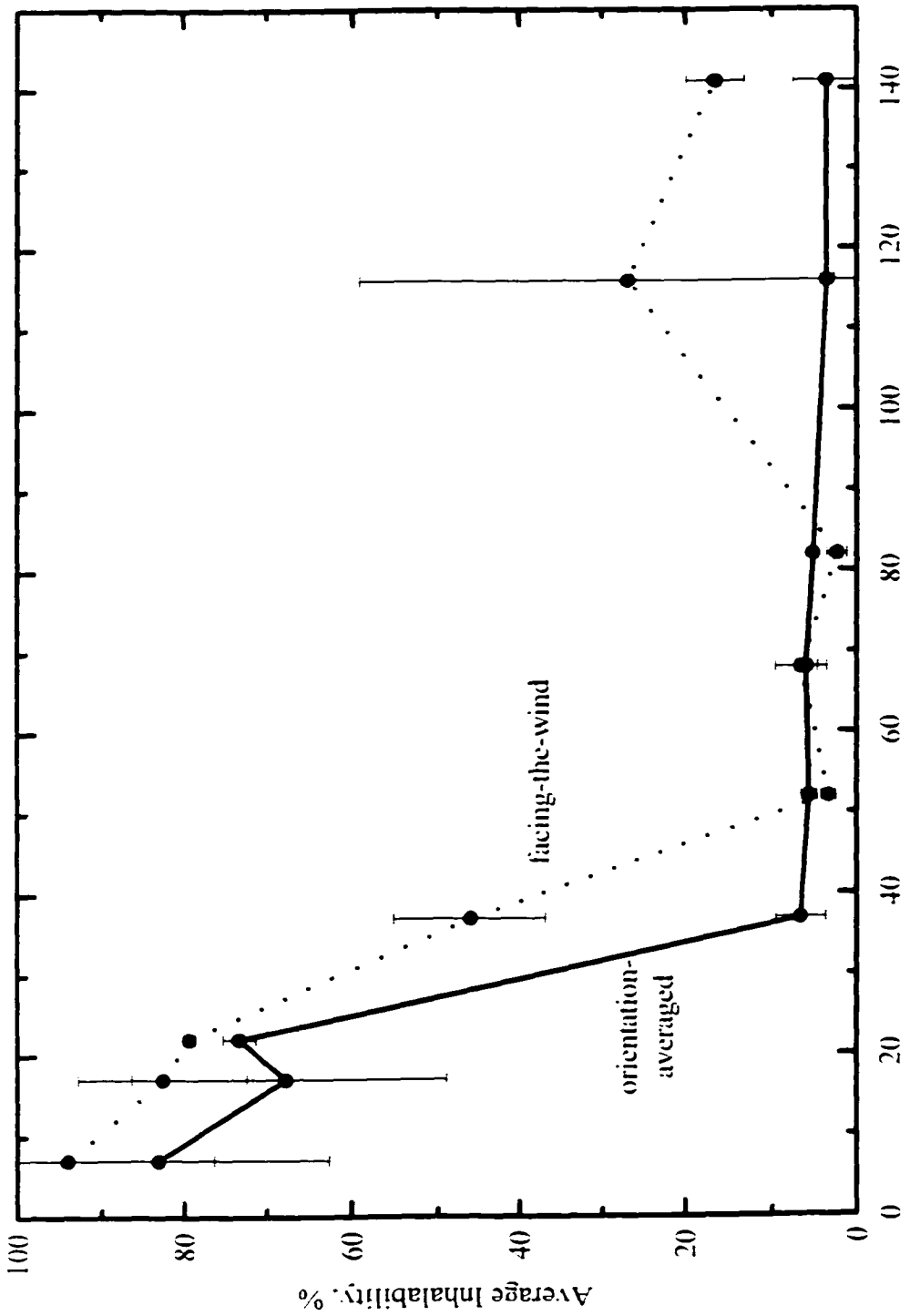

Figure 5-7: Solid particle inhalability for nose breathing.

inhalability for particles larger than 50 μm and on measured orientation-averaged nose inhalability for particles between 20 μm (possibly smaller) and 35 μm.

There was little observed difference between solid and liquid particles for facing-the-wind nose inhalability. Whether this is due to dominance of the effect of mannequin position with respect to wind direction or to some other aerosol dynamic is unclear. Conversely, there was a tremendous difference between solid particles and liquid particles for facing-the-wind mouth inhalability for particles larger than 50 μm. Wind velocity did not have a significant or clear effect on the inhalabilty of solid particles. For liquid particles, orientation-averaged inhalability appears to be affected by wind velocity. A wind velocity of 0.4 m/s was associated with increased inhalability for liquid particles smaller than 80 μm, while wind velocities of 1.0 and 1.6 m/s gave orientation-averaged inhalability curves that were not significantly different from each other. The curve for 0.4 m/s resembles the solid particle inhalability curve for orientation-averaged mouth breathing.

It is a reasonable assumption that liquid particles provide a better estimation of inhalability for humans because they will stick to surfaces they contact, as is the case with particles that strike the soft, moist skin of a worker. The data indicate that the accepted IPM criteria overestimates orientation-averaged mouth inhalability for particles larger than 50 μm. The overestimation may extend to some particle sizes smaller than 50 μm, but this was not clear from the data. Consequently, samplers

designed to meet the IPM criteria will likely overestimate worker exposure to particles larger than 50 μm.

6.0 Conclusions to the Dissertation

The objectives of the research presented in this dissertation were met and the data collected provides information that adds to our current understanding of the inhalability and sampling of large particles. Results for parameters not previously investigated are presented in the preceding chapters; they include:

1. extension of the inhalability criterion to include particles up to 141 μm.
2. evaluations of the effect of wind velocity on inhalability for mouth breathing.
3. evaluation of the effect of breathing pattern on inhalability for mouth breathing,
4. measurements of inhalability for nose breathing,
5. IPM performance evaluations for eight sampling devices,
6. evaluation of the effect of wind velocity on the performance of two common sampling devices, the 37-mm in-line cassette used for "total" dust sampling and the IOM personal inhalable sampler,
7. evaluations of the differences in inhalability and sampler performance due to mannequin position, either facing the wind or orientation-averaged with respect to the oncoming wind.
8. evaluation of inhalability for large liquid particles, and
9. information about the effect of particle bounce on measurements of inhalability.

Along the path of finding answers to the questions posed by the research, several adjunct projects were accomplished. These included improvements and modifications to the UCLA Low-Velocity Wind Tunnel, such as, redesign of the aerosol delivery manifold and solving the problem of particle charge by developing and installing an ion generator and Faraday-cup sampler. A method for determining the mass median aerodynamic diameter of a dust population using optical microscopy and measures of hydrodynamic settling velocity was developed to facilitate sizing of the irregularly shaped particles used in the solid particle studies. In general, working with large particles (> 10 μm) proved to be even more challenging than was anticipated at the onset of the research.

The solid particle inhalabilty results obtained by this work are significantly different from the IPM criterion. Several possibilities were offered to explain the difference and a compelling argument arises from looking at the results of the liquid particle inhalability study. Particle bounce might account for the wide disparity between these data and the IPM criterion for particles larger than 30 μm. The potential for particle bounce is influenced by particle size, the hardness of the materials, and wind velocity.

Three studies were used to develop the IPM criteria. The two that investigated particles larger than 30 μm used solid particles and wind velocities as high as 8 m/s, which is 5 times greater than the highest wind velocity used in this study, 1.6 m/s.

Also, the present investigation found that particle bounce has a tremendous effect when the mannequin faces the oncoming wind. Unlike this study, which used a continuously rotating mannequin to evaluate orientation-averaged inhalability, previous studies determined inhalability using a method that over-emphasizes the facing-the-wind condition (0°). The combined effect of higher wind velocities and over-emphasis of the inhalabilty at angles around 0° with respect to the oncoming wind might explain why the data used to develop the IPM criterion indicate higher inhalability than found by this research.

Measurements of nose inhalability indicate, as expected, that nose inhalability differs greatly from mouth inhalabilty. For the setting of occupational exposure limits, a standard based on mouth inhalabilty will also protect workers who breathe through their nose. The difference becomes an issue for exposure assessment and risk determination because samplers designed to match the IPM criterion will likely overestimate worker exposure to particles larger than 35 μm. It may be necessary to develop sampling devices to monitor the inhalable fraction for nose breathing, as well as, for mouth breathing. This becomes further complicated when one considers that most people are not exclusive mouth or exclusive nose breathers.

While the solid particle study found that particle inhalability is not affected by wind velocity in the range of 0.4 to 1.6 m/s, the results of the liquid particle study showed that inhalabilty was influenced by wind velocity for particles smaller than 80 μm. In

agreement with the findings of Aitken *et al.* (1999), it appears that wind velocity will influence inhalability when wind velocity is below 0.5 m/s.

Breathing pattern did not affect inhalability for a wind velocity of 1.0 m/s. Differences due to breathing pattern were not evaluated for other wind velocities or for liquid particles. Until such determinations are made, the effect of a worker's breathing rate and volume on inhalability will not be fully understood.

The results of the IPM performance evaluation for eight samplers generally confirmed the findings of previous studies. The IOM personal inhalable sampler, the device most commonly used in the US to monitor exposure to inhalable particles, showed reasonable agreement with the IPM criterion. Wind velocity appears to affect the aspiration efficiency of this sampler. A 37-mm in-line cassette with an 8-mm inlet positioned forward also performed well. A general conclusion from the study is that inlet diameter and position with respect to wind direction influence the aspiration efficiency of the sampling device.

The results of the liquid particle study suggest that inhalability should be determined using particles that will not bounce, because bounce has a significant effect on measured inhalability for aerodynamic diameters greater than 50 μm when solid particles are used. The findings were unanticipated and call into question the

appropriateness of an IPM criterion that is based on studies in which the effect of particle bounce was not considered.

Inhalability is apparently more complicated than indicated by the current IPM, which is limited in its application to orientation-averaged mouth breathing for wind velocities between 1 and 4 m/s. Additionally, the IPM criterion may not accurately reflect inhalability for the conditions it does cover because it is based on data that might have been influenced by particle bounce. The results of this research suggest that the IPM criterion needs revision. The recommended revision should:

1. extend beyond 100 μm because particles larger than this are inhalable,
2. be based on data obtained for particles that do not bounce,
3. account for wind velocities below 0.5 m/s,
4. provide for workers who face the oncoming wind during their work, and
5. recognize the difference between nose and mouth breathing.

Revised IPM criteria might include several curves representing ranges of conditions. This could be the best way to handle the complexity of large particle inhalability and sampling. At present, the data for developing such curves are limited. Considering the arduous task of collecting large particle inhalability data, it may be several years before a revision of the IPM criterion is possible.

References

Adachi, M., Pui, D.Y.H., and Liu, B.Y.H. (1993) Aerosol Charge Neutralization by a Corona Ionizer. *Aerosol Sci. Tech.* 18:48-58.

Aitken, R.J., Baldwin, P.E.J., Beaumont, G.C., Kenny, L.C., and Maynard, A.D. (1999) Aerosol Inhalabilty in Low Air Movement Environments. *J. Aerosol Sci.* 30:613-626.

Aizenberg, V., Grinshpun, S.A., Willeke, K., Smith, J., and Baron, P.A. (2000) Measurement of the Sampling Efficiency of Personal Inhalable Aerosol Samplers Using a Simplified Protocol. *J. Aerosol Sci.* 31(2):169-179.

American Conference of Governmental Industrial Hygienists (ACGIH) (1968) *Threshold Limit Values of Airborne Contaminants for 1968*, ACGIH, Cincinnati, OH.

American Conference of Governmental Industrial Hygienists (ACGIH) (1985) *Particle Size-Selective Sampling in the Workplace: Report of the ACGIH Technical Committee on Air Sampling Procedures.* ACGIH, Cincinnati, OH.

American Conference of Governmental Industrial Hygienists (ACGIH) (1995) *Industrial Ventilation A Manual of Recommended Practice*, 22nd ed., ACGIH, Cincinnati, OH.

American Conference of Governmental Industrial Hygienists (ACGIH) (1999) 1999 TLVs® and BEIs®. ACGIH, Cincinnati, OH.

Armbruster, L. and Breuer, H. (1982) Investigations into Defining Inhalable Dust. In *Inhaled Particles V*, W.H. Walton (Ed.), Pergamon, Oxford.

Baines, W.D. and Peterson, E.G. (1951) An Investigation of Flow Through Screens. *Trans. Am. Soc. Mech. Eng.* 73:467-480.

Baldwin, P.E.J. and Maynard, A.D. (1998) A Survey of Windspeeds in Indoor Workplaces. *Ann. Occup. Hyg.* 42:303-313.

Beaulieu, H.J., Fidino, A.V., Kim, M.S., Arlington, L.B., and Buchan, R.M. (1980) A Comparison of Aerosol Techniques: 'Open' versus 'Closed-Face' Filter Cassettes. *Am. Ind. Hyg. Assoc. J.* 41:758-765.

Berglund, R.N. and Liu, B.Y.H. (1973) Generation of Monodisperse Aerosol Standards. *Environ. Sci. Tech.* 7:147-152.

Berry, R.D., and Froude, S. (1989) An Investigation of Wind Conditions in the Workplace to Assess their Effect on the Quantity of Dust Inhaled. Health and Safety Executive Report No. IR/L/DS/89/3. Health and Safety Executive, London, UK.

Breslin, J.A., and Stein, R.L. (1975) Efficiency of Dust Sampling Inlets in Air. *Am. Ind. Hyg. Assoc. J.* 36:576-583.

British Medical Research Council (BMRC) (1952) Recommendations of BMRC Panels Relating to Selective Sampling. From the minutes of a joint meeting of Panels 1, 2, and 3 held on 4 March 1952.

Buchan, R.M., Soderholm, S.C., and Tillery, M.I. (1986) Aerosol Sampling Efficiency of 37-mm Filter Cassettes. *Am. Ind. Hyg. Assoc. J.* 47:825-831.

Bureau of Labor Statistics (BLS) (1998) http://stats.bls.gov/pdf/cpsaat11.pdf, Current Population Survey.

Burgess, W.A., Ellenbecker, M.J., and Treitman, R.D. (1989) *Ventilation for Control of the Work Environment.* Wiley, New York.

Cheng, Y.S. and Yeh, H.C. (1979) Particle Bounce in a Cascade Impactor. *Environ. Sci. Tech.* 13:1392-1296.

Chung, I.P. and Dunn-Rankin, D. (1992) Numerical Simulation of Two-Dimensional Blunt Body Sampling in Viscous Flow. *J. Aerosol Sci.* 23:217-232.

Code of Federal Regulations (1987) CFR Title 40, Section 53.43. July 1, 1987.

Code of Federal Regulations (1997) CFR Title 40, Section 53.62. July 18, 1997.

Comité Européen de Normalisation (CEN) (1993) Workplace Atmospheres. Assessment of Performance of Instruments for Measurement of Airborne Particles. CEN/TC137/WG3/ N125. CEN, Brussels.

Comité Européen de Normalisation (CEN) (1993) Workplace Atmospheres: Size Fraction Definitions for Measurement of Airborne Particles in the Workplace. CEN Standard EN 481. CEN, Brussels.

Cooper, D.W. and Reist, P.C. (1973) Neutralizing Charged Aerosols with Radioactive Sources. *J. Colloid Interface Sci.* 45:17-26.

Courbon, P., Froger, C., and LeBouffant, L. (1983) Personal Dust Sampler CIP10. Presented at the 20th International Conference of Safety in Mines Research Institute, Sheffield, October, Paper L2.

CRC (1983) *CRC Handbook of Chemistry and Physics*, 63rd ed. Weast, R.C. and Astle, M.J., (Eds.), CRC Press, Inc., Boca Raton, FL.

Dahneke, B. (1971) The Capture of Aerosol Particles by Surfaces. *J. Colloid Interface Sci.* 37:342-353.

Dockery, D.W., Pope, C.A., III, Xu, X., Spengler, J.D., Ware, J.H., Fay, M.E., Ferris, B.G., and Speizer, F.E. (1993) Mortality Risks of Air Pollution: A Prospective Cohort Study. *New England J. Med.* 329:1753-1759.

Dockery, D.W., Schwartz, J., and Spengler, J.D. (1992) Air Pollution and Daily Mortality: Associations with Particulates and Acid Aerosols. *Environ. Res.* 59:362-373.

Douglas, D.D. (1991) Respiratory Protective Devices. In *Patty's Industrial Hygiene and Toxicology*, 4th ed., Volume 1 Part A, G.D Clayton and F.E. Clayton (Eds.), Wiley, New York.

Dunnett, S.J. and Ingram, D.B. (1988) An Empirical Model for the Aspiration Efficiencies of Blunt Aerosol Samplers Oriented at an Angle to the Oncoming Flow. *Aerosol Sci. Tech.* 8:245-264.

Dunnett, S.J. and Ingram, D.B. (1988) The Human Head as a Blunt Aerosol Sampler. *J. Aerosol Sci.* 19:365-380.

Erdal, S. and Esmen, N.A. (1995) Human Head Model as an Aerosol Sampler: Calculation of Aspiration Efficiencies for Coarse Particles Using an Idealized Human Head Model Facing the Wind. *J. Aerosol Sci.* 26:253-272.

Fairchild, C.I., Tillery, M.I., Smith, J.P., and Valdez, F.O. (1980) Collection Efficiency of Field Sampling Cassettes. Report No. LA-8640-MS, Los Alamos Scientific Laboratory, Los Alamos, NM.

Hatch, T.F. and Gross, P. (1964) *Pulmonary Deposition and Retention of Inhaled Aerosols*. Academic Press, New York.

Hinds, W.C. (1999) *Aerosol Technology Properties, Behavior and Measurement of Airborne Particles*, 2nd ed., Wiley, New York.

Hinds, W.C. and Kennedy, N.J. (2000) An Ion Generator for Neutralizing Concentrated Aerosols. *Aerosol Sci. Tech.* 32:214-220.

Hinds, W.C. and Kuo, T.-L. (1995) A Low-Velocity Wind Tunnel to Evaluate Inhalability and Sampler Performance for Large Dust Particles. *Appl. Occup. Environ. Hyg.* 10:549-556.

International Standards Organization (ISO) (1981) Ad Hoc Working Group to Technical Committee 146 - Air Quality: Size Definitions for Particle Sampling. *Am. Ind. Hyg. J.* 42:A64-A68.

International Standards Organization (ISO) (1995) Air Quality – Particle Size Fraction Definitions for Health-Related Sampling. ISO Standard 7708. ISO, Geneva.

James, A.C., Stahlhofen, W., Rudolf, G., Köbrich, R., Briant, J.K., Egan, M.J., Nixon, W., and Birchall, A. (1994). Deposition of Inhaled Particles. in *Annals of the ICRP (International Commission on Radiological Protection), Publication 66*, Elsevier Science, Inc., Tarrytown, NY.

John, W. (1980) Particle Charge Effects. In *Generation of Aerosols*, Willeke, K. (Ed.), Ann Arbor Science, Ann Arbor, MI.

Johnson, A.E., Fletcher, B., and Saunders, C.J. (1996) Air Movement Around a Worker in a Low Speed Flow Field. *Ann. Occup. Hyg.* 40:57-64.

Johnston, A.M., Vincent, J.H., and Jones, A.D. (1986) Electric Charge Characteristics of Dry Aerosols Produced by Various Mechanical Generators. *Aerosols: Formation and Reactivity*, 2nd International Aerosol Conference, Pergamon Journals.

Kennedy, N.J., Tatyan, K., and Hinds, W.C. (2000) Comparison of a Simplified and Full-Size Mannequin for Evaluation of Inhalable Samplers. *Aerosol Sci. Tech.* (in press, accepted May 2000).

Kenny, L.C. (2000) The International Conventions for Health-Related Sampling of Aerosols – A Review of Current Status and Future Evolution. *Appl. Occup. Environ. Health* 15:68-71.

Kenny, L.C., Aitken, R., Chalmers, C., Fabriès, J.F., Gonzalez-Fernandez, E., Krombout, H., Lidèn, G., Mark, D., Riediger, G., and Prodi, V. (1997) A Collaborative European Study of Personal Inhalable Aerosol Sampler Performance. *Ann. Occup. Hyg.* 41:135-153.

Kuo, T.-L. (1993) Inhalability Evaluation of Large Dust Particles Using a Full Torso Manikin. Doctoral disseration. UCLA, Los Angeles.

Lioy, P.J., Lippmann, M. and Phalen, R.F. (1985) Rationale for Particle Size-Selective Air Sampling. In *Particle Size-Selective Sampling in the Workplace: Report of the ACGIH Technical Committee on Air Sampling Procedures.* ACGIH, Cincinnati, OH.

Lippmann,, M. (1995) Size-Selective Health Hazard Sampling. in *Air Sampling Instruments for Evaluation of Atmospheric Contaminants*, 8th ed., ACGIH, Cincinnati, OH.

Liu, B.Y.H. and Pui, D.Y.H. (1974) Electrical Neutralization of Aerosols. *J. Aerosol Sci.* 5:465-472.

Liu, B.Y.H. and Pui, D.Y.H. (1981) Aerosol Sampling Inlets and Inhalable Particles. *Atmos. Environ.* 15:589-600.

Lodge, J.P. and Chan, T.L. (eds.) (1986) *Cascade Impactor*. American Industrial Hygiene Association, Akron, OH.

Mark, D. and Vincent, J.H. (1986) A New Personal Air Sampler for Airborne Total Dust in Workplaces. *Ann. Occup. Hyg.* 30:89-102.

Mark, D. and Vincent, J.H. (1986) Investigation of the Entry Characteristics of Dust Samplers of the Type used in the British Nuclear Industry. *Atmos. Environ.* 20:2389-2396.

May, K.R. (1967) Physical Aspects of Sampling Airborne Microbes. *Symp. Soc. Gen. Microbiol.* 17:60-80.

National Research Council (1980) *Measurement and Control of Respirable Dust in Mines*. NMAB-363. National Academy of Sciences, Washington, D.C.

Nelson, G.O., Johnson, R.E., Lindeken, C.L., and Taylor, R.D. (1972) Respirator Cartridge Efficiency Studies III: A Mechanical Breathing Machine to Simulate Human Respiration. *AIHAJ* 33:745-750.

Notø, H., Halgard, K., Daae, H.L., Bentsen, R.K., and Eduard, W. (1996) Comparative Study of an Inhalable and a Total Dust Sampler for Personal Sampling of Dust and Polycyclic Aromatic Hydrocarbons in the Gas and Particulate Phase. *Analyst* 121:1191-1196.

Ogden, T.L. and Birkett, J.L. (1977) The Human Head as a Dust Sampler. In *Inhaled Particles IV*. W.H. Walton (Ed.), Pergamon, Oxford.

Ogden, T.L. and Birkett, J.L. (1978) An Inhalable Dust Sampler for Measuring the Hazard from Total Airborne Particulate. *Ann. Occup. Hyg.* 21:41-50.

Özkaynak, H. and Thurston, G.D. (1987) Association Between 1980 US Mortality Rates and Alternative Measures of Airborne Particle Concentrations. *Risk Anal.* 7:449-461.

Pope, C.A., III, and Dockery, D.W. (1999) Epidemiology of Particle Effects. In *Air Pollution and Health*. Holgate, S.T., Samet, J.S., Koren, H.S., and Maynard, R.L., (Eds.) Academic Press, London.

Pope, C.A., III, Schwartz, J., and Ransom, M.R. (1992) Daily Mortality and PM_{10} Pollution in Utah Valley. *Arch. Environ. Health* 47:211-217.

Pope, C.A., III, Thun, M.J., Namboodiri, M.M., Dockery, D.W., Evans, J.S., Speizer, F.E., and Heath, C.W. (1995) Particulate Air Pollution as a Predictor of Mortality in a Prospective Study of US Adults. *Amer. J. Resp. Crit. Care Med.* 151:669-674.

Prodi, V., Belosi, F., and Mularoni, A. (1986) A Personal Sampler Following ISO Recommendations on Particle Size Definitions. *J. Aerosol Sci.* 17:576-581.

Public Law 91-173 (1969) *Federal Coal Mine Health and Safety Act of 1969*. 91st Congress, December 10, 1969.

Public Law 91-596 (1970) *Occupational Safety and Health Act of 1970*. 91st Congress, December 29, 1970.

Public Law 95-164 (1977) *Federal Mine Safety and Health Act of 1977*. 95th Congress, November 9, 1977.

Ramachandran, G., Sreenath, A. and Vincent, J.H. (1998) Towards a New Method for Experimental Determination of Aerosol Sampler Aspiration Efficiency in Small Wind Tunnels. *J. Aerosol Sci.* 29(7):875-92.

Rodes, C.E., Kamens, R.M., and Weiner, R.W. (1995) Experimental Considerations for the Study of Contaminant Dispersion Near the Body. *Am. Ind. Hyg. Assoc. J.* 56:535-545.

Romay, F.J., Liu, B.Y.H. and Pui, D.Y.H. (1994) A Sonic Jet Corona Ionizer for Electrostatic Discharge and Aerosol Neutralization. *Aerosol Sci. Tech.* 20:31-41.

Silverman, L.G., Plotkin, T., Sawyers, L.A., and Yancey, A.R. (1951) Air Flow Measurements on Human Subjects with and without Respiratory Resistance at Several Work Rates. *Arch. Ind. Hyg. Occup. Med.* 3:461-478.

Soderholm, S.C. (1985) Size-Selective Sampling Criteria for Inspirable Mass Fraction. In *Particle Size-Selective Sampling in the Workplace: Report of the ACGIH Technical Committee on Air Sampling Procedures.* ACGIH, Cincinnati, OH.

Spear, T.M., Werner, M.A., Bootland, J., Harbour, A., Murray, E.P., Rossi, R., and Vincent, J.H. (1997) Comparison of Methods for Personal Sampling of Inhalable and Total Lead and Cadmium-Containing Aerosols in a Primary Lead Smelter. *Am. Ind. Hyg. Assoc. J.* 58:893-899.

Sutton, G.W. and Reno, S.J. (1968) Respirable Mass Concentrations Equivalent to Impinger Count Data. Presented at *American Industrial Hygiene Conference*, St. Loius, MO.

Task Group on Lung Dynamics (1966) Deposition and Retention Models for Internal Dosimetry of the Human Respiratory Tract. *Health Phys.* 12:173-207.

Teague, S.V., Yeh, H.-C., and Newton, G.J. (1978) Fabrication and Use of Krypton-85 Aerosol Discharge Devices. *Health Phys.* 35:392-395.

US Environmental Protection Agency (EPA) (1996) Air Quality Criteria for Particulate Matter. EPA/600/P-95/001cf, April 1996.

Vincent, J.H. (1987) Recent Advances in Aspiration Theory for Thin-Walled and Blunt Aerosol Sampling Probes. *J. Aerosol Sci.* 18:487-498.

Vincent, J.H. (1989) *Aerosol Sampling Science and Practice.* Wiley, New York.

Vincent, J.H. and Mark, D. (1982) Application of Blunt Sampler Theory to the Definition and Measurement of Inhalable Dust. In *Inhaled Particles V*, W.H. Walton (Ed.), Pergamon, Oxford.

Vincent, J.H., Hutson, D., and Mark, D. (1982) The Nature of Air Flow Near the Inlets of Blunt Dust Sampling Probes. *Atmos. Environ.* 15:703-712.

Vincent, J.H., Mark, D., Miller, B.G., Armbruster, L., and Ogden, T.L. (1990) Aerosol Inhalability at Higher Wind Speeds. *J. Aerosol Sci.* 21:577-586.

Vincent, J.H., Mark, D., Parker, I., and Witherspoon, W. (1988) Joint Investigations of New Generations of Dust Sampling Instrument. IOM Report No. TM/88/09. Institute of Occupational Medicine, Edinburgh.

Vinzents, P. (1988) Personal Sampling of Total and Inspirable Dust: Results from a Survey in the Danish Wood and Furniture Industry. *Aerosol Sci.* 19:1437-1439.

Wilsey, P.W., Vincent, J.H., Bishop, M.J., Brosseau, L.M., and Greaves, I.A. (1996) Exposures to Inhalable and "Total" Oil Mist Aerosol by Metal Machining Shop Workers. *Am. Ind. Hyg. Assoc. J.* 57:1149-1153.

Witschger, O., Willeke, K., Grinshpun, S.A., Aizenberg, V., Smith, J., and Baron, P.A. (1998) Simplified Method for Testing Personal Inhalable Aerosol Samplers. *J. Aerosol Sci.* 29:855-874.

Wood, J.D. and Birkett, J.L. (1979) External Airflow Effects on Personal Sampling. *Ann. Occup. Hyg.* 22:299-310.

Yeh, H.-C. (1993) Electrical Techniques. In *Aerosol Measurement*, Willeke, K. and Baron, P.A. (eds.), Van Nostrand Reinhold, New York.

Yoshida, H., Uragami, M., Masuda, H., and Iinoya, K. (1978) Particle Sampling Efficiency in Still Air. *Kagaku Kogaku Ronbunshu* 4:123-128 (HSE translation No. 8586).

Zamorani, E. and Ottobrini, G. (1978) Aerosol Particle Neutralization to Boltzmann's Equilibrium by a.c. Corona Discharge. *J. Aerosol Sci.* 9:31-39.